Award Number: **W81XWH-11-1-0477**

TITLE: Military Vision Research Program

PRINCIPAL INVESTIGATOR: Darlene A. Dartt, Ph.D.

CONTRACTING ORGANIZATION:
Schepens Eye Research Institute

Boston, MA 0214

REPORT DATE: October 2012

TYPE OF REPORT: Annual

PREPARED FOR: U.S. Army Medical Research and Materiel Command
Fort Detrick, Maryland 21702-5012

REPORT DOCUMENTATION PAGE

Form Approved
OMB No. 0704-0188

1. REPORT DATE	2. REPORT TYPE	3. DATES COVERED
1 October 2012	Annual	Sep 19, 2011-Sep 18, 2012

4. TITLE AND SUBTITLE
, 2012
Military Vision Research Program

5a. CONTRACT NUMBER

5b. GRANT NUMBER
W81XWH-11-1-0477

5c. PROGRAM ELEMENT NUMBER

6. AUTHOR(S)
Drs. Darlene Dartt (PI); Sunil Chauhan, Maredith Gregory-Ksander,
Sharmila Masli, James Zieske, Patricia D'Amore, Andrius Kazlauskas,

Joan Stein-Streielin, Dong Feng Chen, Alex Bowers, Peter Bex, Bruce Ksander
E-Mail: darlene.dartt@schepens .harvard.edu

5d. PROJECT NUMBER

5e. TASK NUMBER

5f. WORK UNIT NUMBER

7. PERFORMING ORGANIZATION NAME(S) AND ADDRESS(ES)

Schepens Eye Research Institute
Boston, MA 0214

8. PERFORMING ORGANIZATION REPORT NUMBER

9. SPONSORING / MONITORING AGENCY NAME(S) AND ADDRESS(ES)

U.S. Army Medical Research and Materiel Command
Fort Detrick, Maryland 21702-5012

10. SPONSOR/MONITOR'S ACRONYM(S)

11. SPONSOR/MONITOR'S REPORT NUMBER(S)

12. DISTRIBUTION / AVAILABILITY STATEMENT

Approved for Public Release; Distribution Unlimited

No restrictions.

13. SUPPLEMENTARY NOTES

14. ABSTRACT

EYE INJURIES HAVE INCREASED IN WARFARE OVER THE PAST 200 YEARS. IN THE CURRENT CONFLICT THE EYE IS PARTICULARLY VULNERABLE TO BLAST INJURY AS WELL AS TO ENVIRONMENTAL STRESS FROM THE CURRENT THEATERS OF OPERATION. FOR CLEAR VISION, THE ENTIRE VISUAL AXIS (TEARS, CORNEA, AQUEOUS HUMOR, LENS, VITREOUS, RETINA, AND OPTIC NERVE) MUST BE TRANSPARENT, INTACT, AND HEALTHY AND EACH PART OF THIS AXIS FUNCTIONAL. EACH OF THESE STRUCTURES HAS ITS PARTICULAR VULNERABILITIES. IN THE PRESENT PROPOSAL WE HAVE DESIGNED MULTIPLE PROJECTS TO INVESTIGATE THE SPECIAL VULNERABILITIES OF THE CORNEA, RETINA, OPTIC NERVE, AND BRAIN TO MECHANICAL, LASER, INFECTIOUS, AND ENVIRONMENTAL TRAUMA AND TO DEVISE MEANS TO PREVENT, DIAGNOSE, AND REPAIR THE SEQUELAE OF THESE TRAUMAS.

15. SUBJECT TERMS
injury, laser injury, infection, angiogenesis, stem cells, dry eye, cornea, inflammation, traumatic brain injury, pain receptors, immune response

16. SECURITY CLASSIFICATION OF:			17. LIMITATION OF ABSTRACT	18. NUMBER OF PAGES	19a. NAME OF RESPONSIBLE PERSON
a. REPORT	b. ABSTRACT	c. THIS PAGE			USAMRMC
U	U	U	UU	62	

Table of Contents

DoD FY10 (W81XWH-11-1-0477)
Annual Report
October 18, 2012

INTRODUCTION:

About 10% of all injuries in the current military conflict are eye injuries, the overwhelming majority being blast injuries. Repairing eye trauma and its sequelae, especially in the context of traumatic brain injury (TBI), has unfortunately become the top priority for military vision research. For functional vision to occur the ocular surface (cornea and conjunctiva) must be intact and healthy and the cornea and vitreous must remain transparent. Additionally, the retina and brain must be able to receive and process the information presented to them. The cornea must not only heal in response to blast injuries, but also is susceptible to environmental challenges as it is the interface between the eye and the external environment. The cornea and conjunctiva must protect the eye from pathogens, heal without inflammation, and repair its dense innervation to maintain the health of the cornea. The vitreous, retina, and brain have their unique challenges for repair after traumatic brain and eye injury. The vitreous, retina, and brain do not regenerate and thus repair poorly. There are multiple reasons for this poor repair including deregulated angiogenesis, aberrant immune response, glial scar formation, and destruction of Burch's membrane. For head trauma, it is important to develop vision tests to diagnose the basis of visual impairment. Tasks 1-5 focus on the ocular surface (cornea and conjunctiva) including its repair, response to infection, and susceptibility to dry eye. Tasks 6-9 center on the retina's susceptibility to microclots in blood vessels, regulation of angiogenesis, control of immune response after damage, and optic nerve regeneration. Tasks 10-11 are developing new tests for determining vision loss associated with TBI. Task 12 focuses on methodologies to restore the corneal epithelium.

TASK 1: A Novel Mesenchymal Stem Cell-based Approach for Corneal Epithelium Regeneration (Sunil Chauhan, Ph.D.)

BODY: Corneal injury and inflammatory diseases, ranging from vision-threatening conditions (e.g. trauma and burn) to quality-of-life impairing conditions (e.g. dry eye) impact more than 10 million Americans each year. Many of these conditions lead to epithelial defects and chronic inflammation, and are commonly treated with non-specific anti-inflammatory drugs such as corticosteroids, which are fraught with many side effects such as cataract, glaucoma, and stromal melts. Thus, there is a pressing need for new, effective and safe treatment modalities that can address such corneal diseases. *Bone marrow-derived mesenchymal stem cells (MSC)* are non-hematopoietic stem cells which possess a multilineage differentiation capacity and potent anti-inflammatory functions [1,2]. The availability of bone marrow and the ability to isolate and expand MSC ex vivo make these cells an attractive candidate for drug development for a variety of regenerative and inflammatory disorders. However, MSC therapeutic efficacy and the mechanism of repair in corneal diseases are still not clear. In the current study, using a mouse model of corneal injury and in vitro assays, we systematically investigated the therapeutic potential of MSC in promoting epithelial repair in corneal injury.

Experiment # 1. ***Standardization of technology for culture and characterization of MSC and primary mouse corneal epithelial cells, and mouse model of corneal epithelial injury***

To study MSC function in corneal injury, we first standardized the methodology for *in vitro* culture and characterization of MSC according to the criteria by the Mesenchymal and Tissue Stem Cell Committee of the International Society for Cellular Therapy statement (3,4).

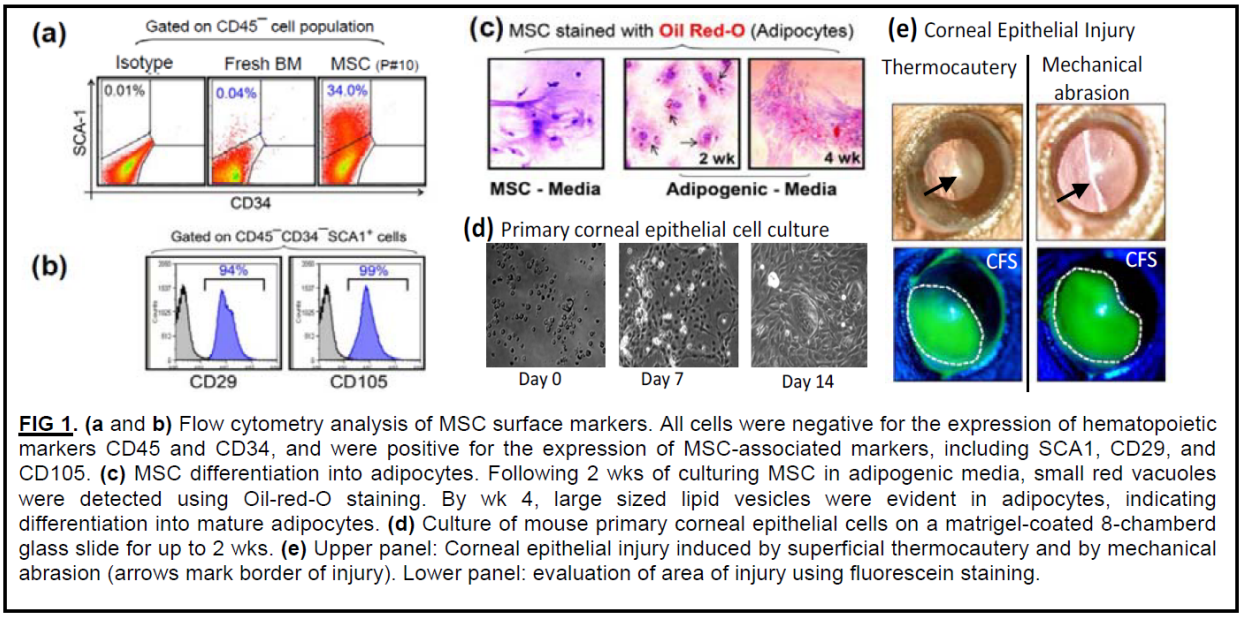

FIG 1. (a and **b)** Flow cytometry analysis of MSC surface markers. All cells were negative for the expression of hematopoietic markers CD45 and CD34, and were positive for the expression of MSC-associated markers, including SCA1, CD29, and CD105. **(c)** MSC differentiation into adipocytes. Following 2 wks of culturing MSC in adipogenic media, small red vacuoles were detected using Oil-red-O staining. By wk 4, large sized lipid vesicles were evident in adipocytes, indicating differentiation into mature adipocytes. **(d)** Culture of mouse primary corneal epithelial cells on a matrigel-coated 8-chamberd glass slide for up to 2 wks. **(e)** Upper panel: Corneal epithelial injury induced by superficial thermocautery and by mechanical abrasion (arrows mark border of injury). Lower panel: evaluation of area of injury using fluorescein staining.

Bone marrow was harvested from euthanized B6 wild type and GFP.B6 mice. MSC were cultured and expanded using the plastic adherence method, and were characterized phenotypically using flow cytometry (FIG 1a and 1b) and functionally by differentiating them into adipocytes (FIG 1c). Similarly, we also standardized the culture of mouse primary corneal epithelial cells. Nearly $15x10^4$ live epithelial cells per cornea can easily be isolated and cultured for up to 2 weeks in a matrigel coated 8 chamber glass slide or culture plate (FIG 1d). Furthermore, we standardized our mouse model of corneal epithelial injury by superficial thermocautery and mechanical abrasion (using Algerbrush-II) (FIG 1e). In our hands, both the techniques are highly reliable for the creation of epithelium-specific injury without creating a stromal wound.

Experiment # 2. ***Corneal injury increases mobilization of MSC and the expression of stem cell chemoattractants.*** To determine if corneal injury has an impact on MSC mobilization and leads to increased expression of putative stem cell-specific chemotactic factors (e.g. Substance P and stromal cell-derived factor-1 (SDF-1)) [5,6], the peripheral blood and corneas were collected at different time points following corneal injury. MSC frequencies were analyzed using flow cytometery, and expression levels of Substance P and SDF-1 were evaluated by ELISA and qPCR. Furthermore, to confirm chemotactic migration of MSC, we investigated MSC expression of homing receptors and their migration toward cornea and sera of mice with corneal injury using a transwell assay.

- Flow cytometric studies showed significantly increased (2-fold) frequencies of $CD45^{-}CD34^{-}SCA1^{+}$ MSC in the peripheral blood of mice with corneal injury at 48h post injury compared to at 0h post injury (FIG 2a).

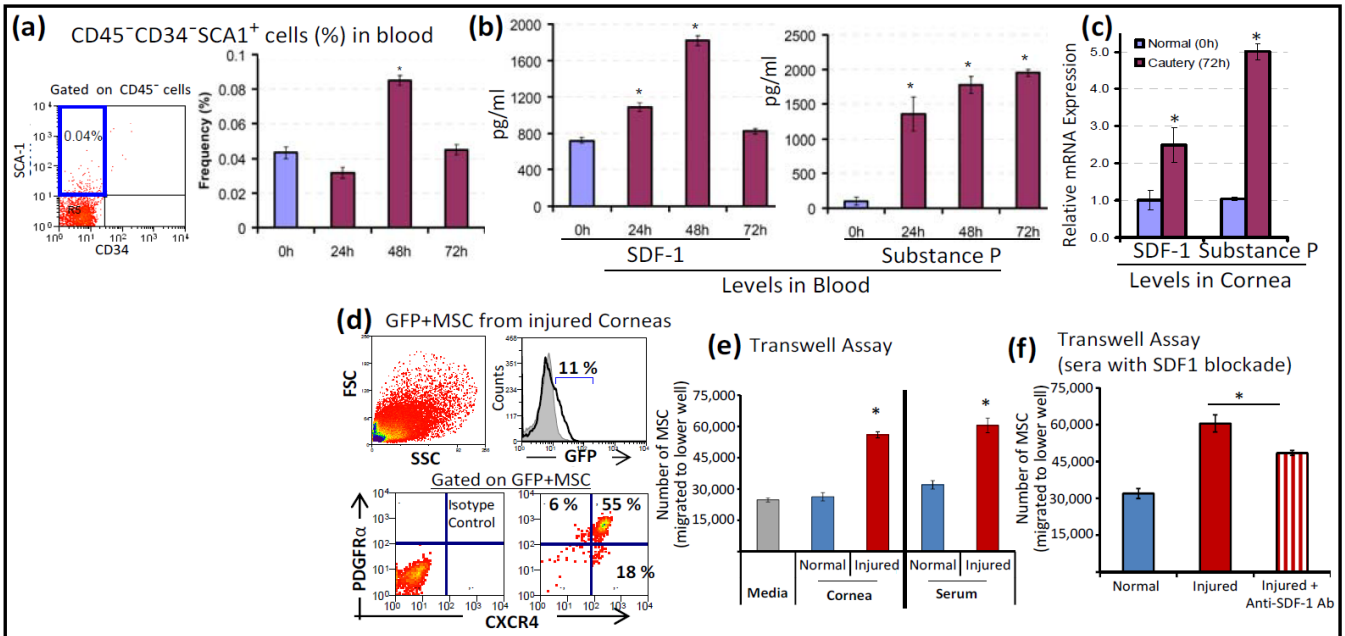

FIG 2. (a) Frequencies of circulating CD45-CD34-SCA1+ MSC in the peripheral blood of mice with corneal injury at different time points post-injury. Expression levels of putative stem cell chemoattaractants SDF-1 and Substance P in the **(b)** peripheral blood and **(c)** corneas of mice after corneal injury. **(d)** Expression of homing receptors CXCR4 and PDGFRa on *in vitro* cultured MSC. **(e)** Frequencies of i.v. administered GFP+MSC in injured corneas and their expression pattern of CXCR4 and PDGFRα. **(f)** Transwell assay showing a significant 2-fold increased chemotactic migration of MSC toward lower well containing corneas and sera of mice with corneal injury compared to normal mice. **(g)** Transwell assay showing partial, but a significant inhibition of MSC migration toward sera of mice with corneal injury when blocking anti-SDF-1 antibodies were added to the lower well. ($p<0.05$).

- Substance P and SDF-1, which have been reported to possess stem cell chemoattractant properties and facilitate mobilization of MSC into blood and to sites of injury [5,6], were observed to be significantly increased in the peripheral blood and cornea following injury. ELISA assays revealed a gradual increase in SDF-1 levels, which peaked at 48h post injury (2.5 fold) and coincided with the increased frequencies of circulating MSC (FIG 2b). A significant (15 fold) increase was observed in substance P levels by 24h, with levels continuing to rise until 72h (FIG 2b). Similarly, there was significantly higher expression of SDF-1 (~3 fold) and substance P (5 fold) in the injured cornea compared to normal corneas (FIG 2c).
- Flow cytometric analysis of single cell suspension of corneas with epithelial injury from GFP+MSC-treated mice showed the presence of ~10% GFP+ cells (of all corneal cells) in the injured cornea (FIG 2d). The majority (55%) of these GFP+MSC expressed both CXCR4 (SDF-1 receptor) and PDGFRa (receptor for PDGF), suggesting a critical role for these homing receptors in the homing of MSC to the injured cornea (FIG 2d) [5,7].
- In a transwell assay, MSC showed a strong chemotactic migration toward cornea and sera of mice with corneal epitheial injury compared to normal mice (FIG 2e). Interestingly, the migration of MSC toward the sera of injured mice could be significantly inhibited by the addition of blocking anti-SDF-1 antibodies (FIG 2f).

These data suggest that (i) corneal injury leads to an increase in the expression of stem cell chemoattractants that can mobilize endogenous MSC into peripheral blood and (ii) increased expression of chemoattractants in injured tissues can augment MSC homing to the site injury.

Experiment # 3. ***MSC home specifically to the injured cornea and promote epithelial regeneration.*** We sought to ascertain whether MSC have the potential to home to corneal tissue by tracking the presence of intravenously injected MSC in both injured and contralateral healthy corneas. MSC homing to cornea following injury was investigated by injecting red Q-dot-labeled or GFP+ bone marrow-derived MSC (GFP+MSC). MSC were injected 1h post injury, and confocal microscopy on corneal wholemounts was used to detect the labeled cells. Furthermore, we studied whether MSC homing to the injured cornea can promote epithelial regeneration.

- At 72h after injury, substantial numbers of Q-dot-labeled MSC were visible in the injured cornea, but not in the contralateral cornea (FIG 3a, upper panel). To determine if MSC remained detectable in the injured cornea at a later time point, we injected GFP+MSC and evaluated the presence of these cells up to 50 days following injury (FIG 3a, lower panel). At this time point, GFP+MSC were similarly observed only in the injured cornea.
- In order to determine the extent of epithelial regeneration following corneal injury in MSC-injected versus control mice, we used corneal fluorescein staining to determine the extent of the epithelial defect (see Fig 4a in our published article [Ref #8]). A smaller epithelial defect, suggestive of more rapid epithelial regeneration, was apparent by 96h in the MSC-injected mice compared to the injury only group (FIG 3b).
- To characterize the impact of MSC on epithelial regeneration at the molecular level, mRNA expression of both stem cell and differentiated corneal epithelial cell markers [9] was quantified in both MSC-injected and control mice following cauterization (FIG 3c). Corneas from mice receiving MSC showed substantially increased (~ 2-fold) mRNA expression of ABCG2, P63, Hes1 and CEBPσ stem cell markers, as well as K12 and K19 differentiated cell markers when compared to control injury-only mice that had not received MSC.

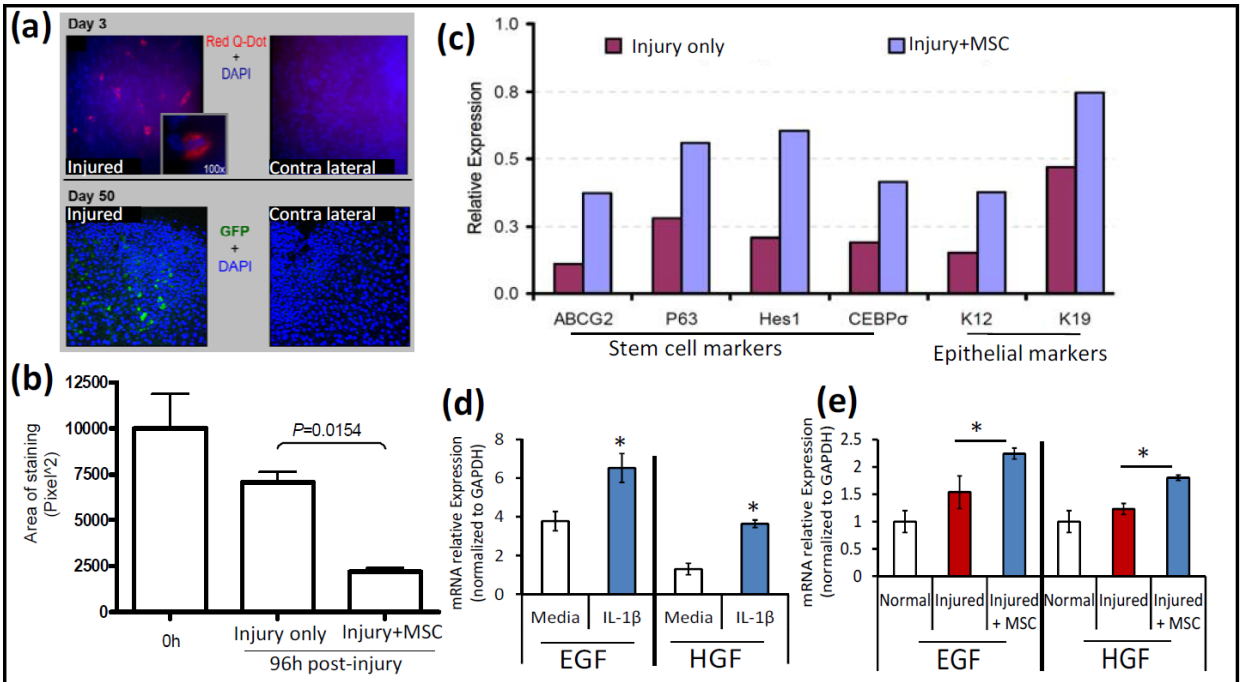

FIG 3. (a) Micrographs showing homing of Q-dot-labeled or GFP+ MSC specifically to injured corneas at Day 3 and Day 50 post-epithelial injury, but not in normal contralateral corneas. **(b)** Quantification of fluorescein staining of injured corneas showing a significantly reduced extent of epithelial defect in MSC-treated injured corneas. **(c)** Real time PCR analysis showing increased expression of both stem cell and epithelial cell markers in MSC-treated injured corneas. **(d)** MSC cultured in the presence of the inflammatory cytokine IL-1β expressed higher levels of growth factors EGF and HGF. **(e)** Injured corneas treated with MSC showed increased expression of EGF and HGF compared to untreated injured or normal corneas. (*p<0.05).

- In addition, we investigated whether administration of MSC can lead to increased expression of epithelial growth factors (e.g. EGF and HGF) [10-12] in the injured cornea. MSC constitutively express both HGF and EGF, and their expression is upregulated in the presence of IL-1β, a pro-inflammatory cytokine known to be present at the ocular surface following injury (FIG 3d). Similarly, injured corneas from MSC-injected mice showed significantly increased expression of these growth factors compared to normal corneas and control injured corneas (FIG 3e).

Together, these finding suggest that (i) MSC not only home to the cornea in response to injury, but also persist at the site of injury for the long term, where they (ii) induce increased expression of epithelial growth factors, and significantly promote corneal epithelial regeneration.

KEY RESEARCH ACCOMPLISHMENTS:

- We standardized the technology for isolation and characterization of murine MSC, and developed mouse models of corneal epithelial injury to study the therapeutic role of MSC.
- Our data demonstrate that corneal injury leads to an increase in the expression of stem cell chemoattractants that can mobilize endogenous MSC into peripheral blood.
- MSC home to the cornea in response to injury, and persist at the site of injury for the long term, where they induce increased expression of epithelial growth factors, and significantly promote corneal epithelial regeneration.

REPORTABLE OUTCOMES:

Manuscript

Lan Y, Kodati S, Lee HS, Omoto M, Jin Y, Chauhan SK. Kinetics and function of mesenchymal stem cells in corneal injury. Invest Ophthalmol Vis Sci. 2012;53(7): 3638-3644. **(Appx. 1)**

Grant

Based on the data derived from this project, an R01 application is submitted to NIH (June 2012 cycle).

CONCLUSION: The present study elucidates the dynamics of MSC trafficking and MSC-mediated regeneration in cornea. These findings provide novel evidence that corneal injury causes significant mobilization of endogenous MSC into blood, and that MSC home specifically to the injured cornea. The demonstration that MSC home to the injured cornea, survive, and promote corneal epithelial regeneration may have therapeutic implications for corneal injuries affecting the limbal stem cell compartment, for which only limited treatment options are available.

REFERENCES:

1. Jiang Y et al. Pluripotency of mesenchymal stem cells derived from adult marrow. Nature. 2002; 418:41.
2. Uccelli A et al. Mesenchymal stem cells in health and disease. Nat Rev Immunol. 2008; 8:726.
3. Horwitz EM et al; International Society for Cellular Therapy. Clarification of the nomenclature for MSC: The International Society for Cellular Therapy position statement. Cytotherapy. 2005;7:393.
4. Dominici M et al. Minimal criteria for defining multipotent mesenchymal stromal cells. The International Society for Cellular Therapy position statement. Cytotherapy. 2006; 8:315.
5. Abbott JD et al. Stromal cell-derived factor-1alpha plays a critical role in stem cell recruitment to the heart after myocardial infarction but is not sufficient to induce homing in the absence of injury. Circulation. 2004;110:3300.
6. Hong HS et al. A new role of substance P as an injury-inducible messenger for mobilization of CD29(+) stromal-like cells. Nat Med. 2009;15:425.
7. Tamai K et al. PDGFRalpha-positive cells in bone marrow are mobilized by high mobility group box 1 to regenerate injured epithelia. Proc Natl Acad Sci USA. 2011;108:6609.
8. Lan Y, Kodati S, Lee HS, Omoto M, Jin Y, Chauhan SK. Kinetics and function of mesenchymal stem cells in corneal injury. Invest Ophthalmol Vis Sci. 2012;53:3638-3644.
9. Chee KY et al. Limbal stem cells: the search for a marker. Clin Exp Ophthalmol. 2006;34:64.
10. Okada H et al. Attenuation of autoimmune myocarditis in rats by mesenchymal stem cell transplantation through enhanced expression of HGF. Int Heart J. 2007;48:6491.
11. Yu Y et al. Antifibrotic effect of hepatocyte growth factor-expressing mesenchymal stem cells in small-for-size liver transplant rats. Stem Cells Dev. 2010;19:903.
12. Amin AH et al. Modified multipotent stromal cells with EGF restore vasculogenesis and blood flow in ischemic hind-limb of type II diabetic mice. Lab Invest. 2010;90:985.

TASK 2: The NALP3 Inflammasome: A Novel Target to Inhibit "Sterile" Destructive Corneal Inflammation (Meredith Gregory-Ksander, Ph.D.)

BODY: The ocular surface is constantly exposed to bacterial pathogens, but is normally highly resistant to infection due to the presence of multiple barriers. However, when these barriers are breached bacterial keratitis can be rapid and aggressive, resulting in significant corneal damage and loss of vision. Corneal epithelial cells defend against infection by (i) serving as a physical barrier to pathogens, and (ii) triggering innate immunity. The innate immune response provides immediate defense against pathogens and serves as a first line of defense against infection. However, if neutrophils persist too long they can mediate non-specific tissue destruction and corneal perforation. Therefore, a better understanding of the triggers of innate mediated inflammation in the cornea will allow us to enhance bacterial clearance, while at the same time limit non-specific tissue destruction and preserve vision. We **hypothesize** that excessive non-specific tissue destruction during the elimination of a pathogen from the cornea is controlled, in part, by the NALP3 inflammasome. Activation of NALP3 in injured and/or stressed cells results in persistent inflammation even after the pathogen is cleared.

We designed 3 aims to test this hypothesis: **Aim 1)** Demonstrate an increased susceptibility to *S. aureus* keratitis in NALP3 deficient mice. **Aim 2)** Demonstrate activation of the NALP3 inflammasome persists after clearance of *S. aureus*. **Aim 3)** Demonstrate inhibition of the NALP3 inflammasome prevents non-specific tissue damage.

Unfortunately, due to a positive MPV test in the UMass animal facility, the NALP3 KO mice required for completion of **Aim 1** had to be re-derived prior to importing them into the Schepens. While we are in the process of rederiving these mice, we were unable to obtain these mice in time to perform the studies in **Aim 1**. However, we believe the results of our studies presented below support the NALP3 inflammasome as a novel target to reduce non-specific corneal damage during inflammation following a wound and/or infection.

The following is a summary of the studies performed as part of **Aim 2)** Demonstrate activation of the NALP3 inflammasome persists after clearance of *S. aureus* and **Aim 3)** Demonstrate inhibition of the NALP3 inflammasome prevents non-specific tissue damage. Using a corneal epithelial debridement wound model, we demonstrate that NALP3 is upregulated in the epithelium of the leading edge of the wound within 1hr (**Figure 1**) and this increased expression precedes the infiltration of neutrophils (**Figure 4**). In an unwounded cornea, NALP3 was constitutively expressed in all epithelial cells except for the most apical layer (**Figure 1A, white arrowhead**). In addition, the NALP3 staining appears to be restricted to the nucleus (**Figure 1A, open arrowhead**). Interestingly, at 1hr post epithelial debridement wound, NALP3 expression is significantly upregulated in the epithelium of the leading edge of the wound (**Figure 1B**). However, the NALP3 expression moved to the cell membrane (**Figure 1B, open arrowhead**) and cytoplasm (**Figure 1B, white arrowhead**). At 48hrs post epithelial debridement, NALP3 remains significantly elevated in the epithelium of the re-epithelialized cornea (**Figure 1C**). The NALP3 expression remains cytoplasmic in the apical epithelial layer (**Figure 1C, white arrowhead**), but returns to the nucleus in the basal epithelial layer (**Figure 1 C, open arrowhead**). The increased expression of NALP3 also correlates with an early neutrophil infiltrate seen at 24hrs post wounding (**Figure 4**).

The second series of studies determined whether upregulation of NALP3 was a critical mediator of wound healing. Using the epithelial debridement wound model, we demonstrate no significant difference in the rate of wound closure in untreated corneas as compared to corneas treated with topical application of a NALP3 inhibitor (Glyburide) (**Figure 2**). By 48hrs post wounding, the epithelium had re-epithelialized in both untreated and Glyburide treated mice (**Figure 2A and 2B**). However, the presence of positive fluorescein staining at 48hrs in untreated eyes (**Figure 2A**), suggests that while the epithelium may have re-epithelialized, the tight junctions have not fully reformed. Interestingly, histologic analysis at 48hrs reveals a much thinner epithelium in untreated corneas (2 cell layers) as compared to the 4 layers of stratified epithelium in the corneas treated with the NALP3 inhibitor (Glyburide) (**Figure 3**). Moreover, the thinner epithelium in the untreated mice is associated with a significant neutrophil infiltrate at 24hrs post wounding, that was greatly reduced following treatment with the NALP3 inhibitor (Glyburide) (**Figure 4**). By 72hrs, however, the corneas of both groups looked healthy, with the multi-layered stratified epithelium. Taken together, these data suggest that blocking the NALP3 inflammasome leads to reduced (but not absent) inflammation, associated with a more efficient restoration of the epithelial barrier. In a setting such as the battlefield, where the threat of infection is high with open wounds, a treatment aimed at accelerating wound healing and restoration of the critical barriers to infection would be highly beneficial.

KEY RESEARCH ACCOMPLISHMENTS:

- We identified the NALP3 inflammsome as a novel target that could be used to (1) reduce non-specific corneal damage during inflammation following a wound and (2) accelerate the restoration of the corneal epithelial barriers to infection.

REPORTABLE OUTCOMES:

A manuscript is currently in preparation.

CONCLUSION: The results of our studies indicate that blocking the NALP3 inflammasome reduces the neutrophil infiltration during corneal wound healing. Moreover, this reduction in innate mediated inflammation correlates with more efficient restoration of the epithelial barriers, critical in protecting against pathogens. Therefore, we propose the NALP3 inflammsome as a novel target that could be used to (1) reduce non-specific corneal damage during inflammation following a wound and (2) accelerate the restoration of the corneal epithelial barriers to infection.

FIGURE 1

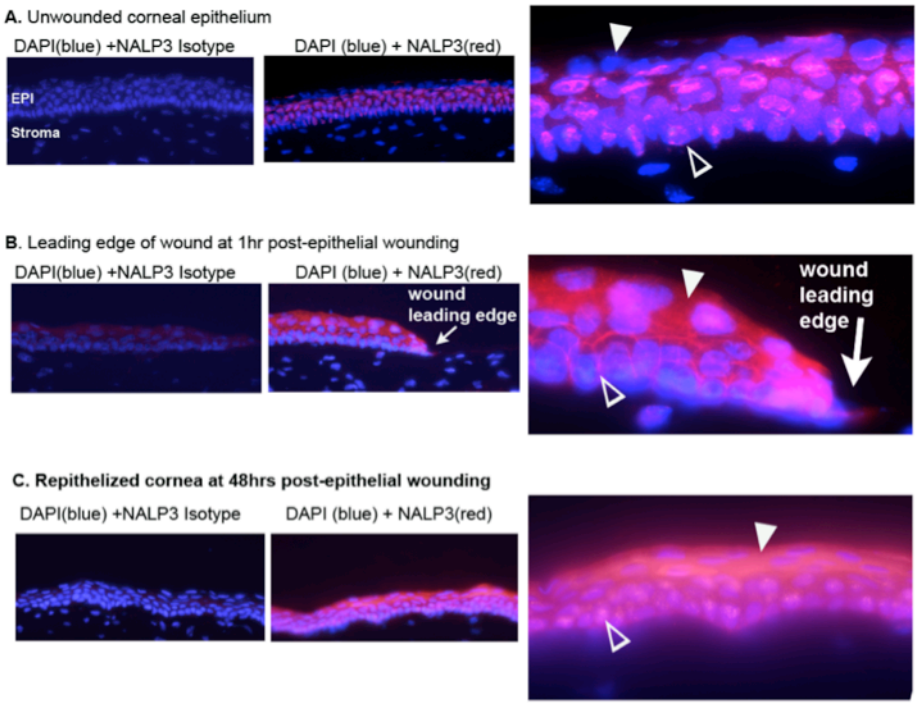

Figure 1. *NALP3 expression in the corneal epithelium following corneal epithelial debridement.* C57BL/6 mice received a corneal epithelial debridement wound and NALP3 expression was determined via immunofluoresence at 0hrs (A), 1hr post wounding (B), and 48hrs post wounding (C). NALP3 = pink, DAPI (nuclear stain)=blue.

Figure 2

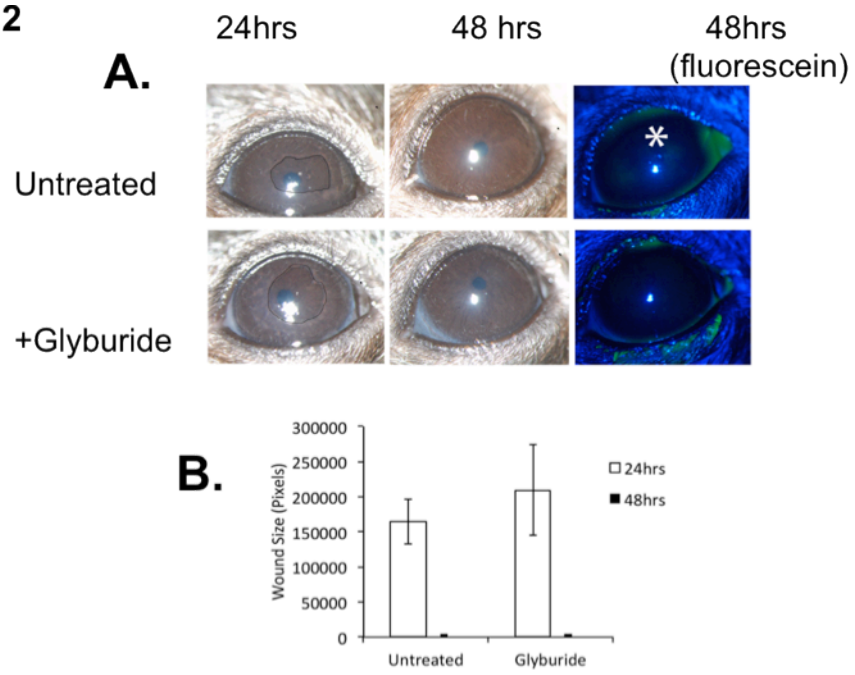

Figure 2- *Rate of wound closure in untreated and Glyburide treated corneas*. C57BL/6 mice received a corneal epithelial debridement wound and received topical application of Glyburide (1ug/5ul PBS) or vehicle control (1xPBS) at the time of wounding and every 24 hrs. Slit lamp microscopy was and fluorescein staining was performed (A) to assess closure of the epithelial wound. ImageJ software was used to analyze the area of the wound at 24 and 48hrs post wounding (B). *= positive fluorescein staining.

Figure 3

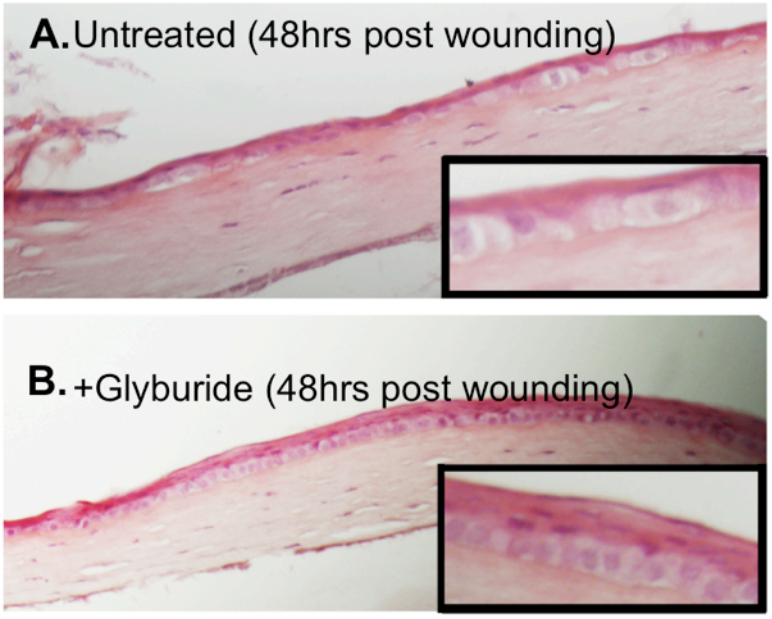

Figure 3- *Stratification of the corneal epithelium at 48hrs post wounding*. C57BL/6 mice received a corneal epithelial debridement wound and received topical application of vehicle control (PBS, untreated) or Glyburide (1ug/5ul PBS) at the time of wounding and every 24 hrs. At 48hrs eyes were enucleated and prepared for H&E staining.

Figure 4

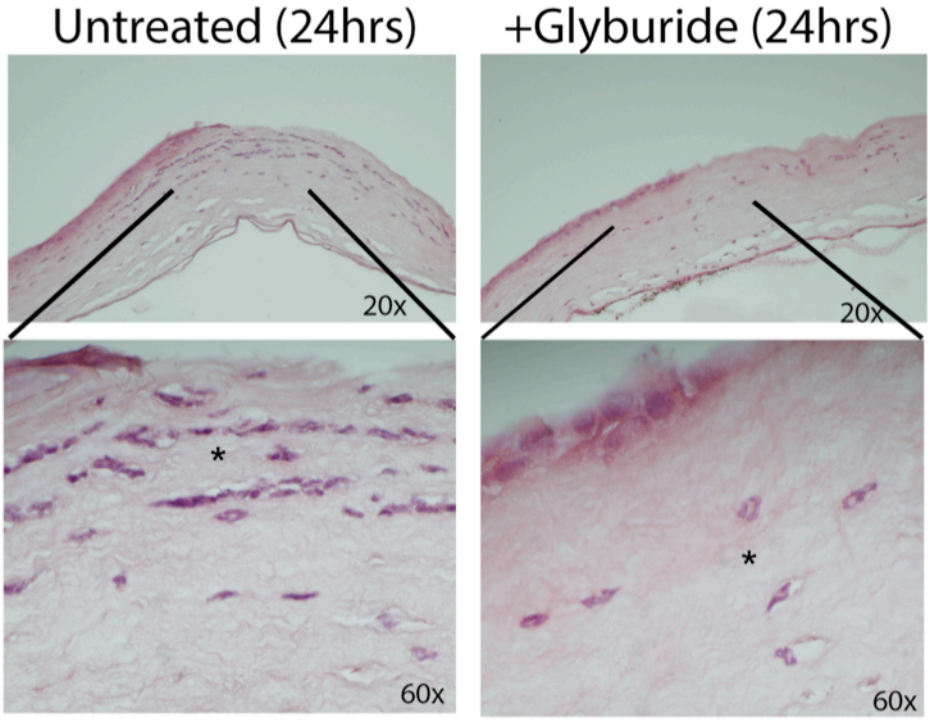

Figure 4- *Neutrophil infiltrate at 24hrs post wounding*. C57BL/6 mice received a corneal epithelial debridement wound and received topical application of vehicle control (PBS, untreated) or Glyburide (1ug/5ul PBS) at the time of wounding and every 24 hrs. At 24hrs eyes were enucleated and prepared for H&E staining. * = presence of neutrophil infiltrate as identified by nuclear morphology.

TASK 3: Association of Thrombospondin-1 polymorphism with predisposition to chronic dry eye after refractive surgery and ocular surface diseases (Sharmila Masli, Ph.D/Darlene A. Dartt, Ph.D.)

BODY: Dry eye is a common problem following refractive surgery such as laser in situ keratomileusis (LASIK) and photorefractive keratectomy (PRK). Perturbation of mucin secreting cells in the conjunctiva results in compromised protection conferred by the mucous layer on the ocular surface leaving eyes vulnerable to environmental assaults including pathogenic stimuli with a consequential inflammation of the ocular surface. Thrombospondin-1 (TSP-1) expressed by epithelial cells of the ocular surface has immunomodulatory properties and is reported as critical for the ocular immune privilege. Absence of TSP-1 expression in mice is associated with development of ocular surface inflammation. Therefore we sought to determine if polymorphism in TSP-1 gene in human subjects is associated with ocular surface inflammation.

To address this aim we used impression cytology samples collected from 140 patients (70 males and 70 females) in the age group 20-40 years. Conjunctival impression cytology (CIC) samples were processed to harvest DNA. Upon quantitation samples (total 133) that generated adequate

DNA (5-10 ng/ml) were genotyped for 5 TSP-1 SNPs - rs2228262 (SNP-1), rs2228261 (SNP-2), rs2292305 (SNP-3), rs1478604 (SNP-4) and rs3743125 (SNP-5) using Sequenom iPLEX Gold platform at Molecular Genetics Core, IDDRC.org of Children's Hospital Boston and Harvard Medical School. Genotyping frequency of selected 5 TSP-1 SNPs were above 75%. For DNA samples included in the association analysis call rates were >85%. Each of the genotyped SNP was tested for Hardy Weinberg equilibrium (HWE). A HWE test value of 0.0023 for SNP-5 suggested a potential departure from Hardy Weinberg Equilibrium ($p< 0.01$) and therefore was excluded from further association analysis. Ancestry informative markers (AIMs) were also genotyped to control for possible population stratification. These included 90 SNPs selected to be maximally informative for differentiating between continental groups based on Hapmap Phase I populations (Caucasians = CEU, Hans Chinese from Beijing = CHB, Japanese from Tokyo = JPT and African from Yoruba tribe of Ibadan, Nigeria = YRB). Genomic inflation factor lamda (l) was calculated from 90 SNPs. Allele frequency divergence among populations is provided in Table-1. The genomic control inflation factor (l) for the population included in this study was less than 1.0 indicating absence of any population stratification and eliminating any need for correcting any test statistics generated in this study. Association studies for each of the selected TSP-1 SNP were performed and results of the allelic analysis are provided in Table-2.

The TSP-1 rs2228262 (SNP-1) G allele was found in 19% of dry eye as well as control group subjects. The TSP-1 rs2228261(SNP-2) T allele or rs2292305(SNP-3) G allele was found in 39% of dry eye patients as against 25% of control subjects ($p=0.0485$, OR1.9, 95% CI 1.1-3.5). These results suggested an increased probability of developing dry eye in subjects with rs2228261 and rs2292305 SNPs of TSP-1. However, allelic analysis of these two SNPs did not result in statistically significant association with dry eye. We noted that TSP-1 rs1478604 (SNP-4) C allele carriers (CT or CC) in dry eye group were 63% as against 44% in control group ($p= 0.003$, OR 2.5, 95% CI 1.4-4.5). Our results indicate statistically significant evidence for association between TSP-1 rs1478604 (SNP-4) and development of dry eye post-refractive surgery.

KEY RESEARCH ACCOMPLISHMENTS:

- Association of TSP-1 SNP with development of dry eye after LASIK or PRK

REPORTABLE OUTCOMES:

Manuscript (under preparation)
Planned submission in 2013 for the renewal of NEI R01 funding to Dr. Dartt

CONCLUSION:

Significant association of TSP-1 SNP with development of dry eye has a potential application as a screening tool to identify individuals predisposed to a risk of chronic ocular inflammation, dry eye and associated complications after refractive surgery. Future studies can be directed towards developing preventive therapeutic strategies that will help avoid such inflammatory complications post-refractive surgery.

SUPPORTING DATA:

Table-1: Allele frequency divergence among populations

	YRI	JPT/CHB	CEU
YRI	-	0.4437	0.4856
JPT/CHB	0.4437	-	0.237
CEU	0.4856	0.237	-

Table-2: Allelic Analysis

rs2228262 (SNP-1): A -> G

Allele	Dry Eye (n=59)	Control (n=16)	OR (90% CI)	p
A	106	29		
G	12	3	1.1 (0.4 – 3.3)	> 0.05

rs2228261 (SNP-2): C -> T

Allele	Dry Eye	Control	OR (90% CI)	p
C	90	28		
T	28	4	2.2 (0.8 – 5.6)	> 0.05

rs2292305 (SNP-3): A -> G

Allele	Dry Eye	Control	OR (90% CI)	p
A	90	28		
G	28	4	2.2 (0.8 – 5.6)	> 0.05

rs1478604 (SNP-4): T -> C

Allele	Dry Eye	Control	OR (90% CI)	p
T	58	23		
C	50	7	2.8 (1.3 – 6.2)	*< 0.05

Statistical comparison with Fisher's exact test.

TASK 4: Prevention of Corneal Scarring by Application of 3-D Self-assembled Corneal Matrix (James Zieske, Ph.D.)

BODY:

This pilot project proposes to test the novel hypothesis that placement of a "scaffold" into a wound site will promote scar-free healing.

BACKGROUND: Even with the increasing use of protective goggles, the cornea is still a major site of military injuries. These injuries include massive damage to the cornea, which require major reconstruction of the eye, resulting in corneal scarring and loss of vision. It is generally accepted that severe corneal wounds will heal with a scar and that the cornea has little ability to regenerate itself in a scar-free manner. However, one of the intriguing findings of current research into producing an artificial cornea is that the cornea may have more ability to remodel than was generally thought. These studies have shown that placement of a "corneal construct" in some wound situations results in healing of the cornea with minimal scarring and a resulting clear cornea. These studies, primarily the work of Dr. May Griffith's group, have shown that placement of a corneal substitute, consisting of cross-linked collagen, on the wound, resulted in the remodeling of the corneal substitute and a far clearer cornea than if the wound was allowed to heal without intervention. Our laboratory has similar results in experiments where we placed a self-assembled corneal construct into a mouse cornea and observed an optically clear cornea in a wound model that normally would result in scarring. These results suggest that placing a template into a wound site of a wound model that would normally result in scars stimulates remodeling of the cornea in a clear manner. If this observation is correct, it has the potential to lead to a new therapeutic option where a temporary scaffold could be placed in a wound to promote regeneration of the cornea without scarring.

Technical objectives - We have previously published a technique to culture human corneal fibroblasts (HCF) in a stable form of ascorbic acid (sAsc) that stimulates the cells to stratify and assemble matrix in a manner that resembles the developing corneal stroma. We propose to generate self-assembled corneal constructs and transplant them into a mouse model of corneal repair. In this model, superficial lamellar keratectomies will be performed in the mice and a corneal construct will be placed in the wound area. The construct will be permanently attached to the wound site by "painting" the wound site with rose bengal followed by irradiation with a green laser. This results in a photoactivation of the chemical to link the collagen in the wound bed with the collagen in the transplant. The Specific Aims are to 1) determine if placement of a self-assembled corneal construct into a wound promotes scar-free healing and 2) determine if placement of a cell-free matrix will promote healing.

METHODS:

Primary Culture of Human Corneal Fibroblasts: Human corneas will be obtained from the National Disease Research Interchange (NDRI; Philadelphia, PA). Corneal epithelium and endothelium will be removed from the stroma by scraping with a razor blade. The stromal tissue will be cut into small pieces (~2x2mm) and put into 6-well plates (4 or 5 pieces per well). Explants will be allowed to adhere to the bottom of the wells and Eagle's Minimum Essential Medium (EMEM: ATCC; Manassas, VA) containing 10% fetal bovine serum

(FBS: ATCC) will be added. After 1-2 weeks of cultivation, the fibroblasts are passaged into a 100mm^2 cell culture plate. The cells are grown to 100% confluency before their use in the culture system.

Fibroblast Assembled Extracellular matrix: The HCF will be plated on Transwell 6-well plates containing polycarbonate membrane inserts with 0.4μm pores (Costar; Charlotte, NC) at a density of 10^6 cells/ml. Fibroblasts will be cultured in EMEM with 10% FBS and 0.5mM 2-O-α-D-glucopyranosyl-L-ascorbic acid (sAsc: Wako Chemicals USA, Inc.; Richmond, VA).

Collagen based matrix: Two ml of Type I bovine dermal collagen (PureCol. Inamed Corp, Fremont, CA) will be added to 0.2ml of 10x EMEM. The collagen solution will be poured into a well, and allowed to set for 1 hour at 37°C.

Transplantation: We will generate HCF self-assembled constructs, as described above, and transplant them into the corneas of BALB/c mice. The constructs will be developed, as described above, transferred and transplanted using an onlay method. In brief, the constructs will be pre-labeled with Fluorescein Dichlorotriazine (DTAF: Invitrogen; Carlsbad, CA) for 2 days before transplantation. A 1.5-mm superficial keratectomy will be performed, removing the epithelium, basement membrane and anterior portion of the stroma. The exposed corneal stroma will be dried with a surgical sponge (Medical Technologies; North Stonington, CT), and Rose Bengal (0.05%) will be painted on the stroma. After 1 minute, a 2mm^2 construct will be placed on the exposed corneal stroma and irradiated with a green laser (Wicked Lasers; Shanghai, China) for 180 seconds. The construct will be tested for attachment by scraping with forceps. Three surgical controls will be used: 1) Contralateral eyes—no wound; 2) Keratectomy only—surgery but no construct or laser applied, and 3) Sham—surgery with laser applied but no construct. In initial experiments a one-week time point was examined.

RESULTS:

Experiment set 1 – In the first series of experiments, a collagen matrix was transplanted into the wound in Balb/C mice. Keratectomy wounds (1.5mm diameter) were created and a 2mm diameter collagen construct was placed on the cornea as described in Methods. Three groups were examined: Sham control, Keratectomy only and Transplant. Corneas were examined at one week using a slit lamp. In addition, corneas were excised and cryostat sections were analyzed for the presence of the construct and overall healing. No obvious difference was seen between the three groups in the slit lamp exam. No consistent difference was observed between groups regarding quality of healing. Technical problems – 1) The collagen constructs were very difficult to place on the wound area without wrinkling. 2) The constructs appeared to dehydrate when the laser was applied. 3) Constructs could not be identified one week after transplant.

Experiment set 2 – In the second set of experiments, a self-assembled fibroblast matrix was used. Protocol was the same as set 1 except that the laser was applied for one minute rather than three. Slit lamp examination appeared to show that the corneas receiving transplants were clearer than the corneas receiving only wounds. Upon evaluation of corneal sections, however, no consistent difference was observed between any of the groups. In addition, it could not be determined if transplants were still in place after one week. Technical problems - 1) The transplants were not clearly labeled by the DTAF. 2) It could not be determined if

the transplant was maintained after one week. 3) The construct appeared to be dehydrated by the laser treatment.

KEY RESEARCH ACCOMPLISHMENTS:

- We have developed a technique to evaluate effect of transplant of a construct.
- Preliminary data are inconclusive regarding the hypothesis that transplant of a scaffold promotes scar-free healing.

REPORTABLE OUTCOMES: - none to date

CONCLUSION: The project was not begun until January 2012 when ACURO approval was received for animal usage. We have also identified several technical problems that have made evaluation of the results difficult. We will continue experiments and analysis for the next three months.

TASK 5: Repair of Conjunctival Injury with Bioengineered Tissue: The First Step to Eyelid Repair (Darlene A. Dartt, Ph.D.)

BODY: Our statement of work was: To begin reconstruction of the eyelid we propose to construct conjunctival equivalents containing goblet, stratified squamous, and undifferentiated cells grown on biocompatible scaffolding that can be used to repair the injured conjunctiva. We proposed the following aims:

Specific Aim 1- Fabricate polymeric scaffolding; **Specific Aim 2**- Determine which types of scaffold polycaprolactone, electrospun collagen, or poly(vinyl alcohol)/collagen induce the optimum cell growth and viability of: 1) mixed goblet and stratified squamous cells and 2) undifferentiated cells.

Specific Aim 1: Our collaborator Dr. Gary Wnek fabricated five different scaffolds by electrospinning. They were poly(vinyl alcohol) (PVA), poly(acrylic acid) (PAA), polycaprolactone (PCL), collagen (Coll), and two composites: 1. 80% poly acrylic acid and 20% poly(lactic-co-glycolic acid (PAA/PLGA) and 2) 20% polycaprolactone and 80% collagen (Coll/PCL).

Specific Aim 2: Human conjunctival tissue was obtained from the Heartland Lions Eye Bank in Kansas City, Missouri, in collaboration with Dr. Wendell Scott. We began our studies by focusing on goblet cells and used media that supported their growth. We grew human conjunctival goblet cells from tissue pieces on glass coverslips as a positive control and the fabricated scaffolds. We found that conjunctival goblet cells did not survive well on PCL and PVA, but did survive and grow on PAA and polyethanolamine (PET) that is tissue culture plastic. From these experiments we concluded that human conjunctival goblet cells prefer negatively charged surfaces. We compared cell growth on the different types of scaffolds by determining outgrowth by bright field microscopy and cellular viability by confocal microscopy using a commercial live/dead stain. We found an increase in outgrowth relative to explant size after 13-15 days of culture of 7.1 (PAA, n=2), 2.3 (PCL, n=4) and no

outgrowth for PVA. The percentage of viable cells after 11-15 days was 9% (PCL, n=5), 89% (PAA, n=5), 89% (PET, n=2), 94% (collagen, n=1) and 0% (PVA, n=3).

We also tried 100% collagen scaffolds that are technically very difficult to fabricate. Although we obtained promising results in terms of outgrowth (3.7 fold) and cellular viability (94%), these membranes were very fragile and not practical for clinical use. We also tried the Coll/PCL mixture that was mechanically stronger, but this scaffold did not improve cell growth.

A modification of the somewhat fragile PAA scaffold was used. The PAA/PLGA composite did not improve cell viability after culture.

We also tried ultrathin PCL (not electrospun), fibronectin-coated PCL, NaOH treated PCL, and collagenase-digested tissue seeding (single cell suspension). None of these scaffolds or methods improved cell outgrowth.

We conclude that the best scaffold that we have tried for culture of human conjunctival epithelial cells is PAA. As it is fragile, in the future we will continue to work with Dr. Wnek to increase the mechanical strength of this material. We will also add growth factors and RGD peptides to improve cell growth. Finally, we will use immunohistochemistry to determine the percentage of cell type of conjunctival epithelium (goblet, stratified squamous, or undifferentiated) present.

KEY RESEARCH ACCOMPLISHMENTS:

- We have identified the optimal technique for the culture and analysis of human conjunctival cells on electrospun polymeric scaffolds.

- We found an increase in outgrowth relative to explant size after 13-15 days of 7.1 (PAA, n=2), 2.3 (PCL, n=4) and no outgrowth for PVA.

- The percentage of viable cells after 11-15 days was 9% (PCL, n=5), 89% (PAA, n=5), 89% (PET, n=2), 94% (collagen, n=1) and 0% (PVA, n=3).

- Of these materials, PCL has the greatest mechanical strength. PAA and collagen need modifications for improved mechanical strength before they can be used for transplantation.

- In one experiment on PCL, large numbers of goblet cells were present in a few localized areas, scattered among many DAPI-positive cells of presumed epithelial origin.

- Composite scaffolds made of PAA/PLGA and Collagen/PCL were not superior to the pure PAA and collagen scaffolds in terms of cellular compatibility.

- An ultrathin continuous PCL membrane was not superior to the electrospun PCL membrane in terms of cellular compatibility.

- Dipcoating PCL with the extracellular matrix protein fibronectin was not superior to the non-dipcoated PCL in terms of cellular compatibility.

REPORTABLE OUTCOMES: We are planning to submit an abstract for ARVO 2013 and will prepare a manuscript for submission.

CONCLUSION: We have successfully fabricated five variations of polymeric scaffolds and developed a method for their use in human conjunctival cell culture, by seeding them with conjunctival tissue explants. We have developed methods to analyze the effect of the scaffolds on conjunctival cellular viability (by confocal laser scanning microscopy), outgrowth (by epifluorescent microscopy) and phenotype (by immunocytochemistry).

We conclude that PAA is the best scaffoled for growth of human conjunctival epithelial cells. But, we will also continue to modify collagen along with PAA for further improvements. Since these scaffolds are extremely fragile, we will improve the mechanical strength to properly match these scaffolds and the native conjunctival tissue.

TASK: 6: The Role of Shear Stress-Induced Endomucin in Leukocyte-Endothelial Cell Interactions (Patricia A. D'Amore, Ph.D.)

BODY: The goal of this project was to test the hypothesize that under normal, non-inflammatory conditions endomucin plays a role in preventing interactions between leukocytes and ECs of postcapillary venules. We had proposed to test this hypothesis with two aims: (1) To investigate the role of endomucin in the maintenance of a non-inflammatory endothelial phenotype; and, (2) To examine the effects of shear stress on endomucin expression by human umbilical vein endothelial cells (HUVEC) in vitro. We have completed the studies that were proposed for both of these aims.

Aim 1: To investigate the role of endomucin in the maintenance of a non-inflammatory endothelial phenotype.

We demonstrated that endomucin was localized on the luminal surface of veins but not arteries. The localization of endomucin on the apical surface of venous endothelium together with its biochemical characteristics suggested a possible role in cell-cell interactions in the endothelium and we speculated that endomucin might be playing a role in the maintenance of the non-inflammatory state.

To examine its functional role we employed a tissue culture model of neutrophil adhesion in which a parallel plate flow chamber was utilized to study the interactions between human neutrophils and human umbilical vein endothelial cells under shear stresses found in the post-capillary venous endothelium. Endomucin was depleted using siRNA; siRNA against endomucin led to an 80% reduction in endomucin protein **(Figure 1).** There was a 4, 5, and 2-fold increase in neutrophil-endothelial cell interactions at low shear stringency, 0.5, 0.75, 1.0 dynes/cm^2, respectively, whereas the scramble control siRNA had no effect **(Figure 2).**

These data demonstrate that under non-inflammatory conditions endomucin blocks neutrophil interactions with the endothelium.

Because human umbilical vein endothelial cells express basal levels of adhesion molecules, we examined whether knockdown of endomucin affected expression of E-selectin, VCAM-1, and ICAM-1. Fluorescent activated cell sorting (FACS) analysis of these adhesion molecules revealed no change in their expression. We did note a higher level of ICAM-1 relative to E-selectin and VCAM-1 in non-activated endothelial cells is consistent with previous reports. In light of these observations, we speculated that the down regulation of endomucin was enabling neutrophil interactions with the endothelium via the constitutively expressed endomucin. To test this, we pre-treated neutrophils with neutralizing antisera against LFA-1 (20 mg/ml) and then allowed to interact under shear stress with human umbilical vein endothelial cells in which endomucin had been knocked down. Results revealed that blocking the interaction of neutrophils with ICAM-1 reduced neutrophil-endothelial cell interactions by more than 60% at shear stress of 1.0, 0.75 and 0.5 dynes/cm^2 **(Figure 3).**

Aim 2: To examine the effects of shear stress on endomucin expression by human umbilical vein endothelial cells in vitro.

The localization of endomucin on the surface endothelium of veins and capillaries and not arteries led to a consideration of how this sialomucin might be regulated. Veins, post capillary venules and arteries are exposed to different fluid shear stresses. It is well established that fluid shear stress in post capillary venules is low compared to arteries to allow for the recruitment of leukocytes into inflamed tissues and increasing shear stress prevents the efficient binding of leukocytes Thus, we hypothesized that endomucin expression was regulated by shear stress.

We hypothesized that the levels of endomucin mRNA and protein would be down regulated by arterial shear stress compared to static cultures. Human umbilical vein endothelial cells were exposed for 24 hr to shear stresses of 10 dynes/cm^2 and 1.5 dynes/cm^2, to model arterial and venous shear stress, respectively.

Real-time PCR analysis of RNA isolated from human umbilical vein endothelial cells exposed to arterial shear stress for 24 hr revealed a 50% reduction in the levels of endomucin mRNA compared to static control cells. In contrast, endomucin mRNA levels in human umbilical vein endothelial cells exposed to venous shear stress for 24 hr was unaffected compared to static control cells (Figure 4).

Given that endomucin is localized to the apical endothelial surface, we were interested in determining how shear stress effects cell surface protein biosynthesis. Cell surface expression of endomucin was determined by biotinylation of Human umbilical vein endothelial cells after exposure to shear stress for 24 hr. Consistent with the reduced levels of mRNA, cell surface endomucin was reduced by approximately 50% in human umbilical vein endothelial cells exposed to arterial shear stress, whereas venous levels of shear stress did not influence the surface levels endomucin in human umbilical vein endothelial cells.

KEY RESEARCH ACCOMPLISHMENTS:

- Demonstrated production of endomucin by bovine aortic and human umbilical veins endothelial cells at the level of mRNA by PCR and protein by western blot analysis.
-
- Demonstrated that endomucin is localized to the surface of endothelium in vivo at the level of light microscopy using confocal immunofluorescent microscopy and biochemically using biotinylation followed by western blot analysis.

- Shown that shear stress characteristic of the arterial tree (10 dynes/cm2) suppresses the expression of endomucin by endothelium at the level of mRNA and protein whereas venular shear stress (1.5 dynes cm2) has no effect.

- Shown that the suppression of endomucin by arterial shear stress is mediated by KLF2. Real-time PCR analysis of EMCN-1 expression in Ad-Ctrl vs. Ad-KLF2 infected HUVEC revealed a down regulation of endomucin when KLF2 was over expressed. Similarly, siRNA knockdown of KLF2 followed by exposure to shear stress did not lead to suppression of endomucin mRNA levels.

- Demonstrated the role of endomucin in the maintenance of the endothelial non-inflammatory surface by using siRNA.

REPORTABLE OUTCOMES:

Alisar Zahr, Pilar Alcaide, Jinling Yang, Alexander Jones, Nathaniel G. dela Paz, Sunita R. Hett, Bruce Ksander, Magali Saint-Geniez, Pablo Argüeso and Patricia A. D'Amore, A critical role for endomucin-1 in suppressing leukocyte-endothelial cell interactions, manuscript in preparation.

CONCLUSION:

Post-capillary venous endothelium is the primary site of leukocyte extravasation during inflammation. A primary function of the endothelium is to maintain an anti-adhesive, non-inflammatory surface by regulating and inhibiting coagulation, and by resisting the adhesion of blood leukocytes. A majority of the work conducted to understand the molecular regulation of leukocyte-endothelial interactions has focused on adhesion molecules responsible for recruitment of blood leukocytes to an activated endothelium. Much less attention has been directed to investigation of anti-adhesive molecules that comprise the endothelial cell surface barrier, the glycocalyx. Our observations introduce the novel paradigm that the down regulation of anti-adhesive molecules may be as important in transforming the endothelial cell surface to a pro-inflammatory state as the elevation in adhesive molecules. Moreover, our in vivo results provide an exciting new therapeutic option for the manipulation of the inflammatory process.

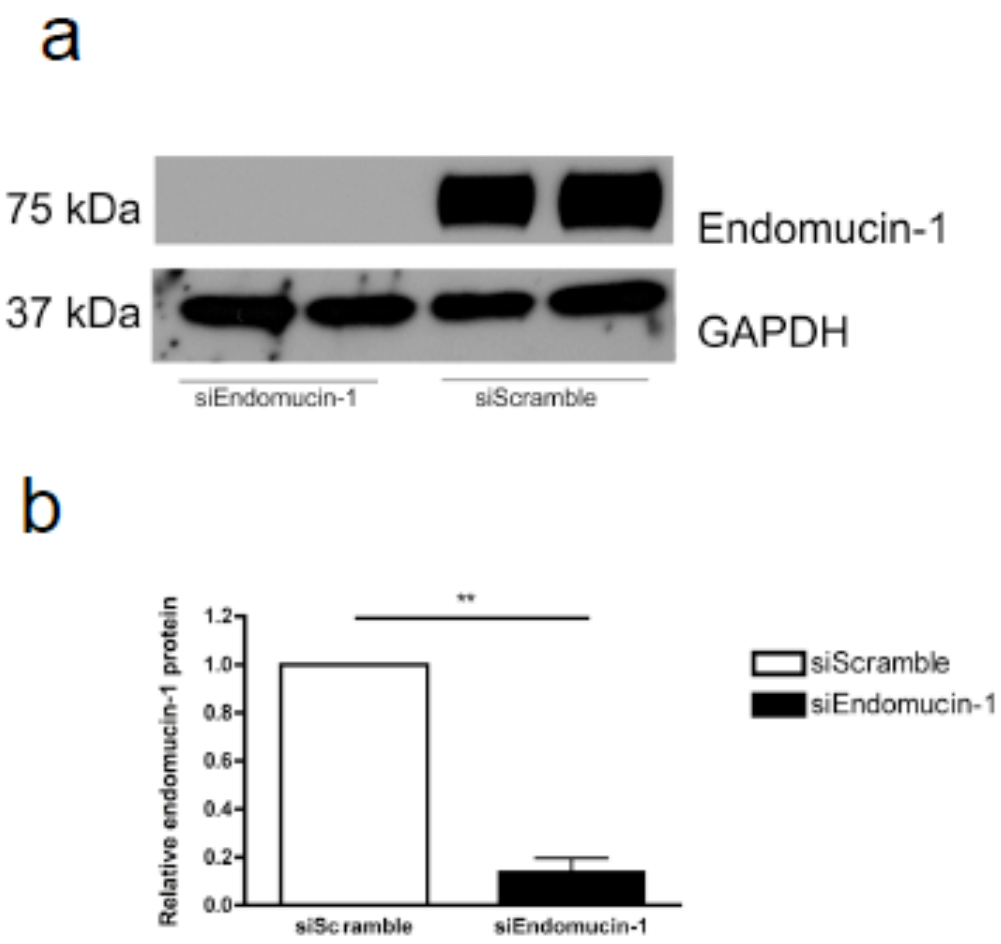
a
75 kDa
Endomucin-1
37 kDa
GAPDH
siEndomucin-1
siScramble
b
Relative endomucin-1 protein
1.2
1.0
0.8
0.6
0.4
0.2
0.0
**
siScramble
siEndomucin-1
siScramble
siEndomucin-1

Figure 1

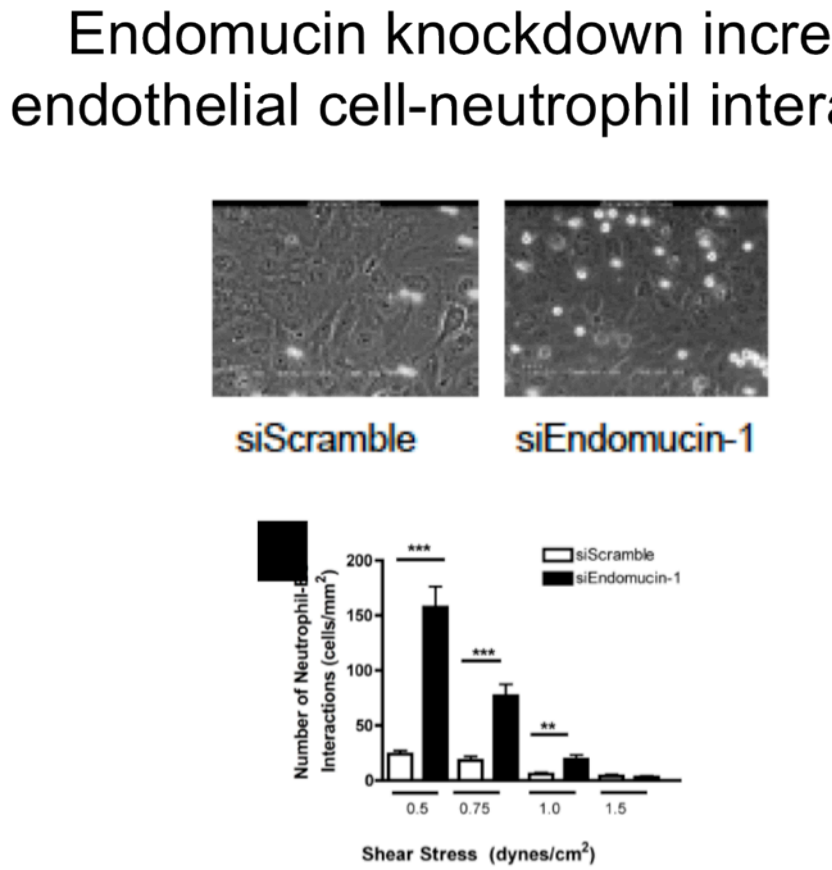

Figure 2

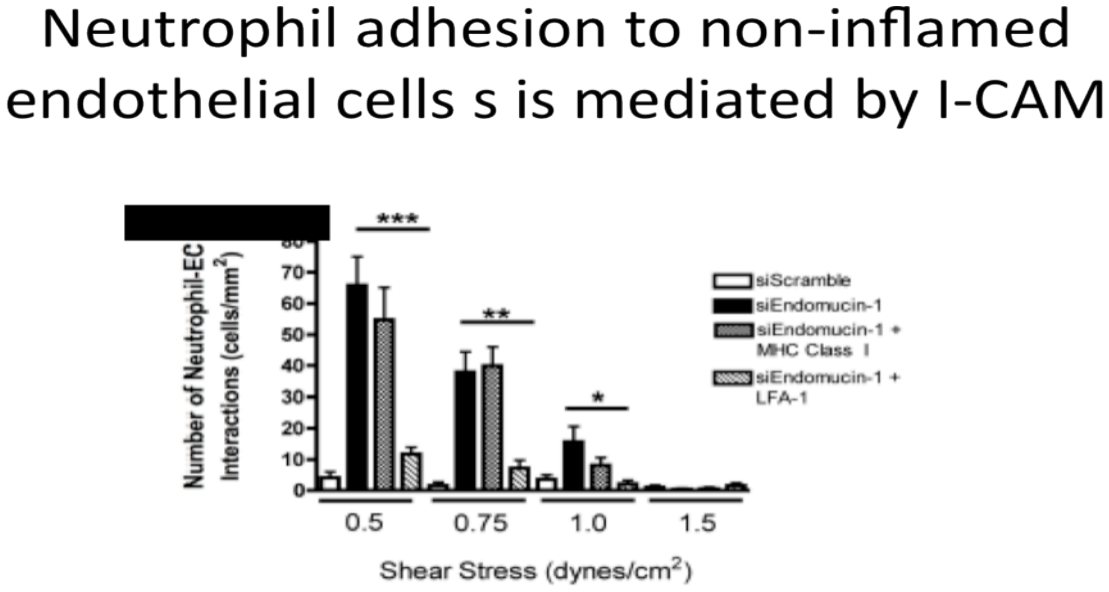

Figure 3

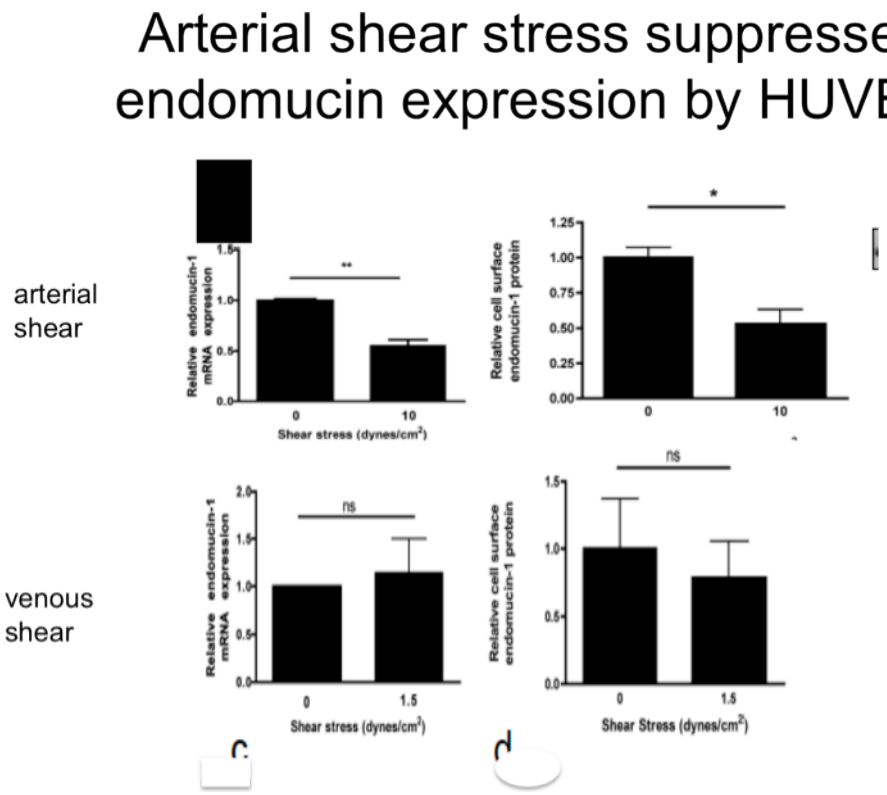

Figure 4

TASK 7: The Role of Endogenous Inhibitors of PDGF Receptors in PVR (Andrius Kazlauskas, Ph.D.)

BODY:

In the first 3 quarters we completed the first aim (Test if agents that neutralize VEGF protect rabbits from developing PVR) and made substantial progress on the second aim ("Determine if neutralizing VEGF in vitreous from PVR patients reduces its PVR potential"). In the fourth quarter we completed the second aim as outlined below.

We completed our biochemical analysis of human PVR vitreous by testing if anti-VEGF (ranibizumab) blocks human PVR vitreous-driven signaling events and cellular responses in primary retinal pigment epithelial cells isolated from a human PVR membrane[1]. As shown in **Fig 1A**, α-VEGF reduced HV-PVR-mediated activation of PDGFRα and the subsequent set of signature signaling events. Furthermore, α-VEGF attenuated the ability of HV-PVR to induce cellular events associated with PVR such as contraction **(Fig 1B)** and survival **(Fig 1C).**

Neutralizing PDGFs (by adding PDGF TRAP) eliminated this observed effect of α-VEGF, while increasing the concentration of PDGF had the same effect as α-VEGF (Fig 1A). As observed for the signaling events, PDGF TRAP mitigated the α -VEGF effect on these cellular events, whereas increasing the level of PDGF mimicked it (Fig 1B-C). These findings are similar to the results with RV-PVR (data shown in the second quarterly report) and indicate that VEGF-A potentiates the PVR potential of HV-PVR due to the VEGF-A/PDGF/non-PDGF relationship. Put another way, α-VEGF diminished the ability of HV-PVR to stimulate signaling events and cellular outcomes associated with PVR by de-repressing vitreal PDGFs.

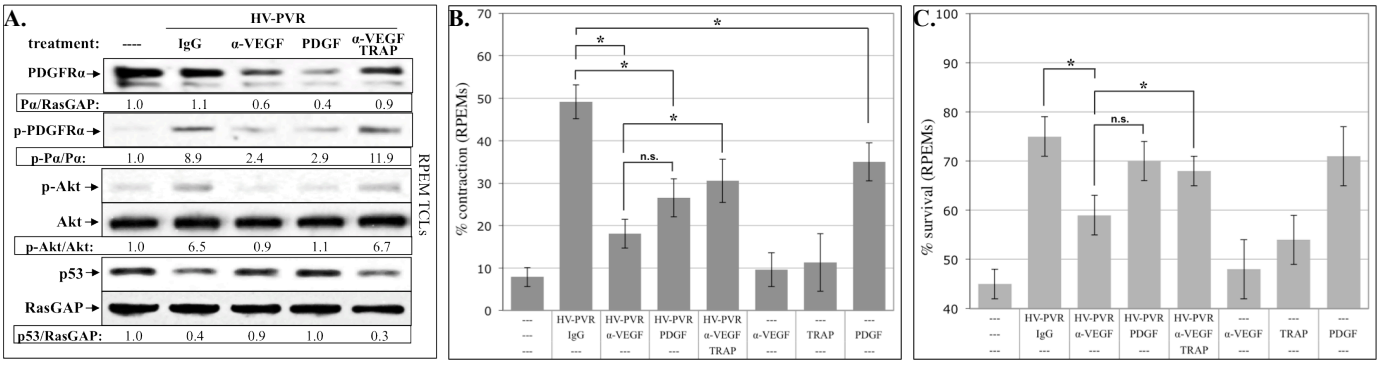

Figure 1. Neutralizing VEGF-A in human PVR vitreous prevented PVR-associated signaling events and cellular outcomes in RPE cells isolated from a human PVR membrane. (**A**) Neutralizing vitreal VEGF-A prevented PVR vitreous-driven signaling events. PVR membrane-derived RPE cells (RPEMs) were serum starved overnight and either lysed immediately (----), or treated for 48 h with human PVR vitreous (HV-PVR, 400 ul) supplemented with non-immune IgG (10 ug/ml), neutralizing anti-VEGF antibody (Ranibizumab, 25 ug/ml), PDGF-A (20 ng/ml), or a combination of anti-VEGF (10 ug/ml) and PDGF-Trap (TRAP, 2 uM). Following treatment, cells were lysed and the resulting total cell lysates (TCLs) subjected to western blot analysis using the indicated antibodies. Results were quantified and ratios representing normalized band intensities are shown under each immunoblot. Blots shown are representative of three independent experiments. **(B)** Neutralizing vitreal VEGF prevented PVR vitreous-driven cell contraction. RPEMs were pre-conditioned for 48 h with either serum-free medium alone (---), or HV-PVR (400 ul) supplemented with non-immune IgG (10 ug/ml), anti-VEGF (25 ug/ml), anti-VEGF + TRAP (2 uM), or PDGF-A (20 ng/ml). Controls included cells pre-conditioned with anti-VEGF, TRAP, or PDGF-A alone. Following pre-conditioning, cells were subjected to the collagen gel contraction assay. Data represents % contraction of collagen gels measured after 72 h; and shows mean % contraction ± standard deviations (SD) obtained for three independent experiments (*, $P < 0.05$ using a paired t test). **(C)** Neutralizing vitreal VEGF prevented PVR vitreous-driven cell survival. Near-confluent RPEMs were placed in starvation medium (DMEM without serum) for 72 h as an inducement of apoptosis, during which time they were conditioned with the same treatments as described in B. At 72 h, surviving cells were quantified as those cells whose nuclei failed to stain positive for apoptosis by TUNEL assay. The graph presents data from three independent experiments showing the mean percentage of cells (± SD) surviving starvation (*, $P < 0.05$ using a paired t test). These data demonstrate that VEGF-A promotes the mode of PDGFRα activation that drives signaling events and cellular responses that are associated with PVR.

In addition, we determined whether vitreal VEGF-A and/or PDGF is a potential biomarker for PVR susceptibility. Analysis of VEGF-A and PDGF levels in vitreous from 32 patients with PVR showed that samples either had low or high levels of both VEGF-A and PDGFs (Fig 2).

This makes sense, since either scenario will be permissive for non-PDGFs to activate PDGFRα. While the majority of vitreal samples had low levels of both VEGF-A and PDGFs, when PDGFs were present, there was also a matched amount of VEGF-A. These observations indicate that the ratio of vitreal VEGF-A/PDGF correlates with clinical PVR and thus is a potential biomarker for PVR susceptibility.

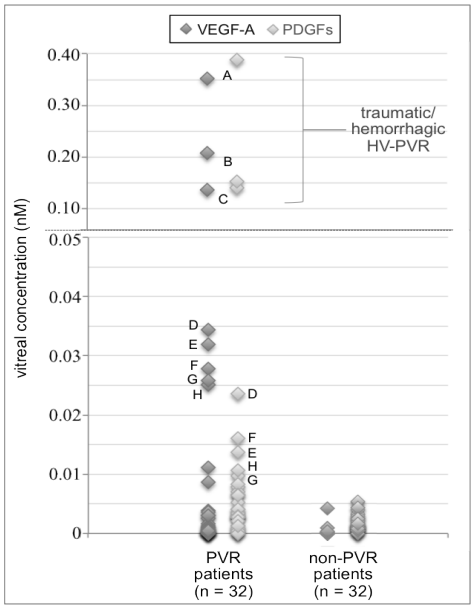

Figure 2. Comparison of VEGF-A and PDGF levels in the vitreous of patients with or without PVR. Vitreous from patients with PVR or non-PVR retinal diseases (macular holes or macular puckers) was subjected to multiplex analysis to determine the concentration of VEGF-A and PDGFs (total of A, AB, and B isoforms). While 94% of PVR samples had a detectable level of VEGF-A, the same was true for only 34% of non-PVR samples. Molar amounts of VEGF-A and PDGFs in each sample were frequently detected at similar levels – symbols labeled with the same letter are the same sample. The majority had low levels of both, whereas when PDGFs were present, there was also a matched amount of VEGF-A. These observations indicate that the ratio of vitreal VEGF-A/PDGF correlates with clinical PVR and is a potential biomarker for PVR susceptibility.

An exciting future direction is to further develop the biomarker concept. Measuring the ratio of PDGF/VEGF is not able to accurately predict which patients will progress to PVR because the ratio is comparable for the majority of both types of patients (Fig 2). Considering other forms of PDGFs, such as PDGF-C, which abounds in vitreous of patients with PVR [2], may lead to a better marker for PVR susceptibility.

KEY RESEARCH ACCOMPLISHMENTS:

- VEGF-A promotes PVR-associated signaling events and cellular outcomes by inhibition of direct activation of PDGFRα
- Ranibizumab, an FDA-approved VEGF-A neutralizing agent, efficiently and effectively protects rabbits from developing PVR
- VEGF promotes the PVR potential of vitreous from patients with PVR
- The VEGF/PDGF ratio in human vitreous is a potential biomarker for PVR potential

REPORTABLE OUTCOMES:

The data obtained in the course of this project were the basis for a recently submitted R21 proposal to the NIH entitled "Can FDA-approved agents protect from PVR?".

CONCLUSIONS:

Altering the growth factor composition of the vitreous can protect from PVR. Clinical studies are the next logical step to test if neutralizing VEGF-A protects patients from PVR as it does in the pre-clinical studies. In addition, clinical testing of the VEGF-A/PDGF ratio from vitreous collected at the time of the initial surgery for RD repair may predict subsequent episodes of PVR

REFERENCES:

1. Wong CA, Potter MJ, Cui JZ, Chang TS, Ma P, Maberley AL, Ross WH, White VA, Samad A, Jia W, Hornan D, Matsubara JA: Induction of proliferative vitreoretinopathy by a unique line of human retinal pigment epithelial cells, Can J Ophthalmol 2002, 37:211-220
2. Lei H, Hovland P, Velez G, Haran A, Gilbertson D, Hirose T, Kazlauskas A: A potential role for PDGF-C in experimental and clinical proliferative vitreoretinopathy, Invest Ophthalmol Vis Sci 2007, 48:2335-2342

TASK 8: Role of Neuropeptides in the Bilateral Loss of Ocular Immune Privilege After Retinal Laser Burn (RLB) Treatment (Joan Stein-Streilein, Ph.D.)

BODY: During the FY 10, we were able to determine that substance P, Tac1, was the neuropeptide responsible for bilateral loss of ocular immunology post unilateral retinal laser burn. This resulted in a manuscript entitled: *Retinal laser burn-induced neuropathy leads to substance P-dependent loss of Ocular Immune Privilege. Published in the Journal of Immunology, 2012, 189: 1237-1242*. Inflammation in the eye is tightly regulated by multiple mechanisms that together contribute to ocular immune privilege. It has been shown that it is very difficult to mitigate the immune privileged mechanism called anterior chamber-associated immune deviation (ACAID). The fact that trauma to the retina mitigates ACAID for an extended period of time provides a clue as to why immune inflammatory diseases may follow post ocular trauma and the studies provide valuable information for understanding Sympathetic Ophthalmia, age related macular degeneration, and uveitis.

During the funding period were showed that both SPANTIDE I and II were effective antagonists of the substance P receptor, NK1R, ruling out the possibility that the release of histamine contributed to the loss of immune privilege. Thus providing proof that SP was the neural messenger that biased the ocular environment post RLB.

We were unable to acquire the antagonist for CGRP, since it is now owned now by a company who has with restrictions on our publications if we use the material.

Previously we reported that SPANTIDE was only able to block the abrogation of immune privilege if delivered 24 h post RLB but not at 7 days. In this funding period we showed that SPANTIDE was able to block the loss of ACAID at 24 h but not at 3 or 5 days post RLB. We conclude that SP initiates a process that once started cannot be reversed. Our future research will be focused on the immune activating process that is initiated by SP post RLB.

In lieu of identifying substance P in the eye we performed Confocal analyses on frozen sections of the eye to show that NK1R was indeed up regulated over time in both eyes of mice that received RLB to the right eye. Since substance P is the significant ligand for the receptor and substance P induces the up regulation of its receptor, we used this as proof that substance P was up regulated in both eyes post RLB. Substance P is very susceptible to neuropeptidases in the eye.

KEY RESEARCH ACCOMPLISHMENTS:

- Introduced a whole new area of research involving neuropeptides in induction of inflammatory conditions in the eye to the field.
- Showed that substance P induces an extended loss of immune privilege.
- The loss of immune privileged by RLB can be blocked by NK1R antagonists if give early post RLB (trauma)

REPORTABLE OUTCOMES:

Publication: Lucas, K, Karamichos, D, Mathew, R, Zieske, JD and Stein-Streilein, J, Retinal laser burn-induced neuropathy leads to substance P-dependent loss of Ocular Immune Privilege. Published in the Journal of Immunology, 2012, 189: 1237-1242 **(Appx. 2)**

Invited Presentation: by Joan Stein-Streilein: Symposium Speaker "Local and distant trauma upsets ocular immune regulation." ARVO annual meeting, FortLauderdale, FL (May 05-10, 2012)

Invited Presentation by Joan Stein-Streilein: 2012 Trauma Induced Neuropeptide Interference With Macrophage Regulation of Ocular Inflammation. ISER Biennial Meeting, Berlin, Germany. (July 21 – 25)

Results from theses studies provided the basis for JS-S application for an NIH RO1. Entitled, Mechanisms *of Immune privilege in the posterior eye. Submitted October 5, 2012*

CONCLUSION: We conclude that neuropeptides contribute to RLB- induced inflammation in the both eyes post trauma to one eye. The work is relevant to the understanding of Sympathetic Ophthalmia and immune inflammatory conditions relevant post battlefield injuries. A potential is raised for development of new therapy to prevent bystander inflammatory damage post ocular trauma. That therapy could involve early treatment with substance P antagonist to the patient.

TASK 9: Stimulating CNS Regeneration And Repair By Insulin-Like Growth Factor (Dong Feng Chen, M.D., Ph.D.)

BODY: The objective of this subtask is to study the mechanisms that regulate the growth and eventually regeneration of the optic nerve in adult mammals with a focus on the insulin-like growth factor I (IGF-I)-mediated signaling pathways. Our goal was to evaluate the effects of IGF-I and its downstream pathways on retinal ganglion cell (RGC) survival and axonal outgrowth in culture using both the gain-of-function and loss-of-function approaches.

Studies from my laboratory and others have shown that IGF-I-mediated signals are critically involved in regulating neuronal survival and axonal outgrowth during development of the central nervous system (CNS),[1,2] but its role in retinal and optic nerve development has not been established. We hypothesize that manipulation of IGF-I signaling may preserve or restore the

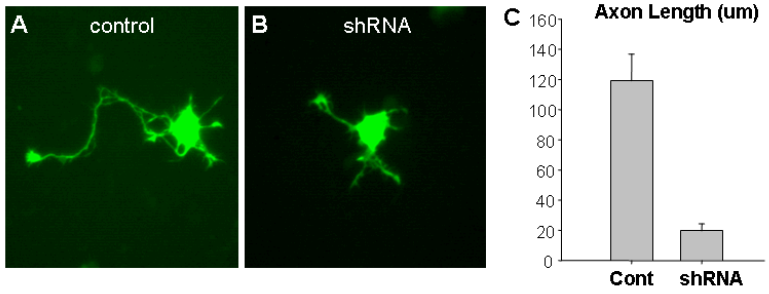

Figure 2. IGF-I shRNA triggers profound reduction in RGC axonal growth in culture. **A,B**, The morphology of RGCs at 4 days after transfection with GFP-tagged shRNA of a scrambled sequence (A; control) or targeting a specific region of IGF-I (B; shRNA). **C**, Quantification of axonal growth in cultured RGCs shows dramatic reduction in axonal length after IGF-I knockdown.

axonal growth machinery in CNS neurons and allow axonal growth and protection after injury. Using gene manipulations in cultured RGCs and genetically modified mice, we plan to test this hypothesis through the following aims: aim 1. To identify the mechanisms by which IGF-I drives axonal elongation during RGC development; aim 2. To define the roles of IGF-I-signaling in DAI development and/or neuron and axon protection in optic nerve injury model.

1. IGF-I and IGF-1R-mediated signaling is essentially involved in RGC axonal growth

To determine the effect of IGF-I on RGC survival and axonal growth, recombinant IGF-I (50 ng/ml; R&D Systems) was added to the medium of P0 RGC cultures. After 3 days of incubation, cells were fixed and stained with a vital dye calcein or immunolabeled with a primary antibody against an RGC specific marker, ß-III-tubulin. Addition of IGF-I not only promoted RGC survival, but strikingly, it also stimulated the cells to extend long neuritis (**Fig. 1**). There was an over 3-fold increase in total neurite length as compared to the untreated control group (**Fig. 1**); the survival effect of IGF-I was less prominent than its growth effect.

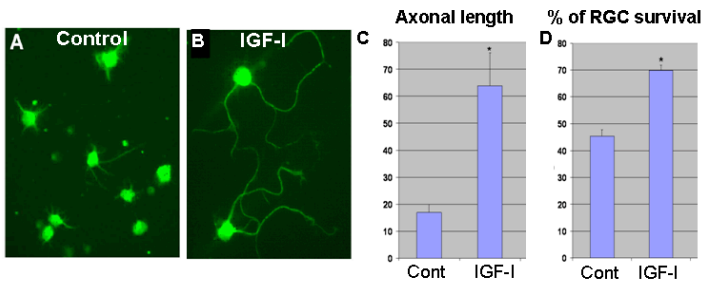

Figure 1. IGF-1 stimulates RGC neurite outgrowth in culture. **A,B**, Epifluorescence photomicrographs of RGCs purified from P0 mouse pups and cultured in the absence (A) and presence (B) of IGF-I (50 ng/ml). Cells were fixed after 72 hr of incubation and labeled with the vital fluorescent dye calcein. **C,D,** Quantification of RGC neurite outgrowth (C) and survival (D). * indicates $P<0.05$ over the control group by two tailed student *t* test.

Next, we used a lentiviral-based method of RNA interference to knockdown IGF-I expression acutely. Infection of lentiviral vector encoding short hairpin RNAs (shRNAs) targeting IGF-I efficiently reduced the expression of IGF-I in RGCs and led to a drastic reduction of neurite outgrowth (**Fig. 2**). Morphometric analysis revealed that axonal length was reduced by 80% relative to control cells (infected with a lentivirus carrying scrambled shRNA). These data suggest that IGF-I is a critical regulator of RGC neurite outgrowth.

Having discovered a role for IGF-I in RGC axonal growth, we next examined if IGF-I acted through IGF-IR to stimulate axonal growth. IGF-IR-mediated signal was blocked using function-blocking antibody against IGF-IR or by adding IGF-1R inhibitor H-1356—the IGF-I analog that competitively binds to IGF-1R—to RGC cultures. RGCs isolated from P0 mouse pups were

cultured in the absence or presence of IGF-I. Addition of either anti-IGF-1R or H-1356 to RGC cultures abolished the axonal growth effect of IGF-I (**Fig. 3**), suggesting that IGF-1R is essentially involved in IGF-I-mediated growth of RGC axons.

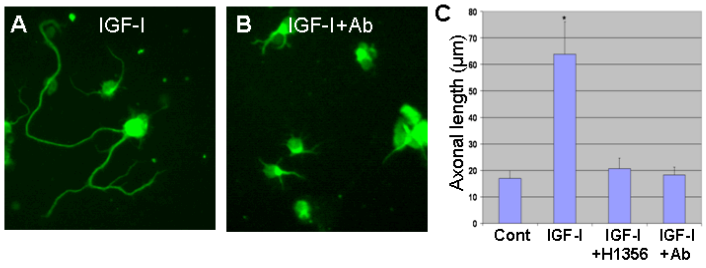

Figure 3. IGF-1R is required for IGF-I-mediated axonal growth. A,B, Epifluorescence photomicrographs of RGCs isolated from P0 mouse pups and cultured in the absence (**A**) and presence (**B**) of IGF-IR neutralizing antibody (Ab). Cells were fixed at 72 hr of incubation and labeled with the vital fluorescent dye calcein. **C,** Quantification of RGC axonal length. * indicates $P<0.05$ as compared to the control group by student *t* test.

We then asked whether overexpression of IGF-1R promotes RGC axonal growth. P0 mouse RGCs were isolated and transfected with a plasmid encoding a human IGF-1R. A plasmid encoding GFP was co-transfected with IGF-1R plasmid so that transfected cells could be visualized directly by their GFP expression. We showed that P0 RGCs transfected with a control GFP plasmid expressed a low level of IGF-1R, as expected; transfection of IGF-1R plasmid induced a high level of IGF-1R expression in postantal RGCs and increased neurite outgrowth as compared to cells expressing a control plasmid (**Fig. 4**). The data further support a role of IGF-I and IGF-1R-mediated signals in the regulation of RGC axonal growth.

2. IGF-I promotes RGC survival and axonal regeneration after optic nerve injury

To study the role of IGF-I in RGC survival and optic nerve regeneration *in vivo*, we performed optic nerve crush injury in adult C57BL/6J mice. IGF-I (25 ng) or phosphate buffered saline (PBS) (as controls) was administrated in adult mice through intracameral injection immediately and at 3 and 6 days post-optic nerve crush. On day 11, mice were received intravitreal injection of anterograde tracer, chlorea toxin subunit B (CTB) to label RGCs, which would pick up CTB and transport along the axons. Regenerating axons thus could be revealed by immunolabel the CTB signal in optic nerve sections.

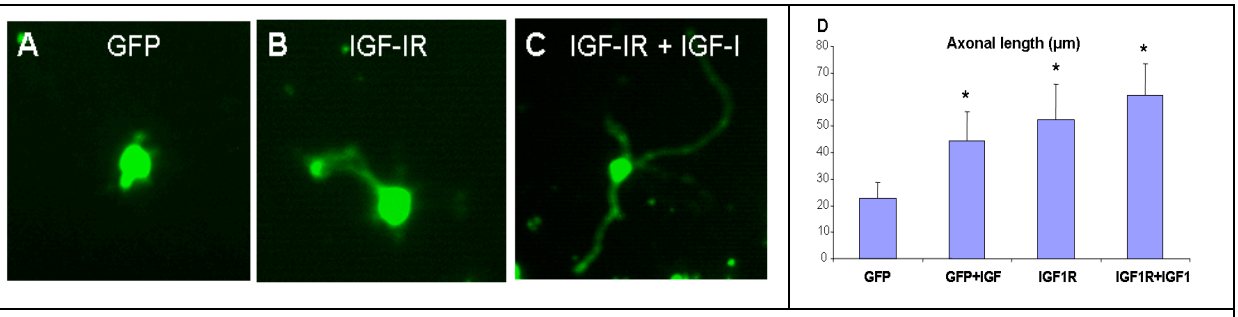

Figure 4. Expression of IGF-1R promotes axonal growth of postnatal RGCs. A-C, Photomicrographs of RGC morphologies that were transfected with a control GFP (**A**) or IGF-1R (**B,C**) plasmid and cultured in the absence (**A,B**) or presence (**C**) of IGF-1 (50 ng/ml). Cells were fixed at 72 hr of incubation and labeled with the vital fluorescent dye calcein. **D,** Quantification of RGC axonal length. * indicates $P < 0.05$ as compared to controls.

After 3-day survival to allow CTB transportation, the mice were sacrificed. Quantification of RGC survival was carried out in retinal whole-mounts that were immunolabeled with mouse anti-Tuj-1 antibody recognizing a specific RGC marker, followed by incubation with Cy3 conjugated secondary antibody. RGCs were counted, and the number of surviving RGCs was compared between the PBS and IGF-I-treated groups (**Fig. 5A**). We showed that treatment of IGF-I significantly enhanced the survival of RGCs following optic nerve crush injury as compared to the control-treated group (**Fig. 5A**).

Next, we quantified RGC axon regeneration in optic nerve sections. The mouse optic nerves were collected and sectioned at 10 μm thickness before immunolabeled with primary antibody for CTB. The regenerating axons were visualized by further incubation of the optic nerve sections with biotinylated mouse anti-goat IgG and then streptavidin Alex Fluor 546 conjugated IgG. CTB+ axons extended beyond the injury site were counted at every 250 μm intervals. Our data indicated that administration o of IGF-I significantly increased the number of regeneration axons at all places counted as compared to the control-treat group (**Fig. 5B**). Together, our data support that IGF-I promotes both the survival and axonal regeneration of RGCs following injury and may be used for treating traumatic optic nerve injury.

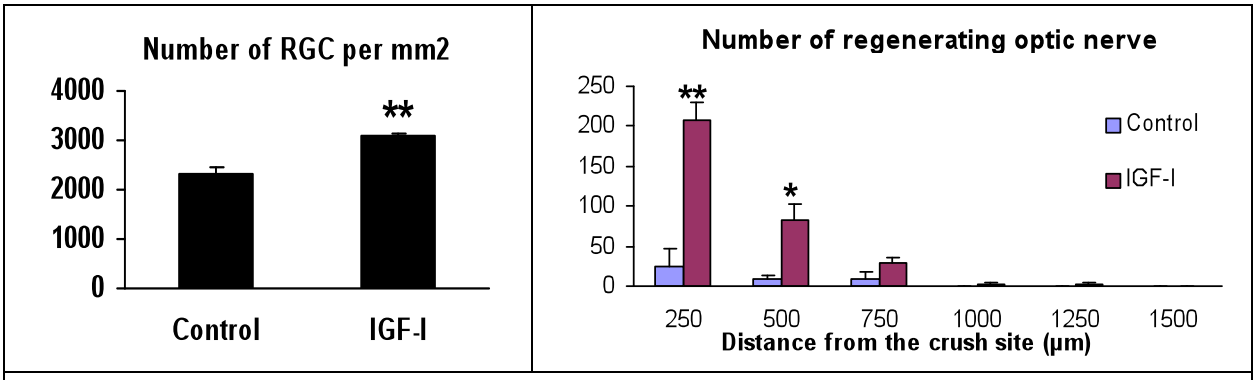

Figure 5. Effect of IGF-I on RGC survival and axon regeneration *in vivo*. A, Quantification of RGC survival in retinal whole-mounts of mice received intracameral injections of either control (PBS) or IGF-I. Administration of IGF-I (25 ng) significantly enhanced RGC survival as compared to the control animals (2,304 ± 159 vs 3,077 ± 70; n=4/group; *P*<0.01 by two-tailed student *t* test). **B,** Administration of IGF-I (25 ng) significantly enhanced the number regenerating axons as compared to PBS-injected control mice after optic nerve crush injury (* represents *P*<0.05; ** represents *P*<0.01 by ANOVA).

KEY RESEARCH ACCOMPLISHMENTS:

- IGF-I and IGF-1R are critically involved in the regulation of retinal ganglion cell survival and axonal growth *in vitro*.
- IGF-I promotes retinal ganglion cell survival and optic nerve regeneration in adult mice and thus may be used as a potential therapy for traumatic optic nerve injury.

REPORTABLE OUTCOMES:

- Guo C, Cho K-S, Tchedre K, Chen H, Malik H, Chen DF. (2012) IGF-I binding protein like protein 1 (IGFBPL-1) promotes axon outgrowth in retinal ganglion cells through the regulation of IGF-I signaling pathway. *ARVO Abstract*.

- Chen, DF & Guo, C. (2012) Composition for controlling axonal outgrowth. US provisional application 61/447.314

CONCLUSION: CNS axons of adult mammals are incapable of regeneration. As a result, optic nerve or brain injury can lead to permanent loss of vision or cognitive functions. Unfortunately, there are currently no medical treatments that can promote CNS nerve regeneration i*n situ*. Therefore, developing a method to stimulate the regrowth and repair of the optic nerve and CNS axons would be highly desirable for functional improvement and restoration after CNS injury. Defining IGF-I and its mediated signals in support of optic nerve regeneration opens up a new avenue for the development of therapeutics to treat brain and optic nerve damage as a result of TBI or other neurodegenerative conditions. Future elucidation of how IGF-I-mediated signals are regulated, for example, by IGF-I-binding proteins during nerve injury, would provide further insights into the mechanisms controlling axonal regrowth and aid our development of more effective therapy.

REFERENCES:

1. Aberg, N.D., Brywe, K.G. & Isgaard, J. Aspects of growth hormone and insulin-like growth factor-I related to neuroprotection, regeneration, and functional plasticity in the adult brain. *ScientificWorldJournal* **6**, 53-80 (2006).
2. Ozdinler, P.H. & Macklis, J.D. IGF-I specifically enhances axon outgrowth of corticospinal motor neurons. *Nat Neurosci* **9**, 1371-1381 (2006).

TASK 10: Realistic Detection Test for Traumatic Brain Injury Vision Losses (Alex Bowers, Ph.D.)

BODY:
We will develop and implement a simple, but realistic test of detection using driving video backgrounds to be applied for the evaluation of traumatic brain injury (TBI) vision losses and rehabilitation interventions

Realistic detection test development
In this 12-month period we have explored two approaches to the development of the realistic detection test, developed a prototype test using the second approach and conducted preliminary evaluations.

In the first approach we used Poser 9 software to create realistic animated human figures and insert them into videos of real-world driving scenes selected from commercially available UK driving hazard detection test videos. We were able to create and program figures to walk along a selected path across a road at a natural speed (relative to real pedestrians on the same crosswalk) and with the correct increase in size on approach **(Figure 1).**

Figure 1: Virtual animated figure of a woman inserted in a driving video clip. The figure walks along a selected path across a crosswalk mimicking the speed and behavior of a real pedestrian (on the same crosswalk in front of the virtual figure) and with the correct increase in size on approach.

While the first method enabled the use of real driving videos, with the natural richness and complexity of real-world scenes, it was very time consuming. We therefore explored a second approach in which we used our driving simulator-scripting environment to create driving scenarios with pedestrians that walked or ran toward the road in a variety of situations **(Figure 2).** A researcher, experienced in driving in the simulator, then drove each scenario while video was recorded directly from the central screen of the simulator. The videos recorded from the simulator were then cut and spliced to create 5 video sequences, each about 3 minutes in duration. Each video sequence included 12 clips with pedestrian appearance events and 5-9 clips without pedestrian events. In each sequence there were an equal number of pedestrian appearances on the right and left of the road. Three of the sequences were based on driving in city environments and two driving on a rural highway.

Figure 2: Example of a walking pedestrian from a video sequence created using our driving simulator environment (central screen of driving simulator only)

Software was developed to record participant responses (a button press to indicate that a pedestrian was seen) and to determine detection rates and responses times from the button presses (response time was the period between the pedestrian appearing and a button press).

Preliminary evaluation of test for patients with homonymous field loss

As we did not receive notification of approval from the military IRB until the 7th June 2012, human subjects testing started later than anticipated. Therefore, only limited testing with patients has been conducted thus far. Six participants (age range 46 to 83 years) with homonymous field loss (3 with hemianopia and 3 with quadranopia) each viewed 5 video sequences displayed on a large rear projection screen (total 30 pedestrian events on the right and left). The viewing distance was selected such that the total angular subtense of the video was similar to that of the central screen of the driving simulator. Participants viewed binocularly and were allowed to use free eye movements during the test.

Preliminary data analyses indicate that the test is sensitive to homonymous visual field loss: detection rates were significantly lower on the blind (non-seeing) side than the seeing side (medians 70% and 100%, respectively, $p = 0.028$; **Figure 3a)** and response times were

significantly longer (medians 1.6s and 0.71s, respectively; p = 0.028; **Figure 3b).** Furthermore, on the blind side, the test was also sensitive to differences in detection performance between pedestrians that initially appeared at large eccentricities (far away from the road) and small eccentricities (close to the road). Specifically, blind side detection rates were significantly lower for pedestrians at large than small eccentricities (medians 50% and 93%, respectively, p = 0.028; **Figure 4a)** and response times were longer (medians 2.7s and 1.4s, respectively; p = 0.068; **Figure 4b**).

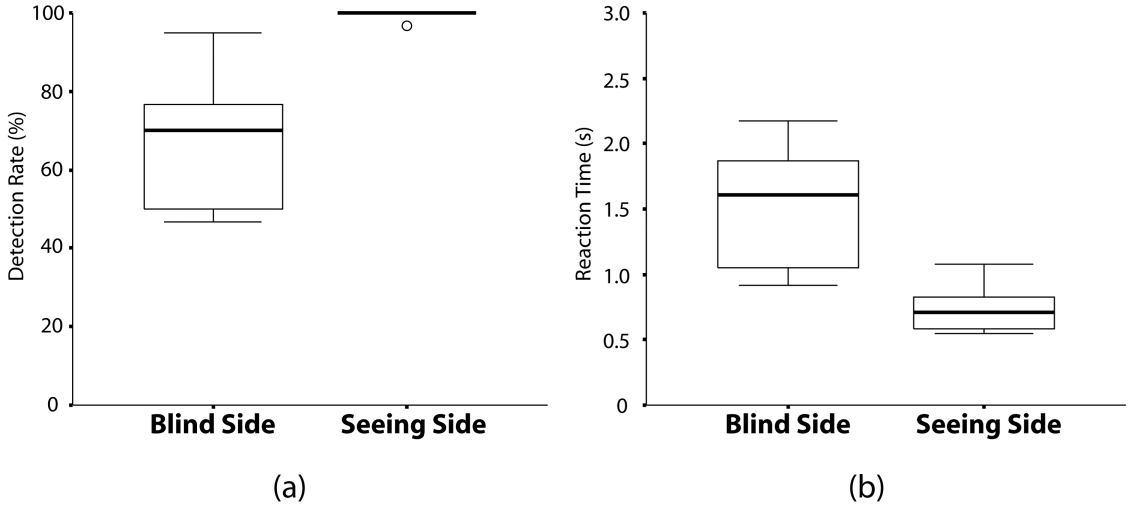

Figure 3. Detection performance for blind and seeing sides for data pooled across small and large eccentricities: **(a)** Median detection rates; and **(b)** Median reaction times. Detection rates were significantly lower (p = 0.028) and reaction times were significantly longer (p = 0.028) on the blind side than the seeing side.

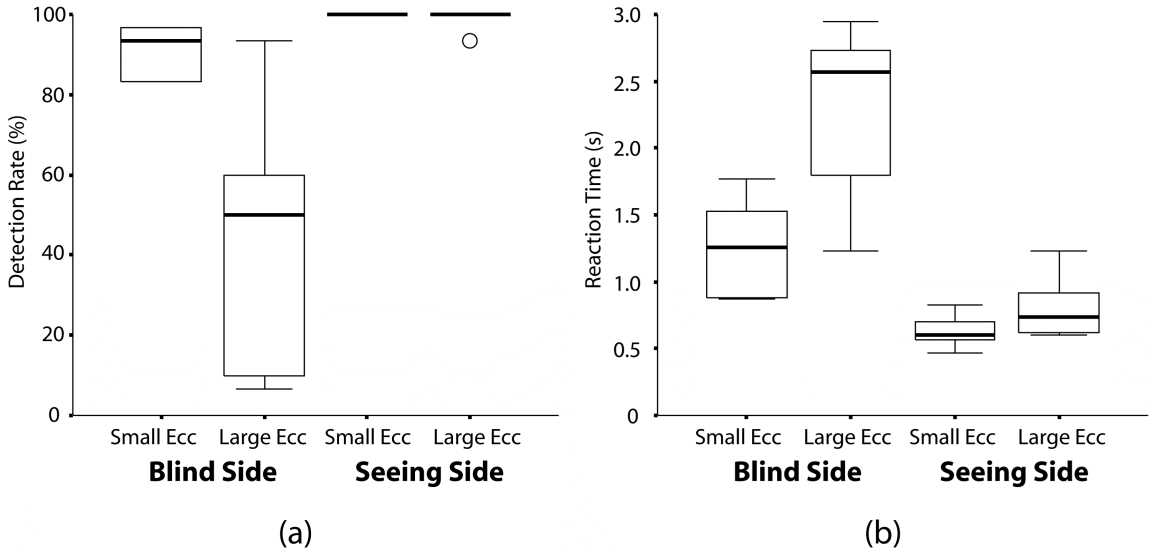

Figure 4. Detection performance for pedestrians at small and large eccentricities on the blind and seeing sides: **(a)** Median detection rates; and **(b)** Median reaction times. On the blind side, detection rates were significantly lower ($p = 0.028$) and reaction times were longer ($p = 0.068$) for pedestrians appearing at large than small eccentricities. The reaction boxplot for the large eccentricity on the blind side includes data from only four participants as two participants detected so few pedestrians at this eccentricity that reaction times could not be computed (required a minimum of 3 detections).

KEY RESEARCH ACCOMPLISHMENTS:

- A prototype video detection test and data analysis software have been developed
- Preliminary evaluations with patients with homonymous visual field loss have been completed

REPORTABLE OUTCOMES:

An abstract reporting preliminary data was submitted for the 5th Military Vision Symposium on Ocular and Vision Injury. The data from this project will be used to support a future grant application to continue development of the test and implement it as an outcome measure in a clinical trial of rehabilitation interventions for patients with homonymous visual field loss due to traumatic brain injury and stroke.

CONCLUSION:

We have successfully developed a simple, video-based detection test for traumatic brain injury vision losses. Preliminary results from 6 patients indicate that the test is sensitive to the type of visual field loss caused by traumatic brain injuries and that further testing with a larger sample is warranted.

TASK 11: Simultaneous Assessment of Structure, Behavior and Electrophysiology (Peter Bex, Ph.D.)

BODY:

People with exudidative and geographic age-related macular degeneration (AMD) frequently report that they experience visual distortions around their scotomas [1 2 3 4], a phenomenon known as *metamorphopsia*. Such distortions are usually most noticeable while viewing straight lines that appear "wavy". The distortions are thought to be caused by displacements of the retinal photoreceptor layers and may be *focal* (i.e. small and generally centered on the fovea, due to central serous chorioretinopathy, best disease, macular holes, cystoid macular edema, central retina vein occlusion) or *diffuse* (over a large retinal area due to subretinal haemorrhaging, choroidal neovascularization, gepgraphic atrophy, drusen or epiretinal membranes).

To measure metamorphopsia, current best practice is to use *Amsler charts* [5] or their modern variants [6 7 8], which are viewed monocularly, while the patient answers structured questions about their distortions. For progressive diseases, patients are often asked to self-monitor distortions and to seek attention when any change is noted. This technique has poor sensitivity - fewer than 60% of people with AMD can discern their scotoma this way [9 10] – and does not

quantify the location or the severity of metamorphopsia. *M-Charts* [11] utilize a series of horizontal and vertical rows of dots with different spacings. The minimum dot-spacing that does not lead to distortion, quantifies the scale but neither the magnitude nor location of distortions. *PHP* (preferential hyperacuity perimetry) [12] is a visual field mapping procedure where patients indicate the location of misaligned series of dots. PHP provides a map of distortions and its parameters correlate with OCT metrics in patients undergoing Lucentis therapy. Interocular size matching has been used to monitor macular holes [13], but actually quantifies dysmetropsia [14] [14] (interocular size difference). None of these methods measure fixation and so the location of distortions is not monitored. *Binocular correspondence perimetry* [15] maps distortion by measuring the deviation in position of points presented simultaneously to the two eyes. This technique relies on the presence of an unaffected eye to provide a reference.

METHODS:

We developed two new methods to quantify and localize metamorphopsia. The first method is hyperacuity-based and is suitable for binocular or monocular metamorphopsia and involves the construction of a figure that is *perceptually* regular, but may be *physically* irregular. The second method is suitable only for monocular metamorphopsia and involves inter-ocular alignment of the points of a regular grid viewed dichoptically.

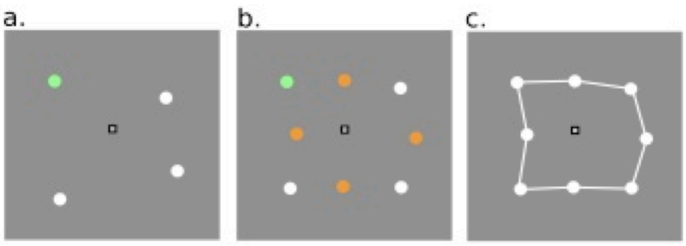

Figure 1 Quantification of Metamorphopsia with Hyperacuity. a) While fixating the central dot, the observer moves the white circles to construct a square. One corner (green) is anchored each trial in random order. b) The center of each side is marked with bisection and vernier alignment. c) example data from 52 year old patient with central serous retinopathy

Hyperacuity-based Metamorphopsia Assessment Subjects construct a square target by first assembling the four corners (line bisection hyperacuity), then by bisecting the mid point of each side of the square (vernier hyperacuity), as illustrated in **Figure 1a,b.** The tasks is repeated 4 times, with the 1st *anchored* dot positioned in each corner at random between repetitions. The mean and standard deviation of the 8 points defined over 4 repetitions at each of 2 eccentricities provide estimates of accuracy and precision. A remote eye tracker is used to ensure compliant fixation on a central point: the alignment dots are removed from the display if the observer fixates >1° away from the fixation point.

Dichoptic Pointing-based Metamorphopsia Assessment We developed a variant of binocular correspondence perimetry that minimize factors that would lead to underestimation of distortion: a) eye tracking ensures compliant fixation, b) nVidia shutter glasses instead of anaglyphs minimize rivalry and improve the cyclopean percept and c) background 1/F fractal naturalistic noise prevents cross-talk. 16 dots on a 4*4 grid subtending 8°*8° are presented only to the dominant eye (assessed with the Porta test [16]) in random order. A mouse-controlled cross-hair is presented only to the non-dominant eye (typically the more impaired eye) - the movement of the cross hairs and attention to them helps overcome dominance and rivalry. The observer's task is to

maintain central fixation (with enforced compliance) and to center the target dot within the cross hairs.

RESULTS:

Figure 2a shows a typical construction of a square based on hyperacuity method and **Figure 2b** shows the results of the inter-ocular pointing task by a 52 year old patient with central serous retinopathy **Figures 2c and 2d** show the appearance of an Amsler grid to this observer. There is close correspondence between the outcomes of these tests. Note that the square construction and dichoptic pointing data should be mirror images because the constructed square appears regular to the observer and therefore must be physically distorted in the opposite direction to invert the patient's metamorphopsia.

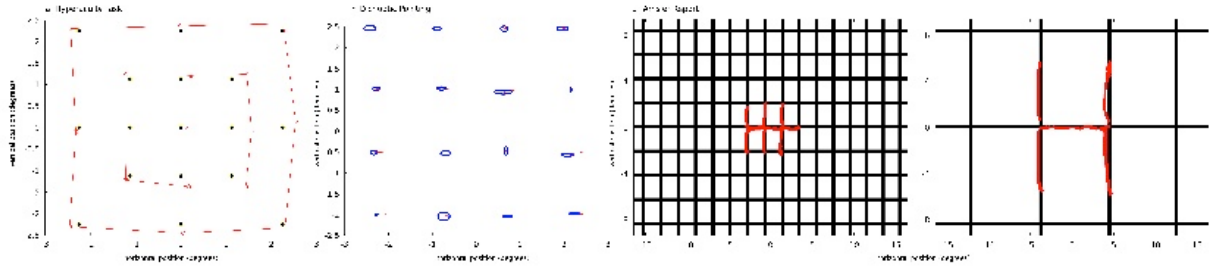

Figure 2. Metamorphopsia in a 52-year-old patient with central serous retinopathy. a) Results of Hyperacuity Assessment b) dichoptic pointing and tracing on a c) fine or d) coarse Amsler grid

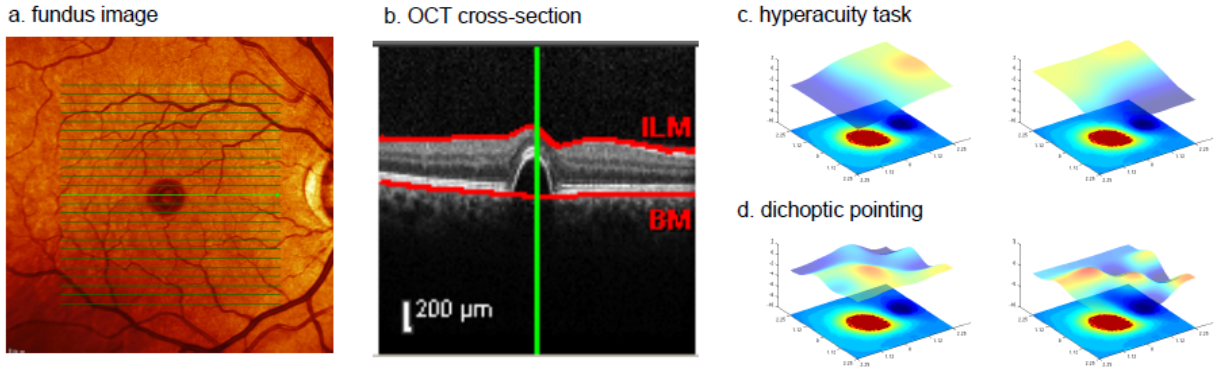

Figure 3a) Fundus image and b) foveal cross section for an observer with central serous retinopathy (c,d) The central lesion location (shown as the lower heat-map in each panel) closely corresponds to areas of distortion identified with c) hyperacuity and d) dichpotic pointing method (shown as the upper land)

Figure 3 shows (a) a fundus image and (b) an OCT image for the same observer. The base of **Figures 3c and 3d** show the retinal thickness, which is abnormally high (red regions) in central vision for this observer, compared to age-matched norms. The elevated surfaces show the estimated level of local distortion for the (c) the hyperacuity and (d) dichoptic pointing tasks **Figure 4** shows analogous data for 10 further patients. In each case, there is a close spatial correspondence between the location of visual distortions and the presence of pathology.

We are currently developing statistical methods to cross correlate the retinal thickness maps (bases of Figure 4) with the local distortion estimates derived behaviorally (elevated surfaces in Figure 4). These data will allow us to compute the relationship between structure and function with these methods. Further more, these data will allow us to estimate when structural pathology is not correlated with functional deficits and when functional deficits occur in the absence of observable pathology. These are important data because they estimate the reliability limits of each method.

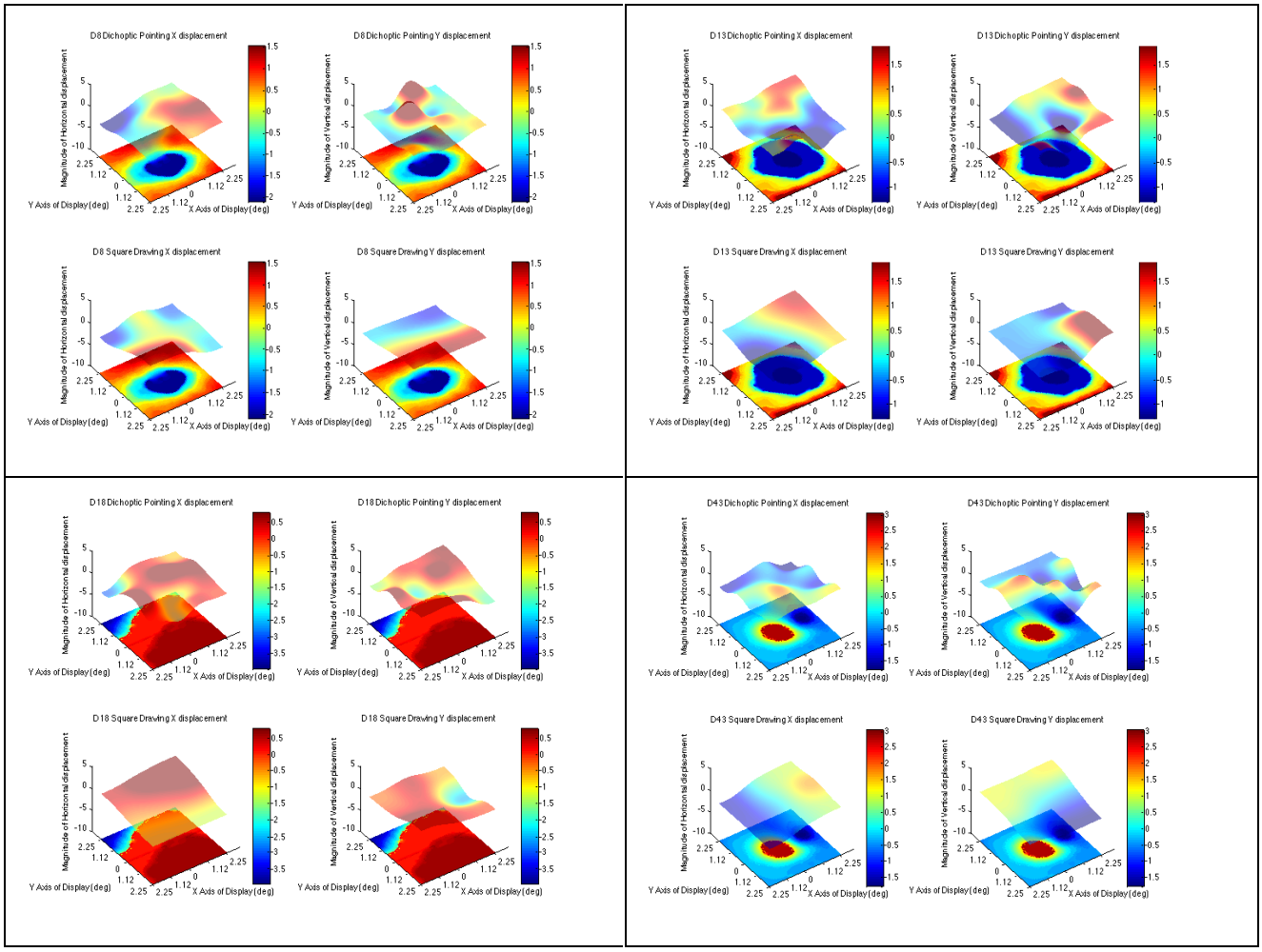

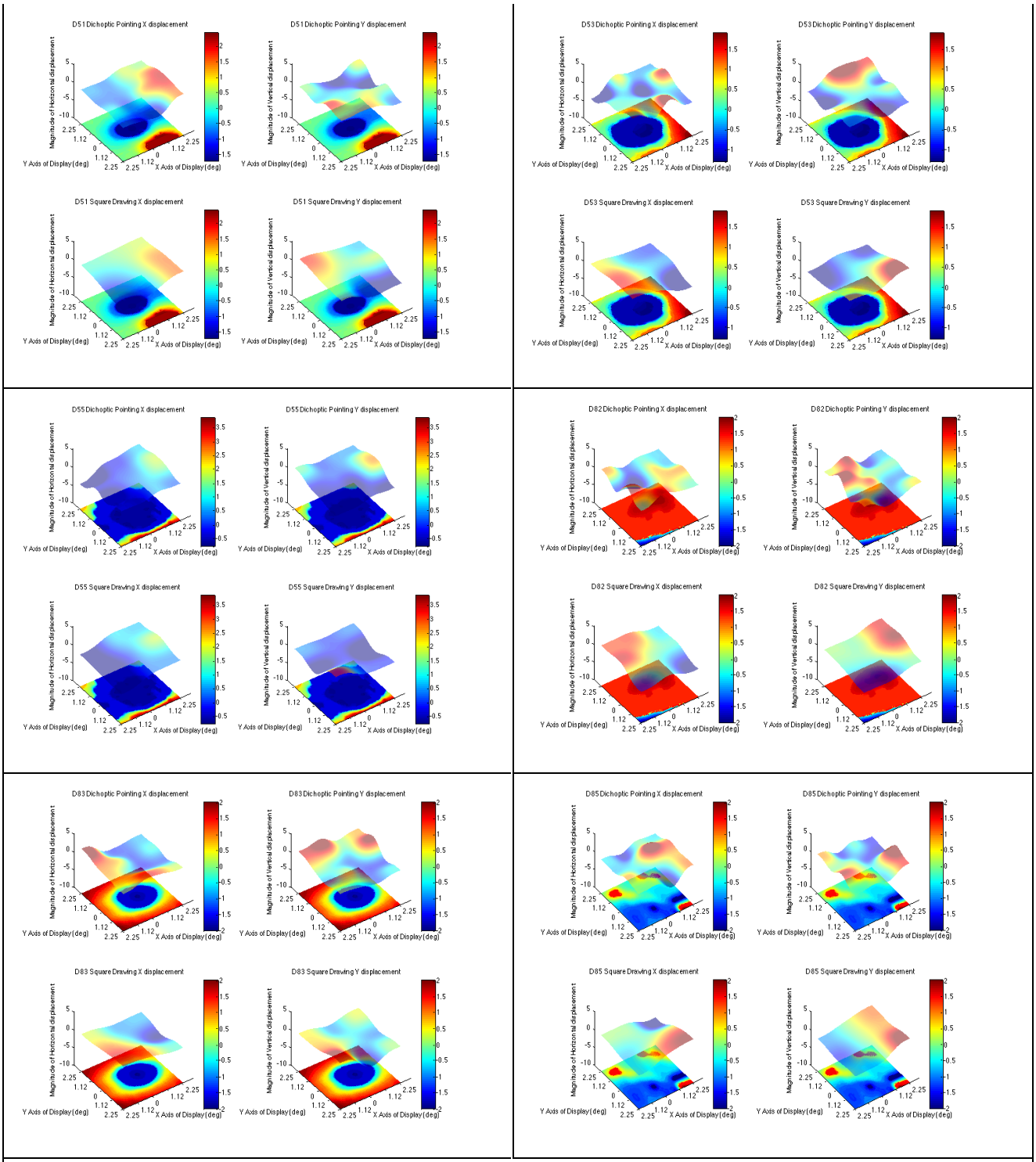

Figure 4 Structural and Functional data for 10 AMD patients who experience metamorphopsia. The base of each figure shows the local retinal thickness from an OCT image relative to age-matched norms. The surface plot in each figure shows the (left) Horizontal and (right) Vertical local distortion measured with (upper) dichoptic or (lower) hyperacuity methods.

KEY RESEARCH ACCOMPLISHMENTS:

- We developed a novel hyperacuity-based method that quantifies the location and magnitude of visual distortions in patients with binocular or monocular metamorphopsia.

- We developed a novel dichoptic-based method that quantifies the location and magnitude of visual distortions in patients with monocular metamorphopsia.

- We demonstrated close correspondence between the location and magnitude of distortion measured with each method.

- We demonstrated close correspondence between the location of subjective metamorphopsia and objective pathological changes in retinal thickness.

REPORTABLE OUTCOMES:

The data and methods developed in this proposal form preliminary data for extra-mural research funding.

CONCLUSION:

Functional deficits are commonly experienced in areas around central vision loss in the form of visual distortions. Such metamorphopsia is therefore associated with areas of disease progression and may serve as an important biomarker. Metamorphopsia is currently monitored with Amsler charts which are inaccurate and imprecise. We developed two novel methods that quantify the location and magnitude of metamorphopsia. We showed that these simple techniques are closely related to pathological changes and may therefore be used to screen for the early signs of vision loss and disease progression.

REFERENCES:

1. Zur, D. & Ullman, S. Filling-in of retinal scotomas. *Vision Res.* **43**, 971–982 (2003).

2. Jensen, O. M. & Larsen, M. Objective assessment of photoreceptor displacement and metamorphopsia: a study of macular holes. *Arch Ophthalmol* **116**, 1303–6 (1998).

3. Cohen, S. Y. *et al.* Filling-in phenomenon in patients with age-related macular degeneration: differences regarding uni- or bilaterality of central scotoma. *Graefes Arch. Clin. Exp. Ophthalmol.* **241**, 785–791 (2003).

4. Burke, W. Psychophysical observations concerned with a foveal lesion (macular hole). *Vision Res.* **39**, 2421–2427 (1999).

5. Amsler, M. L'examen qualitatif de la fonction maculaire. *Ophthalmologica* **114**, 248–261 (1947).

6. Bouwens, M. D. & Meurs, J. C. Sine Amsler Charts: a new method for the follow-up of metamorphopsia in patients undergoing macular pucker surgery. *Graefes Archive for Clinical and Experimental Ophthalmology* **241**, 89–93 (2003).

7. Saito, Y. *et al.* The visual performance and metamorphopsia of patients with macular holes. *Arch Ophthalmol* **118**, 41–6 (2000).

8. Matsumoto, C. *et al.* Quantification of metamorphopsia in patients with epiretinal membranes. *Invest Ophthalmol Vis Sci* **44**, 4012–6 (2003).

9. Schuchard, R. A. Validity and Interpretation of Amsler Grid Reports. *Arch Ophthalmol* **111**, 776–780 (1993).

10. Crossland, M. & Rubin, G. The Amsler chart: absence of evidence is not evidence of absence. *Br J Ophthalmol* **91**, 391–393 (2007).

11. Arimura, E. *et al.* Correlations between M-CHARTS and PHP findings and subjective perception of metamorphopsia in patients with macular diseases. *Invest. Ophthalmol. Vis. Sci* **52**, 128–135 (2011).

12. Das, R., Shi, Y., Silvestri, G. & Chakravarthy, U. Distortion Maps From Preferential Hyperacuity Perimetry Are Helpful In Monitoring Functional Response To Lucentis Therapy. *Retina* **29**, 1013–1018 (2009).

13. Krøyer, K., Christensen, U., Larsen, M. & Cour, M. la Quantification of Metamorphopsia in Patients with Macular Hole. *IOVS* **49**, 3741–3746 (2008).

14. Ugarte, M. & Williamson, T. H. 'Metamorphopsia' Assessment. *IOVS* **51**, 6894–6895 (2010).

15. Kroyer, K., Jensen, O. M. & Larsen, M. Objective signs of photoreceptor displacement by binocular correspondence perimetry: a study of epiretinal membranes. *Invest Ophthalmol Vis Sci* **46**, 1017–22 (2005).

16. Li, J. *et al.* Quantifying Sensory Eye Dominance in the Normal Visual System: A New Technique and Insights into Variation across Traditional Tests. *IOVS* **51**, 6875–6881 (2010).

17. Abscar, S. F. *et al.* Identifying the Roles of Interferon-Gamma Inducible Chemokines in Progression of Age-related Macular Degeneration (AMD). (2012).

TASK 12: Corneal epithelium regeneration via stem cell transplantation (Bruce Ksander, Ph.D.)

INTRODUCTION: Our ***overall hypothesis*** is that the corneal epithelium is derived from an ABCB5+ population of limbal basal epithelial cells that regenerates the corneal surface. ABCB5+ cells in the limbus function as adult stem cells and retain the ability to self-renew and differentiate.

TASK: Determine the differentiation and regeneration potential of tissue-specific adult ABCB5+ stem cells for regenerating the corneal epithelium. Aim 1- The first objective was to test the regenerative potential of human ABCB5+ limbal stem cells. Aim 2- The second objective was to test the regenerative potential of murine ABCB5+ limbal stem cells.

Body-

Aim 1: Experiments were performed to test the regenerative potential of ABCB5 positive and negative limbal stem cells recovered from cadaveric human donor eyes.

Xenotransplantation of *human* ABCB5+ limbal stem cells (LSC) restores the corneal epithelium in NSG mice with an induced LSC deficiency. We investigated the effect of transplanting *human* ABCB5+ LSC (limbal stem cells) on corneal regeneration in NSG mice with an induced LSC deficiency. Our experiments used a proven xenotransplantation model (human donor cells / mouse recipient) where *human* ABCB5+ limbal cells are grafted onto immunodeficient NOD.Cg-*Prkdc*^{scid} *Il2rg*^{tm1Wjl}/SzJ (NSG) mice with an induced limbal stem cell deficiency. NSG mice are a new immunodeficient mouse strain with enhanced ability to accept human transplants.

Isolation and purification of ABCB5+ and ABCB5- cells- ***Human limbal epithelial cells*** were obtained from two sources (i) discarded corneal rims following penetrating keratoplasty (Dr. Victor Perez, Bascom Palmer Eye Institute Cornea Service) and (ii) the Heartland Lions Eye Bank (Iowa). The limbus was dissected and epithelial cells isolated as described previously. ABCB5^{+} or ABCB5^{-} cells were purified by FACS sorting of anti-ABCB5/FITC-labeled samples using the murine anti-ABCB5 mAb 3C2-1D12 (available from AbD Serotec). Post-sort analysis was used to determine sorting purity and cell viability, as previously described for ABCB5-based sorting in other tissues.

Induction of limbal stem cell deficiency in immunodeficient NSG mice- We used a procedure described previously by Winston Kao. Dr. Evi Kolovou (Ksander laboratory) visited Dr. Winston Kao's laboratory where she learned these procedures. Briefly, the entire limbal and corneal epithelium was removed using an Algerbrush II corneal rust ring remover with a 0.5 mm burr. As a control, to demonstrate that we create consistently a limbal stem cell deficiency, mice were either (i) untreated, or (ii) receive a transplant of an empty fibrin carrier. These mice developed conjunctivalization of the corneal surface.

Transplantation of donor cells- Donor cells were transplanted in a fibrin and thrombin carrier using the method described by Winston Kao. Cells were added to the fibrin carrier at the defined cell density and transplanted onto the corneal stroma of recipient mice. The fibrin transplants were anchored to the conjunctiva with four sutures and the mouse eye closed by a tarsorrhaphy. The recipient eye remained closed until the sutures dissolved approximately one week later.

Four treatment groups were tested: (1) fibrin carrier without cells; (2) fibrin carrier seeded with 200 unsegregated limbal cells; (3) fibrin carrier seeded 200 ABCB5- limbal cells, and (4) fibrin carrier seeded with 200 ABCB5+ LSCs (**Figure 1A**). At four weeks post transplantation, grafts containing either no cells, or ABCB5- cells displayed: (i) reduced corneal clarity and increased neovascularization, (ii) a lack of stratified epithelium, and (iii) evidence of goblet cells and no K12+ epithelial cells. Grafts containing unsegregated cells displayed some evidence of restoration (clearer cornea with less neovascularization), but there was no evidence of a stratified

Figure 1

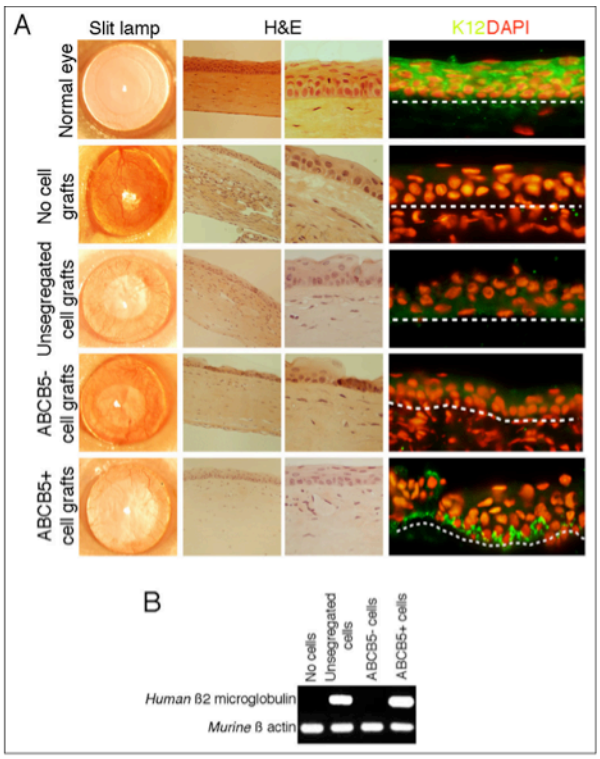

Figure 1. *Analysis of* ***human*** *to NSG mouse xenogeneic transplants at 4 weeks.* **(A)** Corneal transparency evaluated by slit lamp (column 1). H&E staining (column 2- lower magnification; column 3 higher magnification). Keratin12 (K12) staining (column 4).

As a control, normal untreated murine corneas are shown in row 1. As a negative control, mice were treated with a fibrin gel carrier without cells (row 2). Mice treated with fibrin gel grafts containing unsegregated, ABCB5-, or ABCB5+ human limbal epithelial cells are shown in rows 3, 4 and 5, respectively. Only transplants containing ABCB5+ limbal epithelial cells displayed normal corneal histology and expression of K12+ mature corneal epithelial cells. **(B)** RT-PCR analyses of murine and human mRNA transcripts in murine eyes transplanted with the denoted human cell types.

K12+ epithelial layer. By contrast, only grafts containing purified ABCB5+ cells displayed evidence of a stratified epithelial layer containing K12+ cells. While corneal restoration was not complete, we predict that more robust regeneration will occur if transplants contain increased numbers of ABCB5+ cells and/or are allowed to develop more than 5 weeks.

To further support the finding that human donor cells improved corneal wound healing, corneal epithelial cells were isolated from chimeric recipients and examined by RT-PCR for the presence of human-specific β2 microglobulin (β2M) transcripts, an identifier of all cells of human origin. The corneal epithelium of recipients grafted with human ABCB5+ cells, or unsegregated cells contained human-specific β2M transcripts and, as expected, control grafts lacking cells displayed no human transcripts (**Figure 1B**). No human-specific β2M transcripts were detected in recipient eyes that received grafts only containing ABCB5- human limbal epithelial cells, demonstrating preferential engraftment of human ABCB5+ LSC**Aim 2**: Experiments were performed to test the regenerative potential of *murine* ABCB5 positive and negative limbal stem cells.

Murine syngeneic **ABCB5+ LSCs restore corneal epithelium in C57BL/6J mice with an induced LSC deficiency.** To determine the role of ABCB5 as a candidate marker for prospective LSC isolation and enrichment, we examined the *in vivo* cornea regenerative potential

of transplanted syngeneic *murine* ABCB5^{+} or ABCB5^{-} limbal cells in C57BL/6J mice with an induced limbal stem cell deficiency. Four treatment groups were tested: (1) fibrin carrier without cells; (2) fibrin carrier seeded with 200 unsegregated limbal cells; (3) fibrin carrier seeded with 200 ABCB5- limbal cells, and (4) fibrin carrier seeded with 200 ABCB5+ LSCs (**Figure 2**). At five weeks post transplantation, grafts containing either no cells, or ABCB5- cells displayed: (i) opaque corneas, (ii) conjunctivalization with infiltrating goblet cells, and (iii) the absence of K12+ epithelial cells. While grafts containing unsegregated cells displayed some evidence of restoration (a clear cornea with a more normal histology), they still contained goblet cells and no detectable K12+ cells. By contrast, only transplants containing ABCB5+ cells displayed clear corneas with: (i) normal histology, (iii) the absence of goblet cells, and (iv) presence of K12+ corneal epithelial cells.

Figure 2

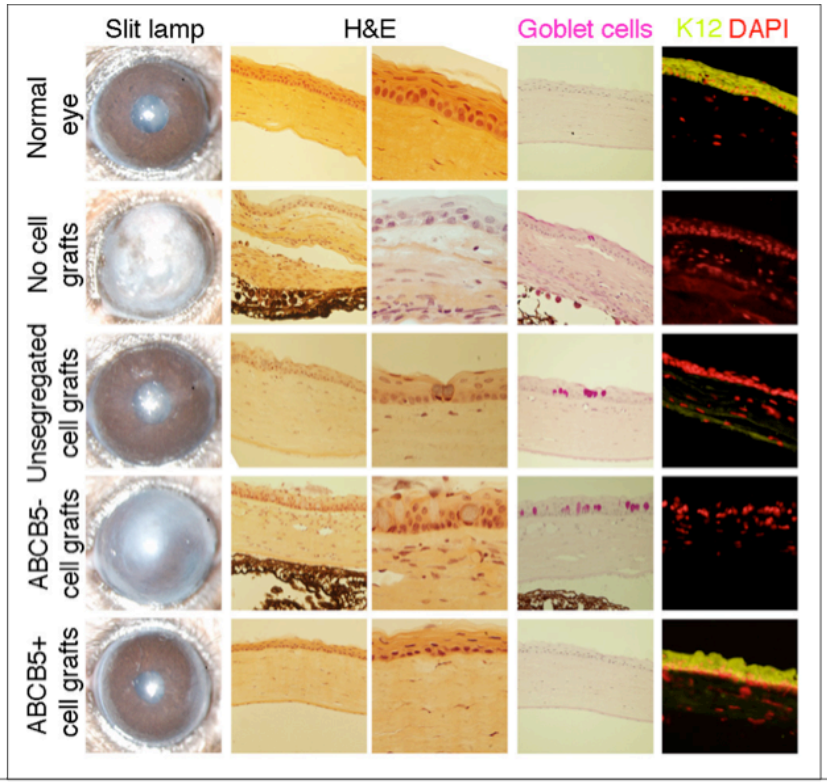

Figure 2. *Analysis of* ***murine syngeneic transplants*** *at 5 weeks.*
Corneal transparency evaluated by slit lamp (column 1). H&E staining (column 2- lower magnification; column 3 higher magnification). Periodic acid–Schiff (PAS) staining to detect Goblet cells (column 4). Keratin12 (K12) staining (column 5).

As a control, normal untreated murine corneas are shown in row 1. As a negative control, mice were treated with a fibrin gel carrier without cells (row 2). Mice treated with fibrin gel grafts containing unsegregated, ABCB5-, or ABCB5+ murine limbal epithelial cells are shown in rows 3, 4 and 5, respectively. Only transplants containing ABCB5+ limbal epithelial cells displayed normal corneal histology, lack of goblet cells, and expression of K12+ mature corneal epithelial cells.

KEY RESEARCH ACCOMPLISHMENTS:

- ABCB5 positive cells recovered from the limbal epithelium of human cadaveric donors were capable of restoring the corneal epithelium when transplanted onto the ocular surface of immunosuppressed mice (NSG mice) with an induced limbal stem cell deficiency.

- Human ABCB5 negative limbal cells were unable to restore the corneal epithelium.

- ABCB5 positive cells recovered from the limbal epithelium of C57BL/6J mice were capable of restoring the corneal epithelium when transplanted onto the ocular surface of syngeneic mice with an induced limbal stem cell deficiency. ABCB5 negative limbal cells were unable to restore the corneal epithelium.

REPORTABLE OUTCOMES: (i) a manuscript describing our data is in the final stages of preparation and will be submitted this month, (ii) an NIH grant was submitted to support funding of future experiments (will be reviewed October 23, 2012.

CONCLUSIONS: Together, these studies (both mouse and human) strongly support our hypothesis that transplantation of human ABCB5+ limbal stem cells, but not ABCB5- limbal cells possess the capacity to restore the corneal epithelium. Moreover, they provide initial proof-of-principle for the specific therapeutic utility of this novel limbal stem cell population for treatment of limbal stem cell deficiency in human patients.

Cornea

Kinetics and Function of Mesenchymal Stem Cells in Corneal Injury

Yinan Lan,[1] Shilpa Kodati,[1] Hyun Soo Lee, Masahiro Omoto, Yiping Jin, and Sunil K. Chauhan

Purpose. Bone marrow-derived mesenchymal stem cells (MSCs) hold great promise for wound healing and tissue regeneration. In the present study, we investigated the impact of corneal injury on the homeostasis of endogenous MSCs, and the potential of MSCs to home to injured tissue and promote corneal repair.

Methods. Corneal injury in mice was induced by thermal cauterization. Circulating MSCs were quantified by flow cytometric analysis. Ex vivo expanded red Q-dot–labeled or GFP+ bone marrow–derived MSCs were intravenously injected after injury and detected using epifluorescence microscopy. Corneal fluorescein staining was performed to evaluate epithelial regeneration.

Results. Following the induction of corneal injury in mice, a 2-fold increase in the frequency of circulating endogenous MSCs was observed within 48 hours of injury, which was accompanied by increased levels of the stem cell chemoattractants, substance P and SDF-1, in both the injured cornea and blood. Systemically administered MSCs homed to the injured cornea, but not to the normal cornea, and showed long-term survival. In addition, in the setting of corneal injury, MSC administration showed significant and rapid corneal epithelial regeneration.

Conclusions. These findings provide novel evidence that corneal injury causes significant mobilization of endogenous MSCs into blood, and that MSCs home specifically to the injured cornea and promote regeneration, highlighting the therapeutic implications of MSC-mediated tissue repair in corneal injury. (*Invest Ophthalmol Vis Sci.* 2012;53:3638–3644) DOI:10.1167/iovs.11-9311

The limbal stem cell (LSC) compartment is the critical source of renewal for the corneal epithelium. Partial or total LSC deficiency is a major cause of corneal transparency loss and ocular morbidity. In addition to trauma and burn injuries, intrinsic factors that lead to LSC deficiency include dysfunction or reduction in the numbers of LSCs due to autoimmune diseases, multiple surgeries, or diabetes.[1] Current therapeutic options for LSCs currently include autologous limbal grafts for unilateral lesions and limbal allografts for extensive or bilateral lesions.[2] However, these strategies are associated with potential adverse effects, including the induction of LSC deficiency in the healthy eye following autologous procurement, and the risks of immunosuppressive therapy post allograft.[3] As a consequence, other strategies, including the potential usage of bone marrow mesenchymal stem cells (MSCs) in corneal injuries, are gaining prominence.[4]

MSCs are self-renewing, nonhematopoietic stromal stem cells comparable to embryonic stem cells in terms of their multipotency and proliferative and differentiation potential.[5] Due to their multilineage differentiation potential and immunomodulatory properties, MSCs present a promising tool for cell therapy, and are currently being tested in Food and Drug Administration–approved clinical trials for myocardial infarction, stroke, meniscus injury, limb ischemia, graft-versus-host disease, and autoimmune disorders (http://clinicaltrial.gov). They have been extensively tested and proven effective in preclinical studies for these disorders.[6] In addition, MSCs have a unique property of homing to the inflamed/injury sites. A significant tissue injury, such as myocardial infarction, stroke, or renal injury, causes the release of cyto-chemokines and other factors, which stimulate bone marrow to mobilize MSCs into the blood and direct their trafficking to the site of injury to promote tissue regeneration/repair.[7,8]

The application of MSCs, or conditioned media derived from MSC cultures, to the injured cornea, has been demonstrated to improve corneal wound healing.[9–12] The impact of corneal injury on the homeostasis of endogenous MSCs, and the homing and engraftment potential of systemically administered MSCs to the cornea are still not well understood, however. In this study, we demonstrate that corneal injury leads to increased frequencies of circulating endogenous MSCs and elevated levels of the putative stem cell-specific chemoattractants in the peripheral blood. Furthermore, intravenously administered MSCs were observed to home specifically to the injured cornea and promote epithelial regeneration.

Methods

Animals

Six- to 8-week-old male C57BL/6 wild-type mice (Charles River Laboratories, Wilmington, MA) and green fluorescent protein (GFP) transgenic mice (Jackson Laboratory, Bar Harbor, ME) were used in these experiments. The protocol was approved by the Schepens Eye Research Institute Animal Care and Use Committee, and all animals were treated according to the ARVO Statement for the Use of Animals in Ophthalmic and Vision Research.

Isolation, Expansion, and Characterization of MSCs

Bone marrow was harvested from euthanized B6 wild-type and GFP.B6 mice. Using the plastic adherence method of MSC cultivation, bone

From the Schepens Eye Research Institute and Massachusetts Eye and Ear Infirmary, Department of Ophthalmology, Harvard Medical School, Boston, Massachusetts.

[1]These authors contributed equally to the work presented here and should therefore be regarded as equivalent authors.

Supported in part by grants from the Department of Defense and the Eleanor and Miles Shore Fellowship for Scholars in Medicine, Harvard Medical School, Boston, Massachusetts.

Submitted for publication December 13, 2011; revised March 29, 2012; accepted April 18, 2012.

Disclosure: **Y. Lan**, None; **S. Kodati**, None; **H.S. Lee**, None; **M. Omoto**, None; **Y. Jin**, None; **S.K. Chauhan**, None

Corresponding author: Sunil K. Chauhan, Department of Ophthalmology, Harvard Medical School, Schepens Eye Research Institute, 20 Staniford Street, Boston, MA 02114; sunil.chauhan@schepens.harvard.edu.

Investigative Ophthalmology & Visual Science, June 2012, Vol. 53, No. 7

marrow cells were cultured in murine MSC-specific MesenCult basal media and supplement (Stem Cell Technologies, Vancouver, BC, Canada) according to manufacturer's instructions. Cells were passaged at every third day, and after 8 to 10 passages, MSCs were characterized phenotypically for the expression of MSC markers by flow cytometry as described later, and functionally by their in vitro differentiation into adipocytes using MesenCult adipogenic stimulatory supplements (Stem Cell Technologies). Oil-red-O (Sigma-Aldrich, St. Louis, MO) staining was used to confirm the differentiation of MSC into the adipocytes.

Model of Corneal Injury and Treatment

Mice were subjected to corneal injury in the right eye under general anesthesia. Using a thermal cautery device (Aaron Medical Industries Inc., St. Petersburg, FL), epithelial cautery was performed on half of the cornea and limbus to induce epithelial injury. Dead corneal and limbal epithelia were mechanically scraped using a surgical blade followed by rinsing with 0.9% NaCl and application of topical antibiotic ointment. To study the kinetics of endogenous MSCs and chemoattractants, mice were killed at 24, 48, and 72 hours post injury to collect blood for flow cytometry and ELISA analyses as described later. To study the homing and therapeutic potential of MSCs, mice were randomly divided into cautery-alone or MSC-recipient groups, with $n = 6$ in each group. In vitro expanded and characterized MSCs, labeled with Alexa 647 Qtracker dots (Invitrogen, Grand Island, NY) or MSCs derived from GFP-B6 mice, were injected into the tail veins of mice 1 hour post injury. Mice were killed at days 3, 21, and 50, and corneas were harvested to examine the presence of MSCs.

Evaluation of Corneal Epithelial Regeneration

Corneal epithelial regeneration following cautery was determined by fluorescein staining of the corneal surface to evaluate the area of epithelial defect, and by molecular analysis using real-time PCR as described later. Corneal fluorescein staining was performed using slit lamp biomicroscopy at baseline before the application of cautery, and then subsequently on the same mice at 24, 48, and 96 hours. Using a micropipette, 1 μL of 2.5% fluorescein (Sigma-Aldrich) was applied to the corneal surface. After 3 minutes, epithelial staining was scored in a masked fashion using slit lamp biomicroscopy under cobalt blue light and photographic images taken. The area of the epithelial defect (green color) was calculated using National Institutes of Health Image J (version 1.34s) software.

Flow Cytometry

Flow cytometry was performed to characterize the phenotype of in vitro expanded MSCs and for the purpose of quantifying the frequencies of circulating MSCs in the peripheral blood following corneal injury. Cultured MSCs in single-cell suspension were stained with conjugated monoclonal antibodies to CD45, CD34, SCA-1, and CD29 or CD105. All the antibodies with their matched isotype controls were purchased from Biolegend (San Diego, CA). Stained cells were analyzed on an EPICS XL flow cytometer (Beckman Coulter, Brea, CA). For analyzing the frequencies of circulating endogenous MSCs, peripheral blood was collected at 24, 48, and 72 hours following injury. Red cells were lysed by the addition of red cell lysing buffer (Sigma-Aldrich) to blood samples, and the final washed single-cell suspension was used for antibody staining.

Real-Time PCR

Corneas were harvested at 96 hours after cautery from each group, and RNA isolated with RNeasy Micro Kit (Qiagen, Valencia, CA) and reverse transcribed using Superscript III Kit (Invitrogen). Real-time PCR was performed using Taqman Universal PCR Mastermix and preformulated primers for murine glyceraldehype-3-phosphate dehydrogenase (GAPDH), ABCG2, P63, Hes1, CEBPσ, K12, K19, TGF-β, and IL-1Ra (Applied Biosystems, Foster City, CA). The results were analyzed by the comparative threshold cycle method, using GAPDH as an internal control and normalized to expression levels in noncauterized cornea tissue.

Fluorescence Microscopy

Freshly excised corneas were washed in PBS and fixed with 4% paraformaldehyde for 15 minutes. Whole corneas were then mounted onto slides with DAPI containing mounting medium (Vectashield; Vector Laboratories, Burlingame, CA), and visualized under epifluorescence microscope (Nikon, Melville, NY) at ×40 magnification to detect red Q-dot-labeled MSCs. In case of detection of GFP+MSC, paraformaldehyde-fixed corneas were permeabilized with 0.5% TritonX-100 for 10 minutes, and then immunostained with Alexa Fluor 488 conjugated anti-GFP (Invitrogen).

ELISA

Levels of SDF-1 and substance P in peripheral blood were analyzed using commercially available murine SDF-1α ELISA kit (R&D Systems,

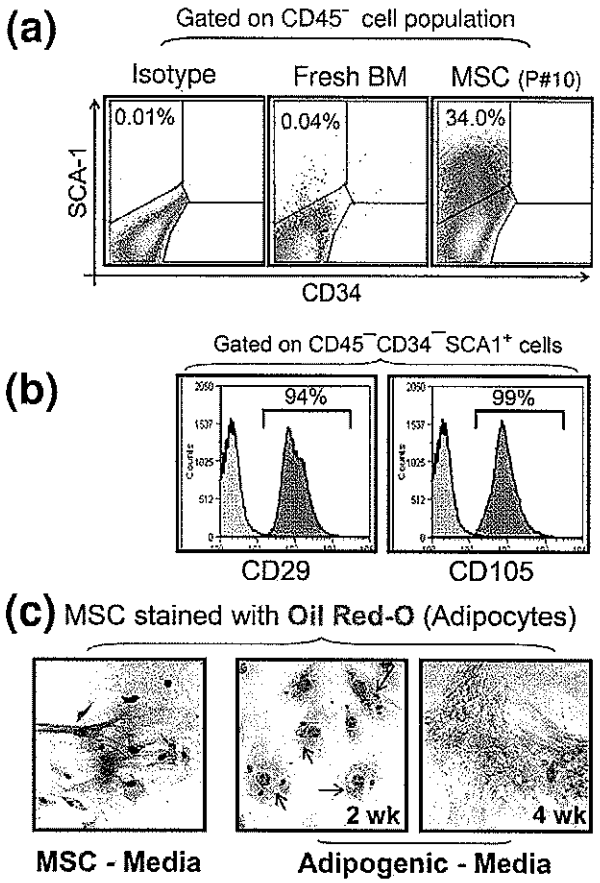

FIGURE 1. Expansion and characterization of MSCs. (a) Representative flow cytometric dot plots showing frequencies of $CD45^-CD34^-SCA1^+$ MSCs in fresh bone marrow (BM) and after 10 culture passages of BM in murine-specific MSC culture media. (b) Representative flow cytometric histograms confirming expression of CD29 (94%) and CD105 (99%) on $CD45^-CD34^-SCA1^+$ MSCs. (c) Microscopic images of MSCs cultured in adipogenic media and stained with Oil-Red-O dye. At 2 weeks, small red color vacuoles (*arrows*) were observed within the cytoplasm. By 4 weeks, mature adipocytes were seen, evident by the coalesced cells and large red vacuoles.

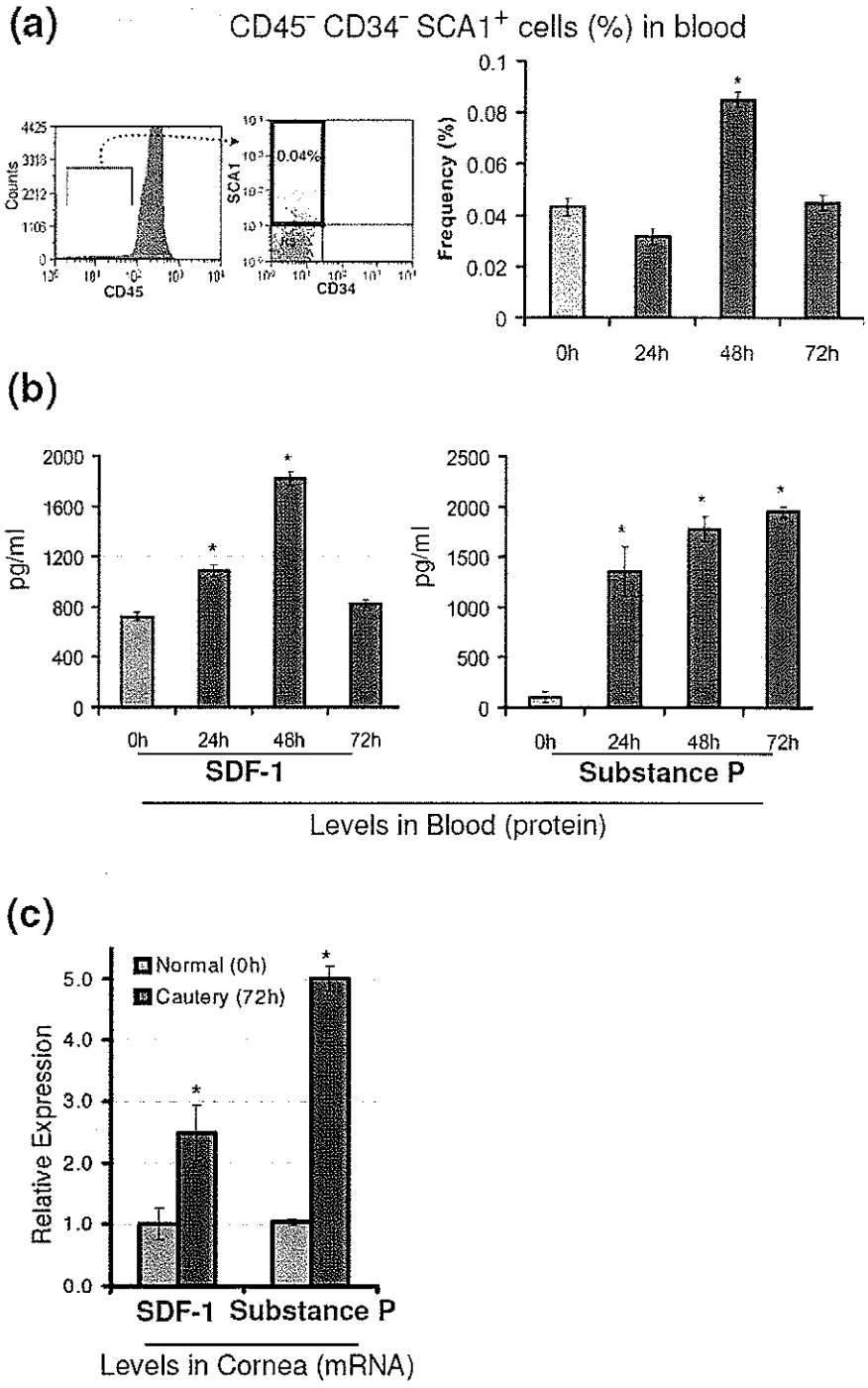

FIGURE 2. Corneal injury leads to increased frequencies of circulating MSCs in peripheral blood with an associated increase in the levels of potential stem cell-specific chemoattractants. (**a**) A significant 2-fold increase in the frequencies of $CD45^{-}CD34^{-}SCA1^{+}$ MSCs was observed in peripheral blood at 48 hours after injury. (**b**) ELISA quantification of chemoattractants in peripheral blood. A progressive and significant increase in the protein levels of SDF-1 was observed, which peaked at 48 hours, and returned to baseline by 72 hours. In contrast, a rapid rise in substance P levels was demonstrated by 24 hours, with levels continuing to increase at all time points evaluated ($n = 3$ mice/time point, $^{*}P < 0.05$). (**c**) Relative mRNA expression of chemoattractants in normal and cauterized cornea at 72 hours following the induction of injury. A significant increase in the expression levels of both SDF-1 and substance P was observed in the injured cornea.

Minneapolis, MN) and substance P assay kit (R&D Systems) as per the manufacturer's instructions.

Statistical Analysis

A two-tailed Student's *t*-test was performed and *P* values less than 0.05 were regarded as statistically significant. Results are presented as the mean ± SEM of at least three experiments.

RESULTS

Characterization and Expansion of MSCs

To study MSCs in corneal injuries, we first standardized the methodology for in vitro culture and characterization of MSCs according to the criteria outlined in the Mesenchymal and Tissue Stem Cell Committee of the International Society for

Cellular Therapy statement.[13] MSCs were cultured and expanded using the plastic adherence method, and after 10 subculture passages, most of cells were spindle shaped and had a fibroblast-like morphology. Cell surface markers were assessed using flow cytometry to phenotypically characterize in vitro expanded MSCs. All the cells were negative for the expression of hematopoietic markers CD45 and CD34, and were positive for the expression of MSC-associated markers, including SCA1, CD29, and CD105 (Figs. 1a, 1b), consistent with previous reports.[13,14] Cultured MSCs were further assessed for their functionality by determining their ability to differentiate into adipocytes. Following 2 weeks of culturing MSCs in adipogenic media, small red vacuoles were detected using Oil-red-O staining. By week 4, adipocytes were coalesced together and large-sized lipid vesicles were evident, indicating differentiation into mature adipocytes (Fig. 1c).

Corneal Injury Alters Homeostasis of Circulating Endogenous MSCs

It has been established that increased frequencies of MSCs are found in the peripheral blood after the stimulus of an injury.[15,16] We herein aimed to determine if corneal injury could have an impact on bone marrow homeostasis and alter the frequencies of circulating endogenous MSCs. Flow cytometric studies performed on peripheral blood of mice with corneal injury showed significantly increased (2-fold) frequencies of $CD45^{-}CD34^{-}SCA1^{+}$ cells at 48 hours post injury compared with naïve mice (Fig. 2a). Furthermore, substance P and stromal cell–derived factor-1 (SDF-1; also known as chemokine C-X-C motif ligand 12 [CXCL12]) have been reported to possess stem cell chemoattractant properties, which can facilitate mobilization of endogenous MSCs from bone marrow into peripheral blood.[7,17] We therefore subsequently quantified the protein levels of substance P and SDF-1 in the peripheral blood following corneal injury (Fig. 2b). ELISA analyses revealed a gradual increase in SDF-1 levels, which peaked at 48 hours post injury (2.5-fold). In contrast, a rapid increase (15-fold) was observed in substance P levels by 24 hours, with levels continuing to rise until 72 hours. To confirm the injured corneal tissue as the potential source of these MSC chemoattractants, we characterized mRNA expression of substance P and SDF-1 in corneal tissue at 72 hours post cautery (Fig. 2c). Significantly increased expression levels were evident at this time point (~2.5- and ~5-fold increase in SDF-1 and substance P respectively). Taken together, these data suggest that corneal injury could lead to an increased expression of stem cell chemoattractants that mobilize endogenous MSCs into peripheral blood.

MSCs Home Specifically to the Injured Cornea

We sought to ascertain whether MSCs have the potential to home to corneal tissue by tracking the presence of intravenously injected MSCs in both injured and contralateral healthy corneas. MSCs homing to cornea following injury was investigated by injecting red Q-dot–labeled or GFP+ bone marrow–derived MSCs (GFP+MSCs). MSCs were injected 1 hour post injury, and epifluorescence microscopy on corneal wholemounts was used to detect the labeled cells (Fig. 3a). At 72 hours after injury, substantial numbers of Q-dot–labeled cells were visible specifically in the injured corneas, but not in the contralateral cornea (Fig. 3b). Next, to determine if MSCs remained detectable in the injured cornea at a later time point, we injected GFP+MSCs and evaluated the presence of these cells up to day 50. GFP+MSCs were similarly observed in the injured cornea at this time point, but not on the contralateral side (Fig. 3b), suggesting that MSCs not only home to the cornea in response to an injury, but also indicating that these cells persist long term at the site of injury.

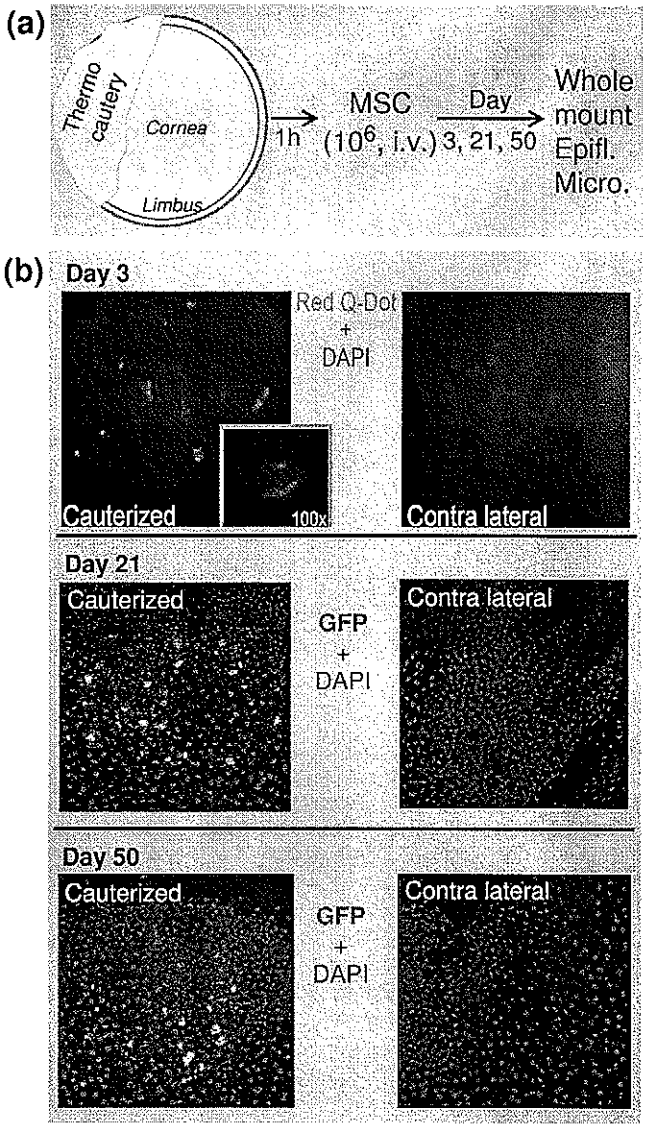

FIGURE 3. MSCs home and persist in the cornea following injury. (a) Schematic diagram of the experimental design to study MSCs homing to the injured cornea. Thermocautery was applied to half of the cornea and limbus to induce epithelial injury. After 1 hour of corneal injury, in vitro expanded and characterized MSCs were injected intravenously to one group of mice ($n = 6$), and then at days 3, 21, and 50, corneas were harvested to examine the presence of MSCs. (b) Epifluorescence micrographs (×40) of corneal wholemounts showing presence of red quantum-dot–labeled MSCs at day 3 in the epithelium of the cauterized cornea but not in the contralateral cornea. Similarly at days 21 and 50, GFP+ MSCs were observed in the cauterized cornea, but remain absent from the contralateral side.

MSCs Promote Corneal Epithelial Regeneration following Injury

We finally studied whether homing and engraftment of MSCs to injured cornea can promote epithelial regeneration. To determine the extent of epithelial regeneration following corneal injury in MSC-injected or control mice, we used corneal fluorescein staining to determine the extent of the epithelial defect. A smaller epithelial defect, suggestive of more rapid epithelial regeneration, was apparent by 96 hours in the

MSC-injected mice compared with the cautery-only group (Fig. 4a). To further characterize the impact of MSCs on epithelial regeneration at the molecular level, mRNA expression of both stem cell and differentiated corneal epithelial cell markers were quantified in both groups of cauterized corneas. Corneas from mice receiving MSCs had substantially increased (~2-fold) mRNA expression of ABCG2, P63, Hes1, and CEBPσ stem cell markers, and K12 and K19 epithelial cell markers compared with control cautery-only mice that had not received MSCs (Fig. 4b). MSCs are known to possess potent anti-inflammatory properties.[6] To ascertain whether MSC administration is associated with an increase in anti-inflammatory factors in the injured cornea, we characterized mRNA expression of TGF-β and IL-1Ra in the two groups of cauterized corneas. Increased expression levels of both TGF-β and IL-1Ra were evident in corneas from MSC recipient mice compared with control mice.

Discussion

We show herein that corneal injury leads to the mobilization of endogenous MSCs and elevation of stem cell chemotactic factors in the peripheral blood, and that systemically administered MSCs home specifically to the injury site and promote corneal epithelial regeneration.

Our characterization of increased frequencies of MSCs in the peripheral blood following corneal injury is the first report showing the impact of corneal injury on endogenous $CD34^{-}CD45^{-}Sca\text{-}1^{+}$ MSC homeostasis and is consistent with previous published findings of injury to other tissues (non-ocular) stimulating enhanced mobilization of MSCs.[15,16] The frequencies of circulating MSCs peaked at 48 hours after corneal injury, suggesting that this insult provides a transient stimulus for MSC release. Furthermore, the release of potential stem cell-specific chemoattractants from injured tissues have been implicated in inducing the mobilization of endogenous

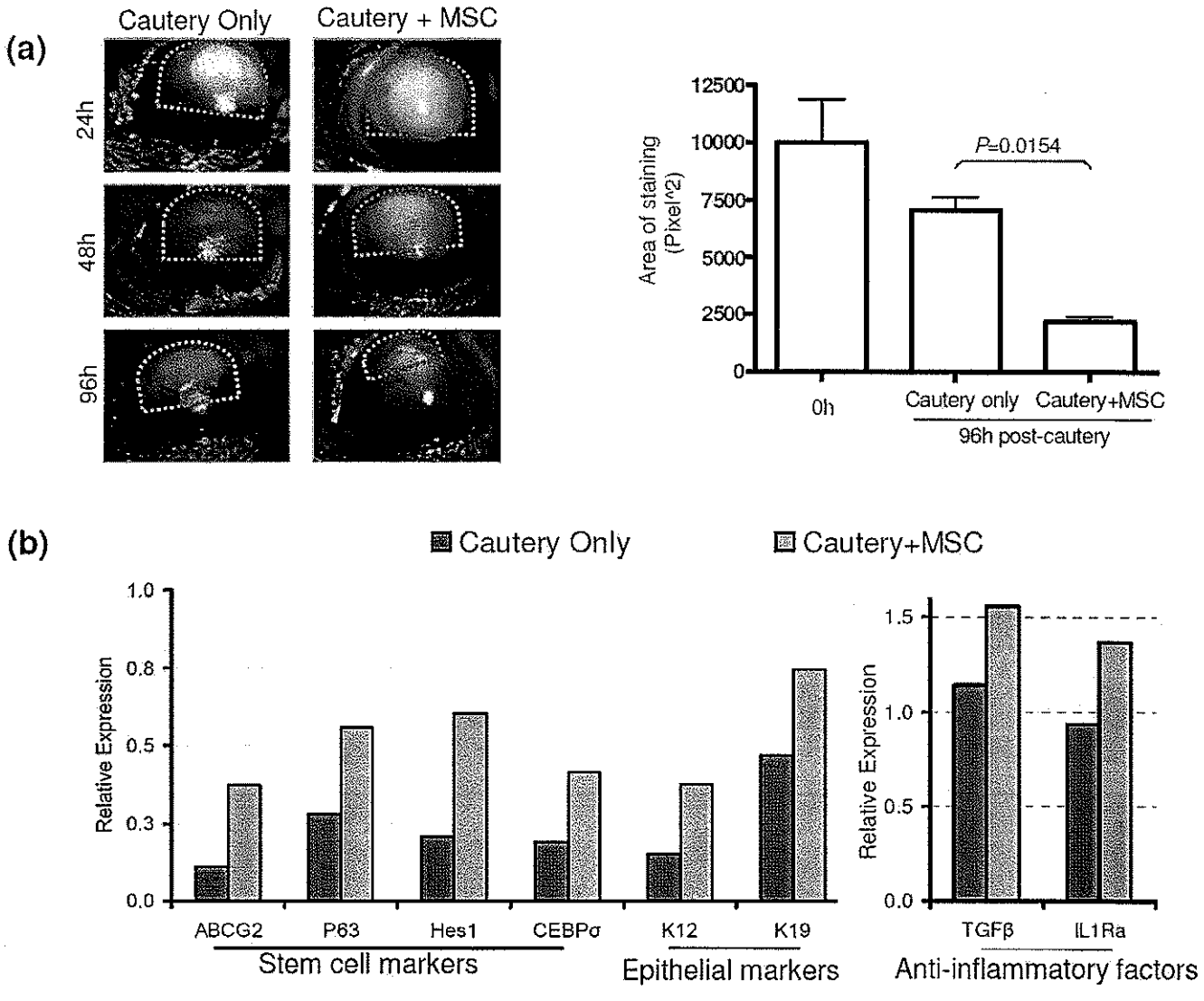

Figure 4. MSCs promote corneal epithelial regeneration. (a) *Left panel*: Representative slit lamp biomicroscopy images of fluorescein-stained corneas at 24, 48, and 96 hours post injury. A smaller area of fluorescein staining, suggestive of a faster rate of regeneration, was seen at 48 and 96 hours post injury in MSC-injected mice compared with the cautery-only group ($n = 6$ mice). *Right panel*: The mean area of fluorescein staining was significantly less in the MSC recipient mice compared with the cautery-only mice at 96 hours ($P < 0.02$). (b) Corneas isolated from MSC-injected mice at 96 hours had a higher mRNA expression of markers of stemness and epithelial cells compared with cautery-only mice. Additionally, higher mRNA expression levels of the anti-inflammatory factors TGF-β and IL-1Ra were observed in corneal tissue derived from MSC-recipient mice. The results were normalized to mRNA expression levels in the cornea of normal mice (defined as 1 on the y-axis).

MSCs into peripheral blood,[18] which is consistent with our results that indicate the coincidence of increased frequencies of circulating MSCs with elevated levels of SDF-1 and substance P after corneal injury. In a similar manner to leukocyte trafficking, the directional migration of MSCs to inflamed and injured tissues is influenced largely by the release of chemoattractants from these affected sites.[19] Our data of elevated levels of SDF-1 and substance P in the cauterized cornea is also suggestive of their role in the mobilization and recruitment of MSCs to the injured cornea. Raised levels of SDF-1 in the peripheral blood and injured tissues are seen in both human and animal models following injury and trauma, and have been implicated in the homing of MSCs to injured tissues, in addition to its function of facilitating MSC mobilization from the bone marrow.[20,21] Similarly, a recent study highlights an important function of neuropeptide substance P as a systemically acting injury-inducible messenger that mobilizes and recruits CD29+ stromal-like cells to the site of injury, resulting in accelerated wound healing.[7]

Using a combination of Q-dot–labeled and GFP+MSCs, we demonstrate MSCs homing to the injured cornea. Although relative specificity for the injured tissue was confirmed by the absence of MSC infiltration into the contralateral uninjured cornea, previous reports have suggested that an element of nonspecific MSC infiltration may occur, evident by small numbers of MSCs migrating into noninjured solid organs.[22,23] Our finding of MSCs homing to the site of injury and promoting repair of the injured cornea corroborates previous reports on MSC infiltration after systemic administration in solid organ injury, including in models of myocardial infarction, cerebral ischemia, pulmonary fibrosis, and nephropathy[8]; however, controversy still remains as to whether these MSCs are capable of persisting long term in the injured cornea.[24] Our observation of MSCs remaining detectable in the cornea up to 50 days post injury is the first report showing long-term survival of MSCs in corneal tissue. In contrast, however, a recent study on the systemic administration of human MSCs in a rat corneal injury model has suggested that the enhanced wound healing was the result of paracrine effects of MSCs from a distant site, rather than their engraftment into corneal tissues.[25] These differences may be in part explained by the usage of human MSCs in animal models, and the potential issues with integration and engraftment of cells across the xeno-species barrier.

It is well established that MSCs possess a series of anti-inflammatory and immunomodulatory properties.[6] Our findings of elevated expression of anti-inflammatory factors in injured corneas from mice receiving intravenously administered MSCs are consistent with these findings. It has been proposed that the suppression of inflammation during the acute phase of injury by the application of MSCs lessens the severity of loss of LSCs, and therefore improves epithelial regeneration. In support of MSCs promoting epithelial wound healing indirectly via suppressing inflammation is the demonstration of high quantities of the anti-inflammatory cytokines IL-10 and TGF-β found in the injured corneas after the application of MSCs to the ocular surface.[26] In addition to this, it has recently been suggested that the MSC-secreted TNF-α stimulated gene 6 (TSG-6) protein has an important role in directly mediating the anti-inflammatory effects of MSCs in corneal wound healing.[25,27] Finally, our observation of increased IL-1Ra expression in corneas from MSC recipient mice is in accord with a previous report demonstrating IL-1Ra expressing populations of murine MSC, and the role of MSC-derived IL-1Ra in promoting lung injury repair.[28] Given the absence of a comparable effect seen after treatment with immunosuppression,[11] however, it is unlikely that the immunomodulatory capabilities of MSCs can fully explain their impact on corneal epithelial regeneration.

In summary, the present study elucidates the dynamics of endogenous MSC trafficking and MSC-mediated regeneration in cornea. However, further investigation is required to delineate the mechanisms through which MSCs facilitate epithelial regeneration, particularly the relative contribution of paracrine effects versus direct differentiation of MSCs. The demonstration that MSCs home to the injured cornea, survive, and promote corneal epithelial regeneration may have therapeutic implications for corneal injuries affecting the LSC compartment, for which only limited treatment options are available.

References

1. Daniels JT, Harris AR, Mason C. Corneal epithelial stem cells in health and disease. *Stem Cell Rev.* 2006;2:247–254.
2. Dua HS, Miri A, Said DG. Contemporary limbal stem cell transplantation—a review. *Clin Experiment Ophthalmol.* 2010;38:104–117.
3. Liang L, Sheha H, Li J, Tseng SC. Limbal stem cell transplantation: new progresses and challenges. *Eye (Lond).* 2009;23:1946–1953.
4. Liu H, Zhang J, Liu CY, Hayashi Y, Kao WW. Bone marrow mesenchymal stem cells can differentiate and assume corneal keratocyte phenotype. *J Cell Mol Med.* 2012;16:1114–1124.
5. Jiang Y, Jahagirdar BN, Reinhardt RL, et al. Pluripotency of mesenchymal stem cells derived from adult marrow. *Nature.* 2002;418:41–49.
6. Uccelli A, Moretta L, Pistoia V. Mesenchymal stem cells in health and disease. *Nat Rev Immunol.* 2008;8:726–736.
7. Hong HS, Lee J, Lee E, et al. A new role of substance P as an injury-inducible messenger for mobilization of CD29(+) stromal-like cells. *Nat Med.* 2009;15:425–435.
8. Karp JM, Leng Teo GS. Mesenchymal stem cell homing: the devil is in the details. *Cell Stem Cell.* 2009;4:206–216.
9. Gu S, Xing C, Han J, Tso MO, Hong J. Differentiation of rabbit bone marrow mesenchymal stem cells into corneal epithelial cells in vivo and ex vivo. *Mol Vis.* 2009;15:99–107.
10. Jiang TS, Cai L, Ji WY, et al. Reconstruction of the corneal epithelium with induced marrow mesenchymal stem cells in rats. *Mol Vis.* 2010;16:1304–1316.
11. Ma Y, Xu Y, Xiao Z, et al. Reconstruction of chemically burned rat corneal surface by bone marrow-derived human mesenchymal stem cells. *Stem Cells.* 2006;24:315–321.
12. Reinshagen H, Auw-Haedrich C, Sorg RV, et al. Corneal surface reconstruction using adult mesenchymal stem cells in experimental limbal stem cell deficiency in rabbits. *Acta Ophthalmol.* 2011;89:741–748.
13. Dominici M, Le Blanc K, Mueller I, et al. Minimal criteria for defining multipotent mesenchymal stromal cells. The International Society for Cellular Therapy Position Statement. *Cytotherapy.* 2006;8:315–317.
14. Meirelles Lda S, Nardi NB. Murine marrow-derived mesenchymal stem cell: isolation, in vitro expansion, and characterization. *Br J Haematol.* 2003;123:702–711.
15. Chen Y, Xiang LX, Shao JZ, et al. Recruitment of endogenous bone marrow mesenchymal stem cells towards injured liver. *J Cell Mol Med.* 2010;14:1494–1508.
16. Rojas M, Xu J, Woods CR, et al. Bone marrow-derived mesenchymal stem cells in repair of the injured lung. *Am J Respir Cell Mol Biol.* 2005;33:145–152.
17. Yu J, Li M, Qu Z, Yan D, Li D, Ruan Q. SDF-1/CXCR4-mediated migration of transplanted bone marrow stromal cells toward areas of heart myocardial infarction through activation of PI3K/Akt. *J Cardiovasc Pharmacol.* 2010;55:496–505.

18. Kucia M, Ratajczak J, Reca R, Janowska-Wieczorek A, Ratajczak MZ. Tissue-specific muscle, neural and liver stem/progenitor cells reside in the bone marrow, respond to an SDF-1 gradient and are mobilized into peripheral blood during stress and tissue injury. *Blood Cells Mol Dis*. 2004;32:52–57.
19. Smith H, Whittall C, Weksler B, Middleton J. Chemokines stimulate bidirectional migration of human mesenchymal stem cells across bone marrow endothelial cells. *Stem Cells Dev*. 2012;21:476–486.
20. Ceradini DJ, Kulkarni AR, Callaghan MJ, et al. Progenitor cell trafficking is regulated by hypoxic gradients through HIF-1 induction of SDF-1. *Nat Med*. 2004;10:858–864.
21. Hannoush EJ, Sifri ZC, Elhassan IO, et al. Impact of enhanced mobilization of bone marrow derived cells to site of injury. *J Trauma*. 2011;71:283–291.
22. Barbash IM, Chouraqui P, Baron J, et al. Systemic delivery of bone marrow-derived mesenchymal stem cells to the infarcted myocardium: feasibility, cell migration, and body distribution. *Circulation*. 2003;108:863–868.
23. Gao J, Dennis JE, Muzic RF, Lundberg M, Caplan AI. The dynamic in vivo distribution of bone marrow-derived mesenchymal stem cells after infusion. *Cells Tissues Organs*. 2001; 169:12–20.
24. Ye J, Yao K, Kim JC. Mesenchymal stem cell transplantation in a rabbit corneal alkali burn model: engraftment and involvement in wound healing. *Eye (Lond)*. 2006;20:482–490.
25. Roddy GW, Oh JY, Lee RH, et al. Action at a distance: systemically administered adult stem/progenitor cells (MSCs) reduce inflammatory damage to the cornea without engraftment and primarily by secretion of TNF-alpha stimulated gene/protein 6. *Stem Cells*. 2011;29:1572–1579.
26. Oh JY, Kim MK, Shin MS, et al. The anti-inflammatory and anti-angiogenic role of mesenchymal stem cells in corneal wound healing following chemical injury. *Stem Cells*. 2008;26:1047–1055.
27. Oh JY, Roddy GW, Choi H, et al. Anti-inflammatory protein TSG-6 reduces inflammatory damage to the cornea following chemical and mechanical injury. *Proc Natl Acad Sci U S A*. 2010;107:16875–16880.
28. Ortiz LA, Dutreil M, Fattman C, et al. Interleukin 1 receptor antagonist mediates the antiinflammatory and antifibrotic effect of mesenchymal stem cells during lung injury. *Proc Natl Acad Sci U S A*. 2007;104:11002–11007.

The Journal of Immunology

Retinal Laser Burn-Induced Neuropathy Leads to Substance P-Dependent Loss of Ocular Immune Privilege

Kenyatta Lucas, Dimitris Karamichos, Rose Mathew, James D. Zieske, and Joan Stein-Streilein

Inflammation in the eye is tightly regulated by multiple mechanisms that together contribute to ocular immune privilege. Many studies have shown that it is very difficult to abrogate the immune privileged mechanism called anterior chamber-associated immune deviation (ACAID). Previously, we showed that retinal laser burn (RLB) to one eye abrogated immune privilege (ACAID) bilaterally for an extended period of time. In an effort to explain the inflammation in the nonburned eye, we postulated that neuronal signals initiated inflammation in the contralateral eye. In this study, we test the role of substance P, a neuroinflamatory peptide, in RLB-induced loss of ACAID. Histological examination of the retina with and without RLB revealed an increase of the substance P-inducible neurokinin 1 receptor (NK1-R) in the retina of first, the burned eye, and then the contralateral eye. Specific antagonists for NK1-R, given locally with Ag within 24 h, but not 3, 5, or 7 d post-RLB treatment, prevented the bilateral loss of ACAID. Substance P knockout (KO) mice retained their ability to develop ACAID post-RLB. These data support the postulate that substance P transmits early inflammatory signals from the RLB eye to the contralateral eye to induce changes to ocular immune privilege and has a central role in the bilateral loss of ACAID. The possibility is raised that blocking of the substance P pathway with NK1-R antagonists postocular trauma may prevent unwanted and perhaps extended consequences of trauma-induced inflammation in the eye. *The Journal of Immunology*, **2012, 189: 1237–1242.**

The eye has a unique environment and contains both neuronal and nonneuronal tissues. Inflammation in the eye is heavily regulated by a wide variety of immunosuppressive factors, cytokines and neuropeptides. Previously, we reported that retinal laser burn (RLB) altered the immune homeostasis/regulation of both the treated and nontreated eye because Ags injected into the anterior chamber (a.c.) of either eye were unable to induce tolerance (1). Further testing showed that after RLB treatment, the aqueous humor from either eye was unable to induce tolerogenic APC in vitro, suggesting that the immunosuppressive environment was altered. The burned eye had evidence of injury but the nonburned eye was not physically compromised, retained its blood ocular barrier, and lacked inflammatory cell infiltration (1). Because there are no known physical connections between the eyes, we posed that neuropeptides might relay signals from the RLB-treated eye to the nontreated eye to upset immune regulation. Such signals could either turn off the existing tolerogenic immune regulation or turn on a strong immune inflammatory response that disturbs immune homeostasis in the eye.

In the eye, family members of the vasoactive intestinal polypeptide and calcitonin gene-related peptide receptor family are immunosuppressive (2). Neuronal signaling throughout the body is carried out by a variety of neuropeptide families including tachykinins. Recently, the tachykinin family member, substance P, was reported to function outside the CNS as a proinflammatory molecule in the immune response (3, 4). Moreover, substance P and its receptor, neurokinin 1 receptor (NK1-R), are expressed by eosinophils, lymphocytes, dendritic cells, macrophages, and lymphocytes (4, 5). Binding of substance P to NK1-R on immune cells causes increased production of proinflammatory molecules such as MIP-1β, IL-6, and TNF-α and exacerbates the inflammatory response (6–8). The ability of substance P to exacerbate inflammation as well as the fact that it is expressed in cells of the amacrine layer of the retina, the cornea, and nerve fibers ending in the ciliary body, iris, and cornea epithelial (9) suggested to us that it may be involved in the loss of immune privilege after RLB.

Immune-privileged sites were originally defined as areas of the body in which foreign tissue grafts survive for extended or indefinite periods of time (10). Since the first report of immune privileged sites by Sir P. Medawar (11), many reports have explored the mechanisms of immune privilege (12–17). A popular experimental model for the study of immune privilege is called anterior chamber-associated immune deviation (ACAID). In the ACAID model, Ag that is introduced in the a.c. of the eye is taken up by indigenous F4/80$^+$APC, processed, and transported to the secondary lymphoid organ (in this case, the spleen) (18). Subsequently, Ag-specific regulatory T cells are generated. F4/80$^+$ cells that leave the eye recruit more F4/80$^+$ cells to the spleen (18). Mice that receive Ag in the a.c. show a suppressed response to the s.c.-inoculated Ag by exhibiting little or no swelling postantigenic challenge in the ear (18).

Immune privilege homeostasis in the eye is due in part to regulatory mechanisms of the resident stromal cells (11, 19–22), indigenous APC (23), the dominance of soluble immunosuppressive molecules in the fluids (24), and the structural barriers of the tissues and outer borders of the eye (25). These multiple overlapping

Schepens Eye Research Institute/Massachusetts Eye and Ear Infirmary, Department of Ophthalmology, Harvard Medical School, Boston, MA 02114

Received for publication November 15, 2011. Accepted for publication May 28, 2012.

This work was supported in part by National Institutes of Health Grants EY11983 (to J.S.-S.), EY016476 (to J.S.-S.), EY020614 (to J.S.-S.), and F32 EY018983 (to K.L.) and Department of Defense Grant W81XWH (to J.S.-S.).

Address correspondence and reprint requests to Dr. Joan Stein-Streilein, Schepens Eye Research Institute, 20 Staniford Street, Boston, MA 02114. E-mail address: joan.stein@schepens.harvard.edu

Abbreviations used in this article: a.c., anterior chamber; ACAID, anterior chamber-associated immune deviation; B6, C57BL/6J; DH, delayed hypersensitivity; KO, knockout; NK1-R, neurokinin 1 receptor; RLB, retinal laser burn.

www.jimmunol.org/cgi/doi/10.4049/jimmunol.1103264

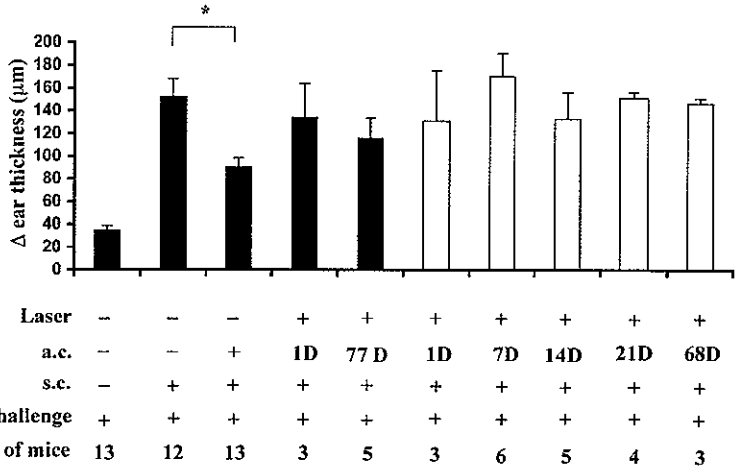

FIGURE 1. DH response after ACAID induction in RLB-treated mice. Change (Δ) in ear thickness is indicated on the ordinate. Experimental treatment of the mice in each group is indicated below each bar on the abscissa. Mice received RLB treatment or not at the time indicated prior to ACAID induction, and 1 wk later, mice were immunized with OVA; the following week, the ear pinnae were challenged with OVA. Ipsilateral, ■; contralateral, □. The time course to 21 d was performed three times. Experiment at 68 and 77 d was performed once. *$p \leq 0.05$, significant difference between the groups.

mechanisms contribute to immune homeostasis and control inflammation in the eye and define ocular immune privilege as we know it (26, 27). Immune privilege is difficult to disrupt even after the direct injection of LPS (28) or the induction of experimental autoimmune uveitis (29). However, we found that multiple aspects of immune privilege were abrogated in both eyes of mice that receive unilateral RLB treatment (1). The goal of this study was to test the hypothesis that the release of substance P after RLB contributes to the loss of immune regulation in both the burned and nonburned eye.

Materials and Methods

Animals

Female C57BL/6J (B6) mice and B6.Cg-Tac1^{tm1Bbm}/J female mice (substance P knockout [KO], B6 background) and B6.129S2-IL6^{tm1Kopf}/J female mice (IL-6 KO, B6 background) were purchased from The Jackson Laboratory (Bar Harbor, ME). Substance P KO mice lack the *tac-1* gene and thus lack substance P and neurokinin A. Mice used in all experiments were 8–12 wk old, unless otherwise stated. All animals were treated humanely and in accordance with the Schepens Eye Research Institute Animal Care and Use Committee and National Institutes of Health guidelines

Reagents and Abs

Substance P peptide, Spantide I, and Spantide II were purchased from Bachem (Torrance, CA). OVA and CFA were purchased from Sigma-Aldrich (St. Louis, MO). NK1-R Ab was purchased from Millipore (Billerica, MA). Alexa Fluor 488-conjugated goat anti-rabbit IgG assays was purchased from Invitrogen (Carlsbad, CA).

Retinal laser burn

Mice were anesthetized with ketamine (120 mg/kg) and xylazine (12 mg/kg), and pupils were dilated with 1% tropicamide. A handheld cover slip was used as a contact lens. A slit lamp was used to deliver a laser beam (wavelength, 810 nm; diameter, 200 nm; power, 50 mW; and duration time, 50 ms) from a diode laser (IRIDEX, Mountain View, CA) to the retina. Four spots (200 nm diameter) were burned on the retina in the right eye of B6 mice.

ACAID assay

ACAID was induced in mice by inoculating OVA (50 μg/2 μl HBSS) into the a.c. 7 d before sensitizing, s.c., with OVA (100 μg/ml HBSS, 50 μl) emulsified in CFA (50 μl). One week after sensitization, mice were challenged in the right ear pinnae of the with OVA-pulsed peritoneal exudate cells (2×10^5 in 10 μl). The thickness of the ear was measured 24 h later with an engineer's micrometer (Mitutoyo, Paramus, NJ), because increased ear thickness was an indication of delayed hypersensitivity (DH).

Histological analyses

Eyes were enucleated from euthanized mice at various times post-RLB treatment. Eyes were placed into Tissue-Tek Optimal Cutting Temperature Compound (Sakura Finetek, Torrance, CA) and frozen on dry ice before storing at −85°C. Horizontal cryosections (10 μm) were prepared by Schepens Eye Institute's Morphology Core.

Frozen cryosections were thawed and rehydrated in PBS for 20 min at 4°C. Slides were then incubated in blocking solution (1% goat serum + 0.1% saponin in PBS) for 1 h at 4°C. Primary staining Ab diluted in blocking solution (1:100) was added, and slides were incubated overnight at 4°C in a humidification chamber. On day 2, slides were washed in PBS and incubated for 1 h at 4°C in Alexa Fluor 488-conjugated goat anti-rabbit Ig in blocking solution. After washing, coverslips were mounted and sealed.

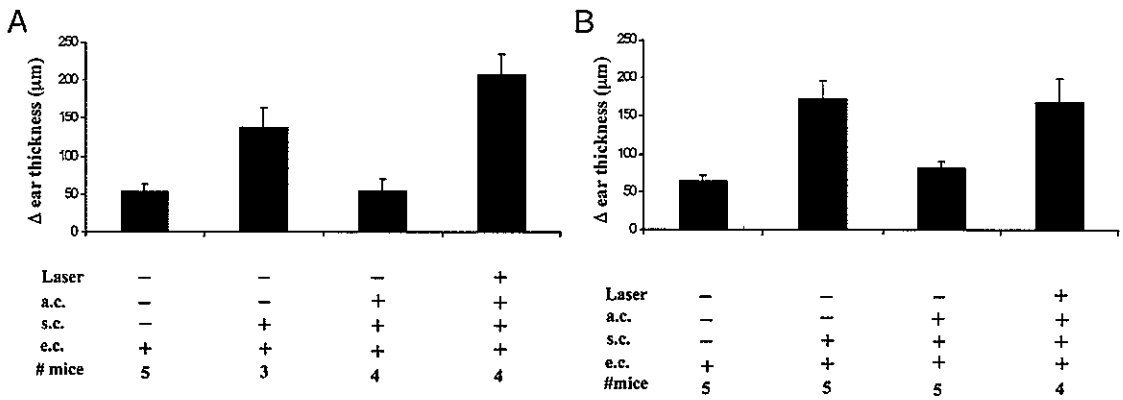

FIGURE 2. Immune privilege in B6 or IL-6KO mice. Change (Δ) in ear thickness is indicated on the ordinate. Experimental treatment of the mice in each group is indicated under the abscissa (a.c., anterior chamber inoculation; e.c., ear challenge; s.c., s.c. inoculation). (**A**) B6 mice. (**B**) IL-6 KO mice. Briefly, mice were treated with OVA 1 d after RLB treatment. One week later, mice were immunized with Ag, and mice were challenged in the ear pinnae with OVA the following week. This experiment was performed twice with similar results.

Photomicrographs were taken using a Leica TCS-SP5 confocal microscope (Leica Microsystems, Bannockburn, IL), and images shown are ×400 magnification.

Data analysis and statistics

Three-dimensional images, three-dimensional cartoons, analysis, and quantification of confocal data as well as calculation of Ab binding intensity were made using Image Pro Plus version 7 (Media Cybernetics, Bethesda, MD). Integrated OD was determined by calculating the binding intensity of NK1-R Ab binding in the slices (Image Pro Plus version 6.3; Media Cybernetics). At least three confocal z-series were used at each time point, and their average was plotted and analyzed. Statistical data were analyzed by ANOVA and Scheffe's test. (The data are presented as mean ± SEM.) A p value ≤ 0.05 was considered significant.

Results

RLB-induced extended loss of ACAID in the contralateral eye

Previously, we reported that the eye that received RLB lost immune privilege for as long as 56 d posttrauma (1), but the time course in the contralateral eye was not studied. In this study, we extended the time course to 77 d in the burned (ipsilateral) eye and tested how long ACAID abrogation lasted in the nonburned (contralateral) eye. ACAID was initiated in nontreated or RLB-treated mice 1, 7, 14, 21, 68, or 77 d post-RLB by injecting Ag into the a.c. As expected, immune privilege was present in nontreated mice (Fig. 1). Mice that received RLB treatment 1 through 77 d prior to Ag injection into the burned eye had no significant difference in ear swelling compared with immunized mice and therefore were unable to develop ACAID (Fig. 1). Mice that received RLB treatment followed by a.c. injection of Ag into the nonburned eye at all time points through 68 d post-RLB also did not develop ACAID. These data show that the loss of immune privilege after RLB treatment is long-lasting in both eyes.

Inflammatory changes to the ocular environment

A logical explanation for the inability of the eyes of RLB-treated mice to develop ACAID is that the local immunosuppressive environment was altered toward inflammation by the trauma. To test whether inflammatory cytokines were increased, eyes were enucleated 1, 3, and 7 d post-RLB, and after dissecting away the lens, the tissue RNA was extracted by standard measures. We observed increases in IL-1β, IL-6, and TNF-α in both the burned and nonburned eye, but there was no consistent pattern to suggest that any of the obvious inflammatory cytokines caused the loss of ACAID (data not shown). Because IL-6 was associated with loss of ACAID in experimental autoimmune uveitis (29), and LPS induced inflammation in the eye (28), we tested whether IL-6 was involved in RLB-induced loss of ACAID. However, IL-6 KO mice who received RLB, such as the IL-6–sufficient B6 mice, were unable to develop ACAID post-RLB (Fig. 2). Thus, IL-6 was not the cause of the RLB-induced loss of immune privilege. We wondered whether the RLB-induced inflammatory molecule might be a neuropeptide.

Immunohistochemistry analysis of NK1-R expression after RLB treatment

In the quiescent retina, 20–30% of the amacrine cells express NK1-R (30), and about one-third of NK1-R–positive cells express substance P (31). However, after RLB trauma, the relative expression of substance P or NK1-R is unknown. Substance P is a neuropeptide of the tachykinin family that exerts biologic activities in the CNS and in peripheral organs and is known to modulate parameters of the immune response (32). Because substance P has a short half-life (33), substance P protein is difficult to measure. Therefore, monitoring its receptor, NK1-R, is an effective measurement for the presence of substance P. In brief, eyes were enucleated from mice at 6 h, 72 h, or 7 d post-RLB. Eyes from untreated mice were used for controls. Cryosections were stained with anti–NK1-R, Alexa Fluor 488 conjugated with goat anti-rabbit Ig, and the nuclear stain, TO-PRO 3, before analyzing by confocal microscopy. Analysis of retinal sections showed that by 72 h, the overall expression of NK1-R in the ipsilateral eye increased in RLB-treated mice compared with untreated mice (Fig. 3). Seven days post-RLB treatment, the ipsilateral eye showed an 8-fold increase of NK1-R, and the contralateral eye had a 10-fold increase over the NK1-R expression in the retina of naive mice (Fig. 3). The amount of NK1-R staining in the retina of both eyes at 72 h and 7 d is statistically significant; $p \leq 0.05$ compared with the amount of staining seen in the naive retina. NK1-R staining of the cornea from RLB mice remained similar to the corneas in naive mice (Fig. 3). These data suggest that the substance P inflammatory pathway is activated in both eyes after RLB to one eye. NK1-R expression in the RLB-treated eye preceded the increase of expression in the contralateral eye, suggesting that the substance P originates in the burned eye, and is the messenger for the loss of

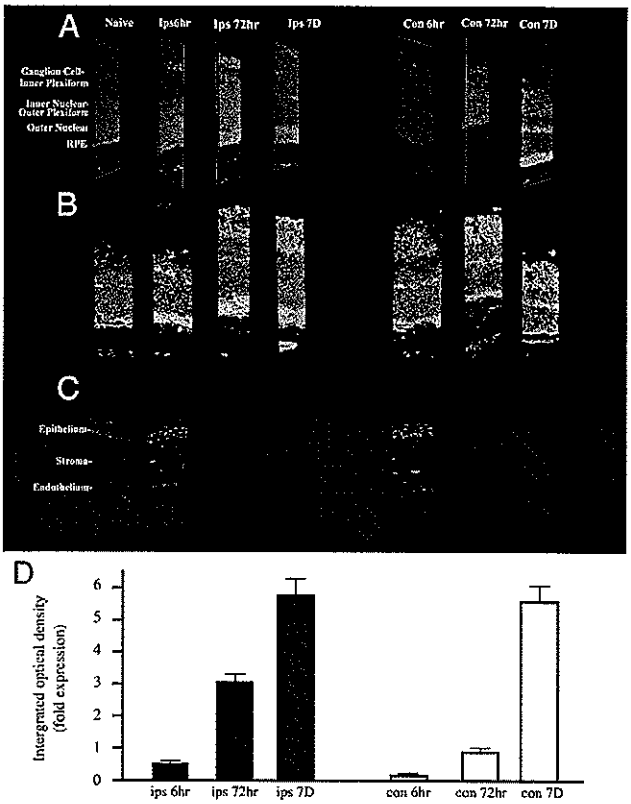

FIGURE 3. Photomicrograph of retina sections stained with NK1-R of mice that received RLB treatment or not. (**A**) Three-dimensional photomicrograph. (**B**) Three-dimensional cartoon representation. For (A) and (B), green indicates NK1-R staining, and red indicates TO-PRO 3 as a nuclear stain. Sections are from the eyes of either nontreated mice or mice that received RLB 6 h, 72 h, or 7 d prior to enucleation. The layers of the eye are indicated to the left of the photomicrograph. (**C**) Green indicates NK1-R staining, and red indicates DAPI 3 as a nuclear stain. Cornea of naive or RLB-treated mice 6 h post-RLB. Original magnification for (A)–(C) ×400. (**D**) Quantification of NKR-1 expression in retina of RLB-treated mice. Integrated OD is shown in fold increase for each group. All groups were repeated at least three times and were normalized to naive (control) mice. Each integrated OD value from the individual groups was normalized to each of the controls, and the fold increase was calculated and plotted. The confocal analysis was performed three times. □, Contralateral; ■, ipsilateral.

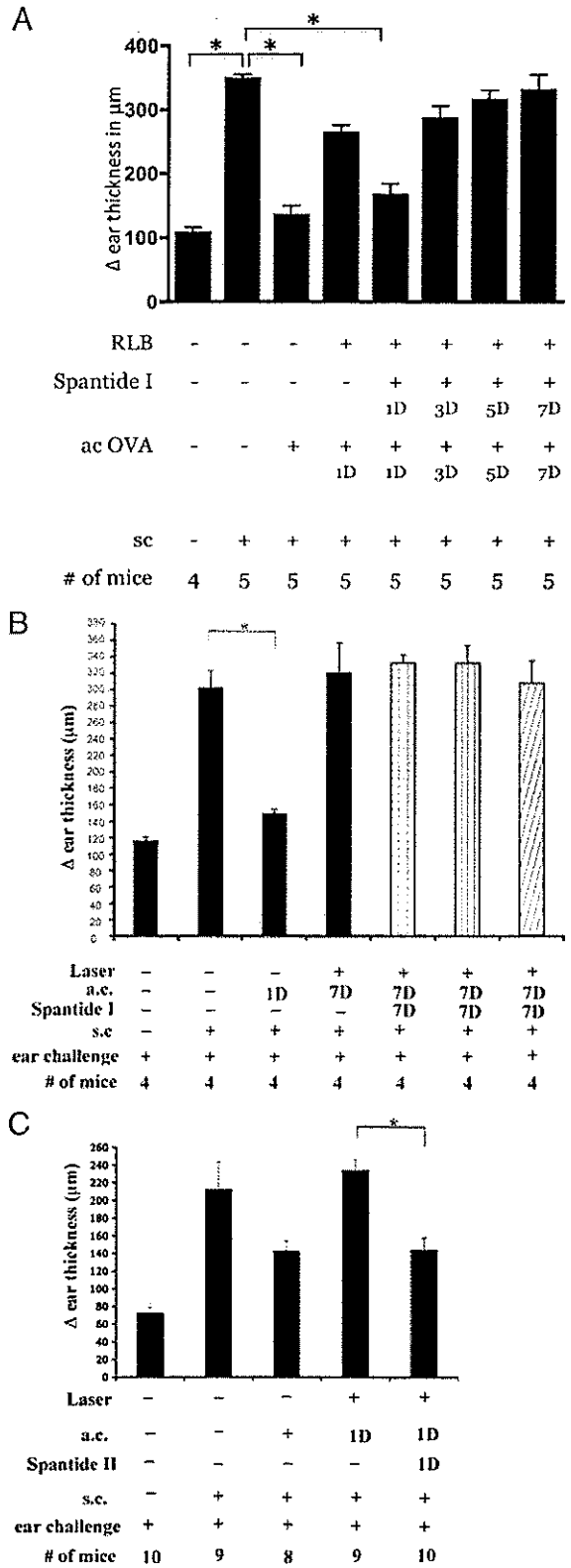

FIGURE 4. DH response after ACAID induction with or without substance P antagonist in RLB-treated mice. Change (Δ) in ear thickness is indicated on the ordinate (a.c., a.c. inoculation; s.c., s.c. inoculation). Experimental treatment of the mice in each group is indicated under the abscissa. (**A**) Spantide I treatment over time. Mice were treated with OVA and substance P antagonist 1, 3, 5, or 7 d after RLB treatment. One week later, mice were immunized with Ag, and mice were challenged in the ear pinnae with OVA the following week. Experiments on 1 and 7 d post-RLB were performed a minimum of three times; induction of ACAID with Spantide I on 3 and 5 d post-RLB was performed once. (**B**) Spantide I treatment at different concentrations. Ipsilateral, black bars; contralateral, white bars; Spantide I treatment 10^{-4} M, bar with check pattern, the dose curve was performed once; Spantide I treatment 10^{-3} M, bar with vertical line pattern; and Spantide I treatment 10^{-2} M, bar with diagonal line pattern. (**C**) Spantide II treatment. Spantide II given with OVA a.c. 1 d post-RLB. Figure shows combined results of two experiments. $^{*}p \leq 0.05$, significant difference between the groups.

immune privilege in the contralateral eye and has a critical role in interfering with immune homeostasis in both eyes.

Effect of blocking substance P receptor of RLB-induced abrogation of ACAID

To test the idea that substance P signaling induced the loss of ACAID, we used commercially available substance P receptor antagonists to block binding signaling by substance P. Spantide I is a full-length modified amino acid sequence of substance P and a selective stereotactic inhibitor for NK1-R (34). In this experiment, ACAID was initiated by injecting (a.c.) OVA with or without Spantide I (10^{-4} M), 1, 3, 5, or 7 d post-RLB treatment (Fig. 4). As before, we were unable to induce ACAID by injection (a.c.) of OVA into either eye of mice that received a unilateral RLB. RLB mice that received Spantide I and OVA (a.c.) in either the ipsilateral or the contralateral eye 1 d after RLB developed ACAID. Interestingly, ACAID was not restored in mice that received Spantide I with OVA in either the ipsilateral or contralateral eye if given after 24 h after RLB treatment. After becoming aware that the NK1-R was increased by a log 7 d post-RLB, we did a dose-response curve for Spantide I treatment at 7 d. Even at a 3-log increase in the dose, the antagonist was unable to interfere with the loss of ACAID 1 wk after RLB (Fig. 4). Because early (1 d) but not delayed treatment with Spantide I blocked the abrogation of ACAID in both eyes, the possibility arises that substance P is critical for initiating or exaggerating the inflammatory response that mitigates the immune privilege response.

Because Spantide I treatment antagonizes the substance P pathway but also induces the release of histamine from mast cells (34), the possibility was raised that histamine, rather than the substance P pathway, may be protective for immune privilege. To test the possibility that histamine contributed to the protection of immune privilege, NK1-R antagonist Spantide II was tested. Spantide II is also a full-length stereotactic inhibitor of NK1-R but did not cause the release of histamine. Thus, if Spantide II did not prevent the loss of ACAID, histamine would be involved. We found that the a.c. inoculation of OVA with Spantide II (10^{-4} M) also mitigated the RLB-induced loss of ACAID (Fig. 4). Thus, the blockade of signaling via the NK1-R, and not histamine release, is responsible for the restoration of ACAID by Spantide post-RLB. These observations support the postulate that substance P signaling through NK1-R abrogates immune privilege in the eye post-RLB.

Effect of RLB on ACAID in substance P KO versus wild-type mice

Another approach to evaluating substance P's role in the loss of ACAID was to use genetically modified mice or mice that are deficient in substance P. In brief, Ag was inoculated (a.c.) into either eye of B6 or substance P KO mice 1 d after the right eye received RLB. As before, B6 mice that received RLB prior to Ag (a.c.) did not develop ACAID, but substance P KO mice that received RLB developed ACAID post (a.c.)-inoculation of Ag (Fig. 5). These data further support the idea that substance P is the neuronal message that disrupts the ability to induce ACAID post-RLB in both eyes.

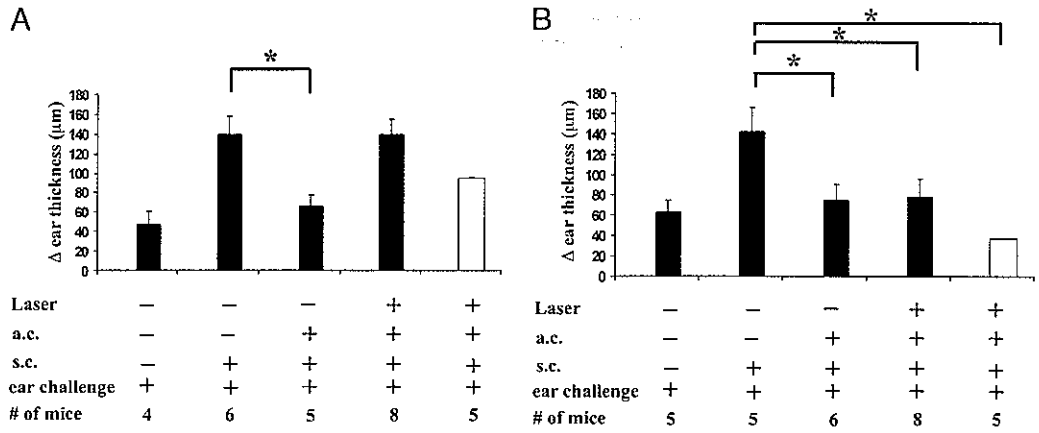

FIGURE 5. DH response after ACAID induction in RLB-treated B6 or substance P KO mice. (**A**) B6 mice. (**B**) Substance P KO mice. Change (Δ) in ear thickness is indicated on the ordinate. Experimental treatment of the mice in each group is indicated under the abscissa. Briefly, B6 or substance P KO mice were inoculated with OVA 1 d after RLB treatment. One week later, mice were immunized with Ag, and mice were challenged in the ear pinnae with OVA the following week. Ipsilateral, ■; contralateral, □. The figure represents the combined results of two experiments. *$p \leq 0.05$, significant difference between the bars.

Effect of substance P treatment in the abrogation immune privilege

Finally, we reasoned that if RLB-induced substance P, and it, in turn, induced the inflammatory signals that interfered with ACAID induction, direct a.c. injection of substance P would mitigate ACAID induction in nonburned mice. In brief, Ag was injected (a.c.) with or without the full-length substance P peptide (10^{-12} M). We observed that mice that received OVA into the a.c. developed ACAID, but mice that received OVA with the substance P peptide were unable to develop ACAID (Fig. 6). These data show that substance P has the capacity to abrogate ACAID.

Discussion

In this study, we show that RLB compromised immune privilege (ACAID) bilaterally for an extended period of time. The extended loss of immune privilege is remarkable and has not been shown before. Other studies attempting to abrogate ACAID show only short-term losses (28, 29, 35). One possibility to explain the bilateral loss of immune privilege after RLB is that cells from the periphery induce inflammatory changes in the ocular environment of both eyes. However, if the loss of immune privilege were due to a systemic signal, one would expect to observe cells infiltrating the contralateral eye, but infiltrating cells were only observed in the ipsilateral eye of mice post-RLB (1). Thus, it is improbable that inflammatory cells recruited from the periphery were responsible for the loss of ACAID in the contralateral eye post-RLB. Furthermore, we did not observe consistent increases in inflammatory cytokines, and IL-6 KO mice still lost ACAID post-RLB.

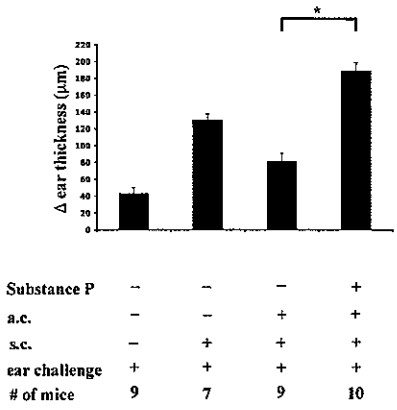

FIGURE 6. DH response after ACAID induction in substance P-treated mice. Change (Δ) in ear thickness is indicated on the ordinate. Experimental treatment of the mice in each group is indicated under the abscissa. Briefly, mice were treated with OVA and substance P peptide 1 wk prior to being immunized with Ag. One week later, mice were challenged in the ear pinnae with OVA. The figure represents the combined results of two experiments. *$p \leq 0.05$, significant difference between the bars.

In this study, we focused on the notion that a neuroinflamatory signal disrupted immune privilege and the ocular environment in both eyes post-RLB. Neuropeptides are polypeptide molecules that act as neurotransmitters to carry information between neuronal tissues. The fluids in the eye contain a variety of factors, including immunosuppressive neuropeptides that contribute to immune suppression (36, 37).

Substance P is an inflammatory neuropeptide that is found in the naive quiescent eye and was shown to contribute to the loss of ACAID in dark-adapted mice (38). Substance P binds exclusively to NK1-R. Furthermore, the binding of substance P to NK1-R induces the upregulation of the NK1-R; thus, an increase is a strong indication for the presence of substance P. Immunohistochemistry analysis showed a bilateral increase of NK1-R in both the ipsilateral and contralateral eye after RLB, suggesting a role for substance P in the neurologic communication between the two eyes. The fact that the increase in NK1-R in the contralateral eye followed the appearance of NK1-R in the burned eye suggests that the burn initiated the neuronal signal. This observation is consistent with other reports that show a unilateral injury to the CNS leads to a bilateral response (39, 40).

To our knowledge, this is the first report to show that neuropeptides are involved in the loss of immune regulation postocular trauma. It is known that in other parts of the body substance P facilitates an array of morphological and functional deficits following injury. Substance P increases vasodilatation, increases permeability of blood–brain barriers, and increases the activity of other cytotoxic neurons post–non-ocular trauma (41, 42). Substance P could be released from amacrine cells to change the immunosuppressive ocular environment to support inflammation bilaterally. Ligation of substance P to NK1-R initiates production of inflammatory cytokines from resident macrophages and microglia and recruits immune cells, including eosinophils, lymphocytes, dendritic cells, macrophages, and lymphocytes from the periphery (4, 5). Substance P ligation to NK1-R has been shown to initiate down-

stream cascade, resulting in increased production of proinflammatory molecules such as MIP-1β, IL-6, and TNF-α (6–8). Thus, substance P has the potential to promote an inflammatory environment that in turn activates resident macrophages and microglia. A change in the suppressive microenvironment of the eye could interfere with the immune homeostasis and ocular immune privilege.

The possibility arises that targeting substance P pathway with NK1-R antagonists may be therapeutically advantageous for treatment of patients postocular trauma to prevent or curb the subsequent inflammation. NK1-R antagonists have the potential to prevent the ability of substance P to amplify itself in an autocrine and paracrine fashion, to interfere with substance P initiated recruitment of peripheral inflammatory cells, and to prevent the subsequent production of many inflammatory cytokines.

Acknowledgments

We thank Thomas Flynn for preparation and submission of this manuscript. We also thank the technical training our staff received from Don Pottle for the confocal microscope. We thank Peter Mallen for expert help with figures and graphs in this manuscript.

Disclosures

The authors have no financial conflicts of interest.

References

1. Qiao, H., K. Lucas, and J. Stein-Streilein. 2009. Retinal laser burn disrupts immune privilege in the eye. *Am. J. Pathol.* 174: 414–422.
2. Taylor, A. W. 2002-2003. Neuroimmunomodulation and immune privilege: the role of neuropeptides in ocular immunosuppression. *Neuroimmunomodulation* 10: 189–198.
3. Maggi, C. A. 1997. The effects of tachykinins on inflammatory and immune cells. *Regul. Pept.* 70: 75–90.
4. O'Connor, T. M., J. O'Connell, D. I. O'Brien, T. Goode, C. P. Bredin, and F. Shanahan. 2004. The role of substance P in inflammatory disease. *J. Cell. Physiol.* 201: 167–180.
5. Douglas, S. D., J. P. Lai, F. Tuluc, L. Schwartz, and L. E. Kilpatrick. 2008. Neurokinin-1 receptor expression and function in human macrophages and brain: perspective on the role in HIV neuropathogenesis. *Ann. N. Y. Acad. Sci.* 1144: 90–96.
6. Sio, S. W., M. K. Puthia, J. Lu, S. Moochhala, and M. Bhatia. 2008. The neuropeptide substance P is a critical mediator of burn-induced acute lung injury. *J. Immunol.* 180: 8333–8341.
7. Arsenescu, R., A. M. Blum, A. Metwali, D. E. Elliott, and J. V. Weinstock. 2005. IL-12 induction of mRNA encoding substance P in murine macrophages from the spleen and sites of inflammation. *J. Immunol.* 174: 3906–3911.
8. Lotz, M., J. H. Vaughan, and D. A. Carson. 1988. Effect of neuropeptides on production of inflammatory cytokines by human monocytes. *Science* 241: 1218–1221.
9. Tervo, T., K. Tervo, and L. Eränkö. 1982. Ocular neuropeptides. *Med. Biol.* 60: 53–60.
10. Streilein, J. W. 2003. Ocular immune privilege: therapeutic opportunities from an experiment of nature. *Nat. Rev. Immunol.* 3: 879–889.
11. Medawar, P. B. 1948. Immunity to homologous grafted skin; the fate of skin homografts transplanted to the brain, to subcutaneous tissue, and to the anterior chamber of the eye. *Br. J. Exp. Pathol.* 29: 58–69.
12. Li, J. H., D. Rosen, P. Sondel, and G. Berke. 2002. Immune privilege and FasL: two ways to inactivate effector cytotoxic T lymphocytes by FasL-expressing cells. *Immunology* 105: 267–277.
13. Streilein, J. W., K. Ohta, J. S. Mo, and A. W. Taylor. 2002. Ocular immune privilege and the impact of intraocular inflammation. *DNA Cell Biol.* 21: 453–459.
14. Suter, T., G. Biollaz, D. Gatto, L. Bernasconi, T. Herren, W. Reith, and A. Fontana. 2003. The brain as an immune privileged site: dendritic cells of the central nervous system inhibit T cell activation. *Eur. J. Immunol.* 33: 2998–3006.
15. Li, X., S. Taylor, B. Zegarelli, S. Shen, J. O'Rourke, and R. E. Cone. 2004. The induction of splenic suppressor T cells through an immune-privileged site requires an intact sympathetic nervous system. *J. Neuroimmunol.* 153: 40–49.
16. Dai, Z., I. W. Nasr, M. Reel, S. Deng, L. Diggs, C. P. Larsen, D. M. Rothstein, and F. G. Lakkis. 2005. Impaired recall of CD8 memory T cells in immunologically privileged tissue. *J. Immunol.* 174: 1165–1170.
17. Sonoda, K. H., T. Sakamoto, H. Qiao, T. Hisatomi, T. Oshima, C. Tsutsumi-Miyahara, M. Exley, S. P. Balk, M. Taniguchi, and T. Ishibashi. 2005. The analysis of systemic tolerance elicited by antigen inoculation into the vitreous cavity: vitreous cavity-associated immune deviation. *Immunology* 116: 390–399.
18. Faunce, D. E., K.-H. Sonoda, and J. Stein-Streilein. 2001. MIP-2 recruits NKT cells to the spleen during tolerance induction. *J. Immunol.* 166: 313–321.
19. Sugita, S., Y. Usui, S. Horie, Y. Futagami, H. Aburatani, T. Okazaki, T. Honjo, M. Takeuchi, and M. Mochizuki. 2009. T-cell suppression by programmed cell death 1 ligand 1 on retinal pigment epithelium during inflammatory conditions. *Invest. Ophthalmol. Vis. Sci.* 50: 2862–2870.
20. Sugita, S., S. Horie, O. Nakamura, K. Maruyama, H. Takase, Y. Usui, M. Takeuchi, K. Ishidoh, M. Koike, Y. Uchiyama, et al. 2009. Acquisition of T regulatory function in cathepsin L-inhibited T cells by eye-derived CTLA-2α during inflammatory conditions. *J. Immunol.* 183: 5013–5022.
21. Zamiri, P., S. Sugita, and J. W. Streilein. 2007. Immunosuppressive properties of the pigmented epithelial cells and the subretinal space. *Chem. Immunol. Allergy* 92: 86–93.
22. Ishida, K., N. Panjwani, Z. Cao, and J. W. Streilein. 2003. Participation of pigment epithelium in ocular immune privilege. 3. Epithelia cultured from iris, ciliary body, and retina suppress T-cell activation by partially non-overlapping mechanisms. *Ocul. Immunol. Inflamm.* 11: 91–105.
23. Wilbanks, G. A., and J. W. Streilein. 1992. Macrophages capable of inducing anterior chamber associated immune deviation demonstrate spleen-seeking migratory properties. *Reg. Immunol.* 4: 130–137.
24. Taylor, A. W. 2009. Neuropeptides, aqueous humor, and ocular immune privilege. In *Neuropeptides in the Eye.* J. Troger, G. Kieslbach, and N. Bechrakis, eds. Research Signpost, Kerala, India, p. 79–91.
25. Crane, I. J., and J. Liversidge. 2008. Mechanisms of leukocyte migration across the blood-retina barrier. *Semin. Immunopathol.* 30: 165–177.
26. Stein-Streilein, J., and J. W. Streilein. 2002. Anterior chamber associated immune deviation (ACAID): regulation, biological relevance, and implications for therapy. *Int. Rev. Immunol.* 21: 123–152.
27. Stein-Streilein, J. 2008. Immune regulation and the eye. *Trends Immunol.* 29: 503–586.
28. Mo, J. S., and J. W. Streilein. 2001. Immune privilege persists in eyes with extreme inflammation induced by intravitreal LPS. *Eur. J. Immunol.* 31: 3806–3815.
29. Ohta, K., B. Wiggert, A. W. Taylor, and J. W. Streilein. 1999. Effects of experimental ocular inflammation on ocular immune privilege. *Invest. Ophthalmol. Vis. Sci.* 40: 2010–2018.
30. Casini, G., D. W. Rickman, C. Sternini, and N. C. Brecha. 1997. Neurokinin 1 receptor expression in the rat retina. *J. Comp. Neurol.* 389: 496–507.
31. Catalani, E., C. Gangitano, L. Bosco, and G. Casini. 2004. Expression of the neurokinin 1 receptor in the mouse retina. *Neuroscience* 128: 519–530.
32. Ansel, J. C., J. R. Brown, D. G. Payan, and M. A. Brown. 1993. Substance P selectively activates TNF-alpha gene expression in murine mast cells. *J. Immunol.* 150: 4478–4485.
33. Matsas, R., A. J. Kenny, and A. J. Turner. 1984. The metabolism of neuropeptides: the hydrolysis of peptides, including enkephalins, tachykinins and their analogues, by endopeptidase-24.11. *Biochem. J.* 223: 433–440.
34. Folkers, K., R. Håkanson, J. Hörig, J. C. Xu, and S. Leander. 1984. Biological evaluation of substance P antagonists. *Br. J. Pharmacol.* 83: 449–456.
35. Ohta, K., S. Yamagami, A. W. Taylor, and J. W. Streilein. 2000. IL-6 antagonizes TGF-β and abolishes immune privilege in eyes with endotoxin-induced uveitis. *Invest. Ophthalmol. Vis. Sci.* 41: 2591–2599.
36. Streilein, J. W., and S. W. Cousins. 1990. Aqueous humor factors and their effect on the immune response in the anterior chamber. *Curr. Eye Res.* 9(Suppl): 175–182.
37. Taylor, A. W., J. W. Streilein, and S. W. Cousins. 1994. Immunoreactive vasoactive intestinal peptide contributes to the immunosuppressive activity of normal aqueous humor. *J. Immunol.* 153: 1080–1086.
38. Ferguson, T. A., S. Fletcher, J. Herndon, and T. S. Griffith. 1995. Neuropeptides modulate immune deviation induced via the anterior chamber of the eye. *J. Immunol.* 155: 1746–1756.
39. Jegliński, W., D. Koczyk, M. Zaremba, and B. Oderfeld-Nowak. 1995. Bilateral gliosis in unilaterally lesioned septohippocampal system: changes in GFAP immunoreactivity and content. *J. Neurosci. Res.* 41: 394–402.
40. Decaris, E., C. Guingamp, M. Chat, L. Philippe, J. P. Grillasca, A. Abid, A. Minn, P. Gillet, P. Netter, and B. Terlain. 1999. Evidence for neurogenic transmission inducing degenerative cartilage damage distant from local inflammation. *Arthritis Rheum.* 42: 1951–1960.
41. Donkin, J. J., R. J. Turner, I. Hassan, and R. Vink. 2007. Substance P in traumatic brain injury. *Prog. Brain Res.* 161: 97–109.
42. Stjernschantz, J., M. Sears, and H. Mishima. 1982. Role of substance P in the antidromic vasodilation, neurogenic plasma extravasation and disruption of the blood-aqueous barrier in the rabbit eye. *Naunyn Schmiedebergs Arch. Pharmacol.* 321: 329–335.